A STUDY ON ACID-BASE REACTIONS OF HALIDES AND OXIDE HALIDES IN ANHYDROUS INORGANIC SOLVENTS

1996

YASUSHI KATAYAMA

A STUDY ON ACID-BASE REACTIONS OF HALIDES AND OXIDE HALIDES IN ANHYDROUS INORGANIC SOLVENTS

1 9 9 6

YASUSHI KATAYAMA

CONTENTS

CHAPTER 1

General introduction

Some anhydrous inorganic solvents have unique characteristics as reaction media which enable chemical reactions not possible in aqueous or organic solutions to be performed for synthesizing novel compounds.

Anhydrous hydrogen fluoride (HF) is a volatile liquid at room temperature, the boiling and melting point being 19.51°C and –83.55°C, respectively[1]. It has a high dielectric constant, 83.6 at 0°C and 175 at –73°C[2], and is therefore a good solvent for ionic solutes. However, it must be used with caution because it is highly toxic and corrosive. The experiments in this study were carried out with a special equipment as described in Chapter 2.

Fluorine is a strong oxidizer to form a number of binary fluorides and oxide fluorides with high oxidation states, for example, $Ag^{III}F_3$[3], $Ni^{IV}F_4$, $Ru^{IV}F_4$, $Os^{IV}F_4$[4], $Au^{V}F_5$[5], $Pt^{VI}F_6$[6], $Os^{VII}OF_5$[7], $Xe^{VI}F_6$[8], $Kr^{II}F_2$[9] and so on. These are stable in an inert atmosphere but easily react with reductive materials like moisture. Preparations and chemical reactions of such fluorides and oxide fluorides have been sometimes performed in HF because of its wide electrochemical window of ~4.5V[2] which is suitable for studying such strong oxidizing species. The early works of acid-base reactions of several fluorides in HF were reported by Clifford *et al.*[10,11,12]. A number of complex salts of fluorides and oxide fluorides with unusual oxidation states have been prepared in HF[13]. The high oxidation states are stabilized in the form of complex anions coordinated by fluorine atoms in the compounds such as $KAu^{III}F_4$, $CsCu^{III}F_4$[13], $KAg^{III}F_4$[14], $MAu^{V}F_6$ (M = AgF, Xe_2F_{11}, XeF_5, Cs, K, NO, O_2)[15,16], $O_2Pt^{V}F_6$[17], $Cs_3Nd^{IV}F_7$, $Cs_3Dy^{IV}F_7$[13]. However, fundamental data, for example, the standard values of the enthalpy of formation of complex salts, the solubility in HF and the fluoride ion affinities of fluorides and oxide fluorides, especially of rare earth and actinide elements, are not

enough to elucidate acid-base reactions in HF.

LiCl-KCl eutectic system is also a good reaction media having a wide electrochemical window of 3.626 V[18] which makes it possible to prepare base metals such as alkaline, alkaline earth, rare earth metals and their intermetallic compounds. However, hygroscopic nature of these chlorides causes more or less contamination of oxide species which occasionally affect the electrochemical syntheses and measurements. It is important for practical use to clarify the chemical behavior of oxide ion in LiCl-KCl eutectic system.

In this study, acid-base reactions of some halides and oxide halides of rare earth elements, tungsten and uranium in HF (Chapter 3 to 7) and LiCl-KCl eutectic (Chapter 8) are focused from a viewpoint of fundamental research for syntheses of functional materials and reprocessing of spent nuclear fuels.

Handling of some halides and oxide halides is not straightforward because of their hygroscopic natures. Chapter 2 describes techniques for handling and characterization of these materials without exposing to air. Moreover, safe handling of reactive gases and liquids are mentioned.

Chapter 3 describes reactions of silver (I and II) fluorides (AgF and AgF_2) and tungsten oxide tetrafluoride (WOF_4) in HF[19]. The physical and chemical properties of the compounds obtained by their reactions are also discussed.

In Chapter 4, reactions of silver(I) fluoride (AgF) and uranium hexafluoride (UF_6) are examined in HF[20], demonstrating the strong oxidizing ability of the latter. The unstable intermediate compound, argentus octafluorouranate (Ag_2UF_8), is discussed.

Chapters 5 and 6 deal with properties of uranyl fluoride (uranium dioxide difluoride, UO_2F_2) as a fluoroacid and fluorobase in HF[19]. In chapter 5, the property of UO_2F_2 in a basic HF solution of alkaline metal and silver(I) fluorides is discussed. The new complex oxofluorouranate ($AgUO_2F_3$) is characterized. In Chapter 6, the property of UO_2F_2 is focused on the reactions with strong fluoroacids in HF. The compounds of

uranyl fluoride and some pentafluorides are studied with the aids of X-ray powder diffraction and vibrational spectroscopy.

The properties of trivalent rare earth trifluorides as a fluoroacid and fluorobase in HF are investigated and described in Chapter 7[21]. The obtained compounds are characterized by X-ray diffraction and vibrational spectroscopy.

In Chapter 8, chemical behaviors of trivalent rare earth trichlorides in LiCl-KCl eutectic are discussed[22]. From the estimation of thermodynamic properties of rare earth oxide chlorides, the conditions of the formation of rare earth oxides and oxide chlorides are predicted and verified by experiments.

References

1 D. R. Lide ed., "*HANDBOOK of CHEMISTRY and PHYSICS*," 74th ed., CRC press (1993-1994).

2 T. A. O'Donnell, "*Superacids and Acidic Melts as Inorganic Chemical Reaction Media*," VCH, (1993).

3 B. Žemva, K. Lutar, A. Jesih, W. J. Casteel, Jr., A. P. Wilkinson, D. E. Cox, R. B. von Dreele, H. Borrmann and N. Bartlett, *J. Am. Chem. Soc.*, **113**, 4192 (1991).

4 B. Žemva, K. Lutar, A. Jesih, W. J. Casteel, Jr. and N. Bartlett, *J. Chem. Soc., Chem. Commun.*, 346 (1989).

5 M. J. Vasile, T. J. Richardson, F. A. Stevie and W. E. Falconer, *J. Chem. Soc. Dalton Trans*, 351, (1976).

6 N. Bartlett, *Angew. Chem. Internat. Edit.*, **7**, 6, 433 (1968).

7 N. Bartlett and N. K. Jha, *J. Chem. Soc.*, **A**, 536 (1968).

8 J. G. Malm, C. L. Chernick, *Inorg. Synth.*, **8**, 258 (1966).

9 J. Slivnick, A. Smalc, K. Lutar, B. Žemva, B. Frlec, *J. Fluorine Chem.*, **5**, 273 (1975).

10 A. F. Clifford, H. C. Beachell and W. M. Jack, *J. Inorg. Nucl. Chem.*, **5**, 57 (1957).

11 A. F. Clifford, H. C. Beachell and W. M. Jack, *J. Inorg. Nucl. Chem.*, **5**, 71 (1957).

12 A. F. Clifford, H. C. Beachell and W. M. Jack, *J. Inorg. Nucl. Chem.*, **5**, 76 (1957).

13 R. Hoppe, *Angew. Chem. Int. Ed. Engl.*, **20**, 63 (1981).

14 R. Hoppe, *Z. Anorg. Allg. Chem.*, **292**, 28 (1957).

15 N. Bartlett and K. Leary, *Rev. Chimie Minérale*, **13**, 82 (1976).

16 W. J. Casteel, Jr., G. Lucier, R. Hagiwara, H. Borrmann and N. Bartlett, *J. Solid State Chem.*, **96**, 84 (1992).

17 F. O. Sladky, P. A. Bulliner, N. Bartlett, *J. Chem. Soc.*, **A**, 2179 (1969).

18 A. J. Bard, "*Encyclopedia of Electrochemistry of the Elements Vol. X Fused Salt Systems*," Marcel Dekker, Inc., New York (1976).

19 Y. Katayama, R. Hagiwara and Y. Ito, *J. Fluorine Chem.*, Vol. **74**, No. 1, 89 (1995).

20 R. Hagiwara, Y. Katayama, K. Ema and Y. Ito, *Eur. J. Solid State Inorg. Chem.*, **32**, 283 (1995).

21 K. Hironaka, Y. Katayama, R. Hagiwara and Y. Ito, to be submitted to *J. Fluorine Chem.*

22 Y. Katayama, R. Hagiwara and Y. Ito, *J. Electrochem. Soc.*, Vol. **142**, No. 7, 2196 (1995).

CHAPTER 2

Experimental techniques

2.1 Material handling

In general, most of materials used in this study must be handled in a glove box of argon atmosphere with a continuous gas refining instrument (Miwa Seisaku-sho, MDB-2BL-T1000+MS-H60W-O). The concentration of water was always monitored and maintained at less than 800 ppb (~ −100°C in a dew point). The concentration of oxygen was less than 500 ppb. This section describes the handling of reactive solids, gases and liquids without exposing them to air.

2.1.1 Solids

Hygroscopic materials must be dried under vacuum with elevating temperature. Drying was usually carried out in a Pyrex glass container (see 2.2.3). Drying over 500°C was made in a quartz glass container. The container was connected to a vacuum line constructed for vacuum drying (Fig. 2-1). Drying was usually performed by an oil diffusion pump until the pressure reaches 10^{-3} torr. After evacuating the gases, the container was heated to a fixed temperature in an electric furnace. Some special treatments were necessary for rare earth trichloride hydrates as described in Chapter 7. The container was then cooled and transferred in the glove box. The dried materials were stored in containers made of Pyrex glass, PFA (tetrafluoroethylene-perfluoroalkylvinylether copolymer) or FEP (tetrafluoroethylene-hexafluoropropylene copolymer). Some highly oxidative materials were stored in FEP tubes (Sanyo, 1/2' o.d.) with Teflon caps. Silver compounds were stored in containers covered with aluminum foil to avoid decomposition by the irradiation of light.

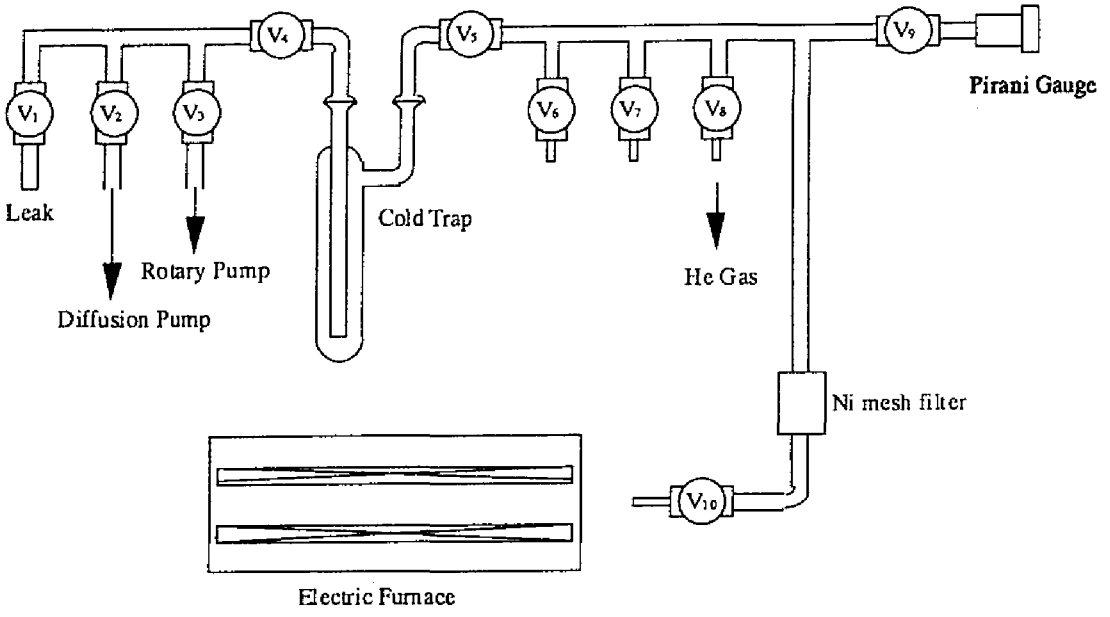

Fig. 2-1 Vacuum line for drying.

The air sensitive reagents were weighed by an electric balance (Shimadzu, EB-430H) settled in the glove box. The error was approximately ±3 mg due to the instability of the measurement caused by static electricity and circulation of gas in the glove box.

2.1.2 Gases

Gaseous materials were handled in a vacuum line constructed for corrosive gases such as fluorine, hydrogen fluoride and reactive fluorides. Fig. 2-2 shows a schematic illustration of the vacuum line. All the tubes and valves (Nupro, SS-8BK-TSW, Kel-F tip) used in the vacuum line are made of argon arc-welded stainless steel (SUS-316). The inner surface of the vacuum line was pre-passivated with fluorine gas (~1 atm) for 10 ~ 20 hours at room temperature. The pressure was monitored by Bourdon and Pirani gauges. The latter must not be exposed to reactive gases filled in the line. The volumes of each part of the line were tensimetrically measured prior to the experiment.

The reactive gases were disposed through a series of chemical trap columns, a sodium fluoride (NaF) column for trapping gaseous fluoroacids and a soda lime column

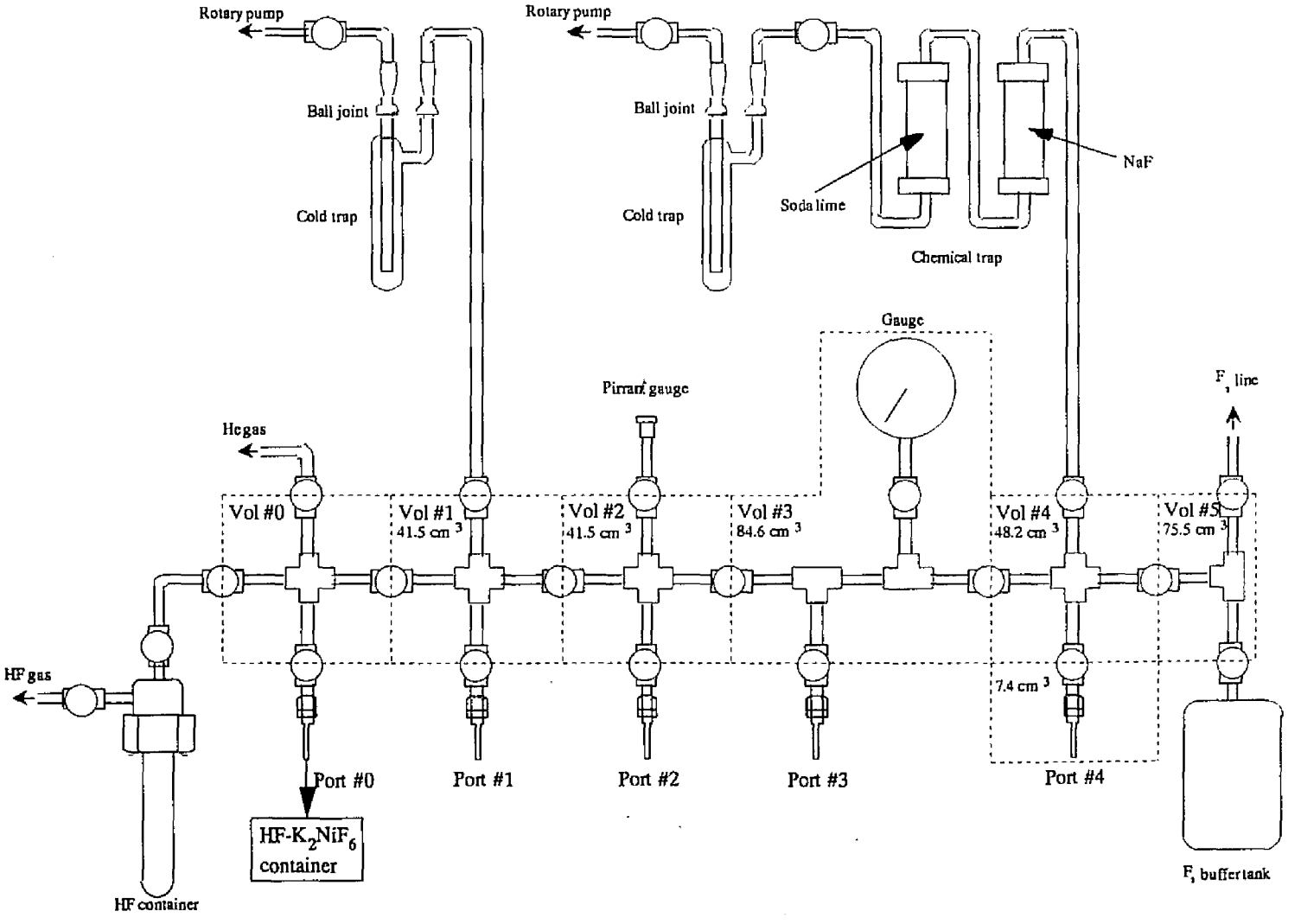

Fig. 2-2 Vacuum line for handling of fluorine, hydrogen fluoride and fluoride gases.

for trapping fluorine and other fluoroacids passed through the NaF column, the reactions in the traps being represented as follows:

$$MF_n + mNaF \rightarrow Na_mMF_{m+n} \quad (1)$$

$$F_2 + CaO \rightarrow CaF_2 + 1/2\ O_2 \quad (2)$$

Pumping of the chemical traps was performed through a cold trap.

The amount of gases for reactions was measured by tensimetry. In some cases, the gases were introduced in reactors by condensation. Fluorine gas, for example, is a liquid with vapor pressure of ~0.4 atm at liquid nitrogen temperature (-176°C). It should be noted that wrong handling in condensation process may cause serious accidents like a pressure explosion of a reactor when it is warmed up. It is necessary to calculate precisely the amount and pressure of gases to be condensed in a reactor. A high pressure reaction needs the protection against explosion such as protection glasses and a thick plastic shield in front of the reactor.

The impurities in the gases were checked by infrared absorption spectroscopy using a gas cell with AgCl crystal windows (See 2.7.2). Gaseous fluorides prepared by the reactions of metals or metal oxides with fluorine were purified by a trap-to-trap distillation.

2.1.3 Liquids

Liquid materials used at room temperature in this study were HF (m.p. -83.1°C, b.p. 19.54°C[1]), WF_6 (m.p. 2.5°C, b.p. 17.5°C[1]), SbF_5 (m.p. 7°C, b.p. 149.5°C[1]) and acetonitrile (CH_3CN, m.p. -45.7°C, b.p. 81.6°C[1]). At high temperature, LiCl-KCl eutectic (LiCl : KCl = 58.5 : 41.5 in mol%, m.p. 354°C) was employed as a solvent.

HF is a colorless liquid and the vapor pressure is ~1.3 atm[2] at room temperature. It was stored in a container made of Kel-F tube to avoid formation of hydrogen by the reactions with metals. A small amount of HF was transferred to an FEP container (3/4' o.d.) in which a strong oxidizer, K_2NiF_6 (Ozark-Mahoning), was placed in order to

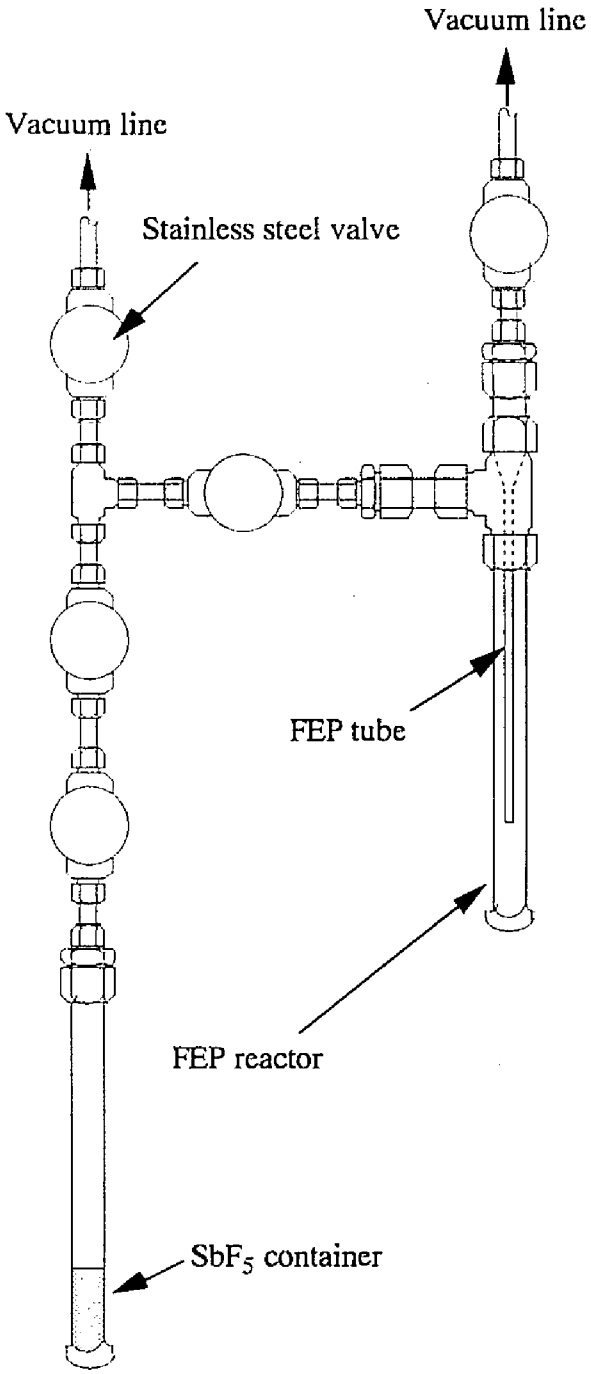

Fig. 2-3 Apparatus of the reactor for handling SbF_5.

eliminate reducing materials, such as water and hydrogen. HF was distilled from the K_2NiF_6 solution to a reactor cooled at –196°C.

Vapor pressure of WF_6 at room temperature is also ~1.3 atm[2]. Therefore, the handling is similar to that of HF. However, a Kel-F container must be used for storage

since WF_6 penetrates FEP wall.

SbF_5 is a colorless viscous liquid with a low vapor pressure (~4 torr at 25°C[2]). Liquid SbF_5 was handled in the glove box. A special apparatus was used to transfer SbF_5 in the vacuum line (Fig. 2-3). SbF_5 was condensed on the cooled surface of outer tube applying a dynamic vacuum through an inner FEP tube.

LiCl-KCl powder mixture was loaded in a Pyrex glass reactor in the glove box and it was connected to the manifold line in order to keep argon atmosphere over the melts. The salts were heated by a transparent electric furnace (see 2.3) monitoring the melting and precipitation of compounds. The temperature of the melts was monitored by a thermocouple attached to the bottom of the reactor.

The volume of a liquid in a cylindrical reactor was estimated from the inner diameter and the height of the liquid-level from the bottom of the reactor.

2.2 Reactors

2.2.1 FEP reactors

FEP reactors were used for the reactions performed in liquid HF at room temperature (Fig. 2-4). The one end of an FEP tube (10 mm, 1/2 or 3/4' o.d., 150 ~ 200 mm long) was heat-sealed pressing by pliers. The other end was connected to a stainless steel valve (Whitey, SS-1KS4, with Kel-F tips) via a reducing union with Swagelok Teflon fittings. The maximum working pressure and temperature were less than ~3 atm and ~120°C, respectively.

T-shaped FEP reactors were occasionally used for decantation to separate a solid from liquid, or wash a solid with HF. Fig. 2-5 shows a T-shaped FEP reactor. Two FEP tubes (10 mm or 1/2' o.d.) with a sealed end are connected to Teflon T-union (Sanyo) with compression fittings so that the liquid does not contact with metal by decantation.

The stirring of the liquid in the FEP tube was carried out by snapping it with fingers

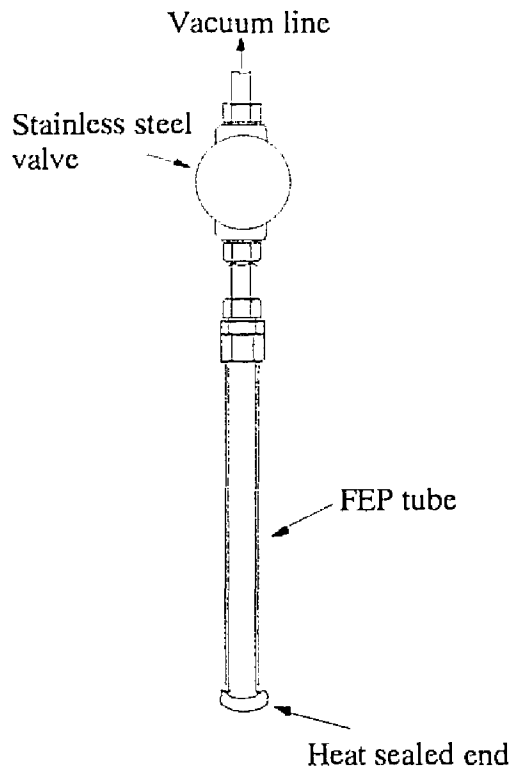

Fig. 2-4 FEP reactor.

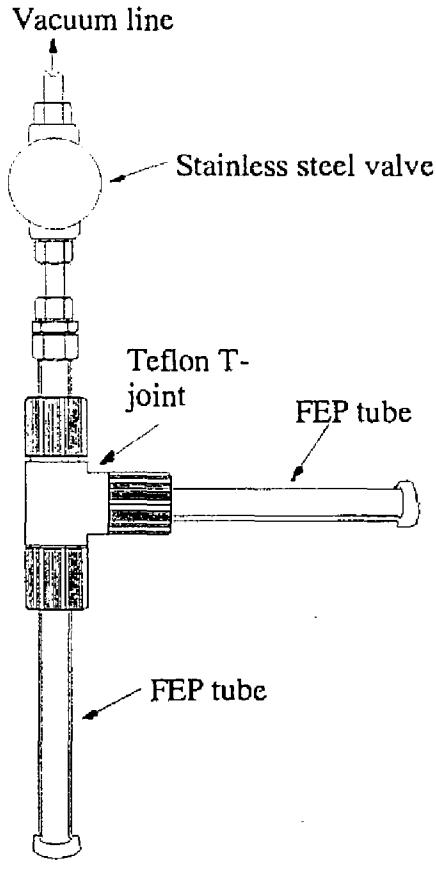

Fig. 2-5 T-shaped reactor.

or magnetically spinning a small magnet coated with Teflon in the reactor.

2.2.2 Monel reactors

Monel (an alloy of nickel and copper) reactors were used when reactions of corrosive gases were performed at high temperature and/or high pressure. Figure 2-6 shows a typical Monel reactor. All the parts contacting with gases are made of argon arc-welded Monel metal. A Teflon packing was used to seal between the body and lid. The lid was cooled by a water flow through a jacket to protect the Teflon packing. The reactor was passivated with fluorine for several hours at room temperature before use. The maximum temperature and pressure for reactions in the presence of fluorine were ~ 500°C and ~ 12 atm, respectively. Samples were usually put on nickel foil cups. The Monel reactor was heated by a ribbon heater wound around it. The temperature was monitored

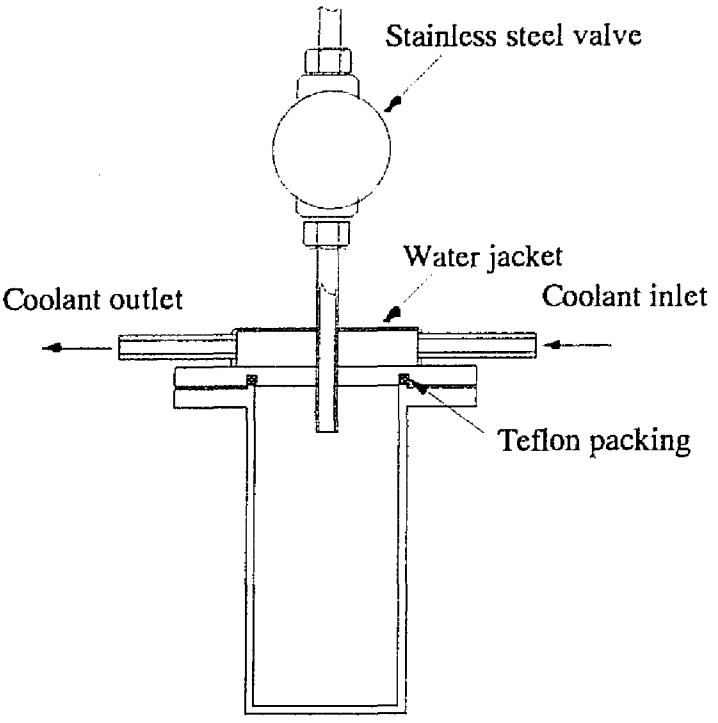

Fig. 2-6 Monel reactor.

by a thermocouple attached on the outer surface near the bottom of the reactor.

When the product is sublimable, it deposits on the inner surface of the lid. Pure tungsten oxide tetrafluoride and bismuth pentafluoride were collected without further purification (see Appendix).

2.2.3 Pyrex and quartz glass reactors

Pyrex and quartz glass reactors were used for vacuum drying of the reagents and the reactions performed at higher temperatures including LiCl-KCl molten salts. A Pyrex glass reactor is illustrated in Fig. 2-7. The tube was connected to a stainless steel valve via Swagelok fitting with Teflon ferrule. The temperature was maintained lower than ~ 500°C. When a higher temperature was required, quartz glass reactors were used.

A large quartz glass reactor (25 mm o.d.) with a joint was used for drying a large amount of solid reagents and capillaries for X-ray powder diffraction and Raman spectroscopy (Fig. 2-8).

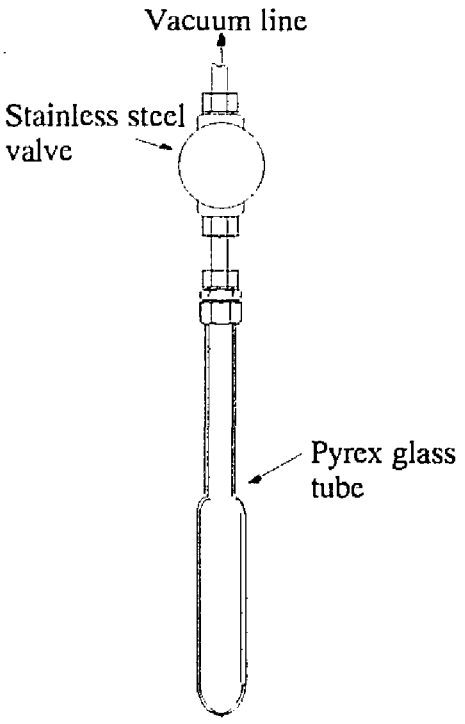

Fig. 2-7 Pyrex glass reactor.

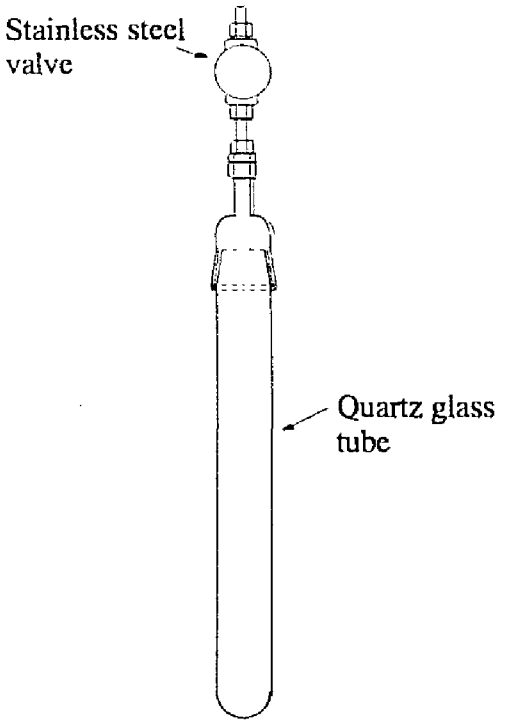

Fig. 2-8 Quartz glass reactor.

2.2.4 Sublimation apparatus

Some reagents were purified by sublimation. Fig. 2-9 shows a sublimation apparatus made of Pyrex glass. A Byton o-ring was used to seal between the vessel and lid. A crude material was placed at the bottom of the vessel. The vessel was then warmed up under reduced pressure while the cold finger to collect the sublimed material was cooled by a water flow.

2.3 Transparent electric furnace

Fig. 2-10 shows a transparent electric furnace made of quartz glass. A nichrome wire was wound around the inner quartz glass tube. The outer tube was placed for heat insulation. The tubes were flexibly held with spring screws to protect from break by heat expansion. A thermocouple covered with an alumina tube was inserted in a brass holder at the center of the bottom. A reactor was inserted from the top and fixed so that the bottom touches on the top of the thermocouple.

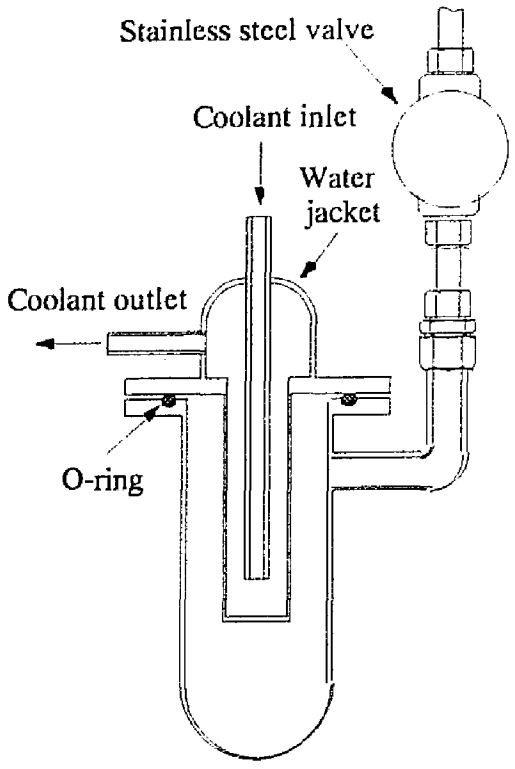

Fig. 2-9 Sublimation apparatus.

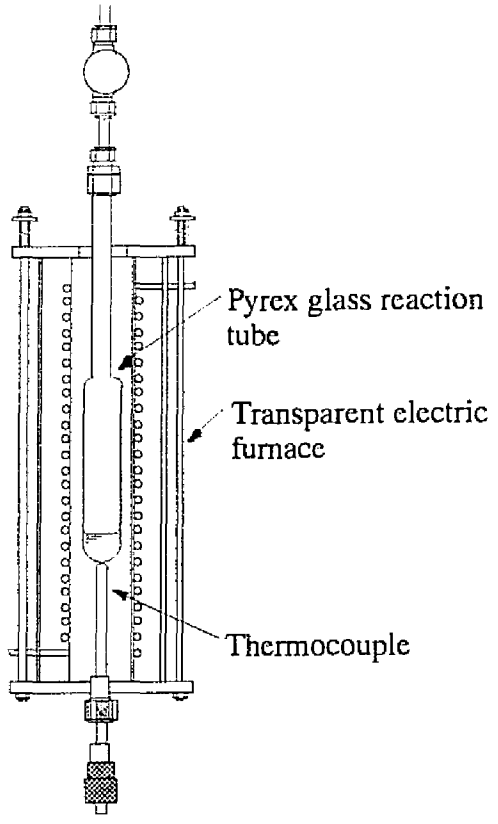

Fig. 2-10 Transparent electric furnace.

2.4 Experimental techniques

2.4.1 Experimental technique for handling anhydrous hydrogen fluoride

Solid reagents were loaded in an FEP reactor in the glove box. The reactor was connected to the vacuum line via Swagelok fitting with Teflon ferrule. The gases in the reactor was evacuated after evacuating air in the connecting part between the reactor and the vacuum line. HF was distilled from a solution of K_2NiF_6 to the reactor. The amount of HF transferred was estimated by the liquid-level of the K_2NiF_6 solution. The reactor was warmed up slowly to room temperature. The reaction was continued for 2-20 hours with/without stirring. HF was evacuated slowly from the reactor after the reaction. Occasionally, the evacuation rate was controlled by a needle valve (Nupro, SS-4BMG) placed between the reactor and the vacuum line. The reactor was then transferred into the

glove box. The product was charged in a quartz glass capillary to prepare the sample for X-ray powder diffraction and Raman spectroscopy.

Single crystal growth was carried out in a T-shaped FEP reactor. A sample or mixture of reagents was loaded in one arm (Tube A) of the reactor and HF was condensed on it. The supernatant solution was decanted to another arm (Tube B). Then, HF in Tube B was condensed slowly back to Tube A cooled by water. Slow elimination of HF controlled by a needle valve was also successful in single crystal growth. In most cases, single crystal growth takes several days.

2.4.2 Experimental technique for handling molten chlorides

Reagents were mixed with LiCl-KCl eutectic mixture and loaded in a Pyrex glass reactor. Ambient pressure of Ar was kept in the reactor. The temperature was elevated to 450°C by the transparent electric furnace to monitor melting of the mixture and formation of precipitate. After holding the temperature for several hours, the reactor was cooled slowly and transferred to the glove box. The precipitate was collected from the cooled melts and charged in a quartz glass capillary to prepare the sample for X-ray powder diffraction as described in the next section.

2.5 X-ray powder diffraction

X-ray powder diffraction patterns were obtained by a Debye-Scherrer camera of 115-mm in diameter with Rigaku apparatus using CuKα radiation (Ni-filtered). Samples were usually packed in 0.3 or 0.5 mm o.d. quartz glass capillaries (Overseas X-ray) in the glove box. The capillaries were temporarily sealed by grease and transferred outside of the glove box. Then they were sealed by drawing down in a small flame of an oxygen burner.

The d-spacing of X-ray powder diffraction patterns was usually measured by a

comparator (Shimadzu). The patterns were occasionally transferred to a personal computer with the aid of a scanner to measure the intensities of diffraction peaks although they are not rigorously proportional to the real intensities. There is a tendency that the transmittance saturates as the intensity of a peak increases. Recently, imaging plates were introduced for the measurement of X-ray powder diffraction patterns instead of films giving proportional intensities of the diffraction.

2.6 Raman spectroscopy of solid samples

The Raman spectra of the solid samples were obtained by NR-1000S (Nippon Spectroscopic), 512.5 and 488 nm lines of Ar laser (NEC), or 647.1 nm line of Kr laser (Spectra Physics) being used as excitation lines. The samples were loaded in 0.5 or 1.0 mm o.d. quartz glass capillaries in the same way as for the samples of X-ray powder diffraction. The Raman scattering light was introduced to the spectrometer from the direction perpendicular to the excitation beam. Colored samples should be irradiated by laser as shortly as possible otherwise the absorption of light causes decomposition. This may be avoided by changing the wavelength and/or power of the laser.

2.7 IR Spectroscopy

2.7.1 Solid samples

A finely grounded powder of a solid sample was sandwiched between two AgCl crystal windows in an air-tight solid cell (Fig. 2-11). The surfaces of AgCl windows were scratched by a sand paper to avoid interference. The spectrum of the sample was measured on FTIR spectrometers (FT/IR-5M, Nippon Spectroscopic or BIORAD FTS 165).

2.7.2 Gaseous samples

Gaseous sample (50~100 torr) was introduced in a gas cell with AgCl crystal windows (Fig. 2-12). A cold finger is equipped to collect gases by condensation. The spectra were recorded using an FTIR spectrometer (BIORAD FTS 165).

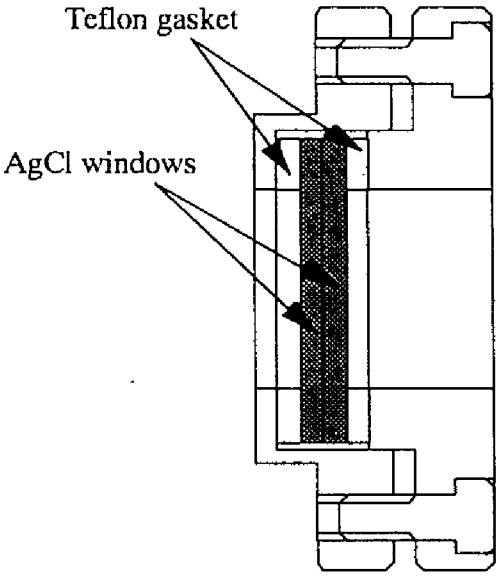

Fig. 2-11 IR cell for solid samples.

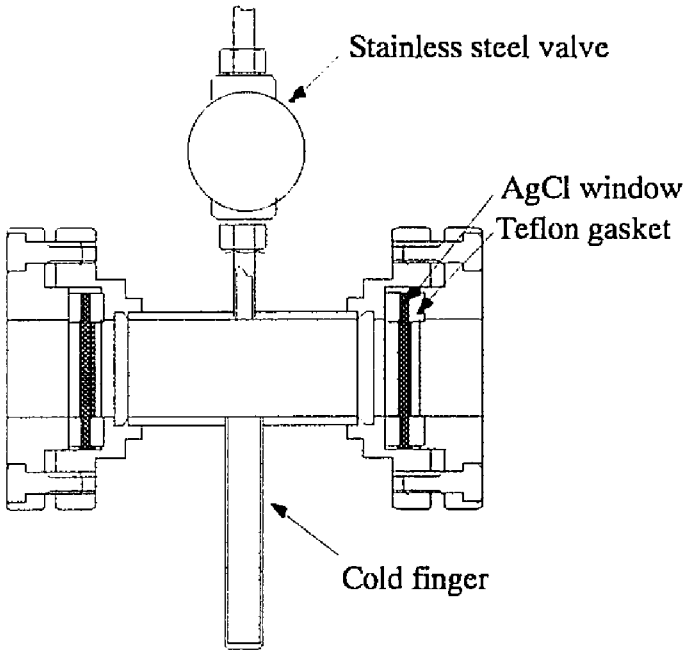

Fig. 2-12 IR cell for gaseous samples.

References

1 D. R. Lide ed., "*HANDBOOK of CHEMISTRY and PHYSICS*," 74th ed., CRC press (1993-1994).

2 N. P. Galkina ed., "*Osnovnye Svojstva Neorganicheskih Ftoridov*," Moskva Atomizdat, (1976).

CHAPTER 3

Reactions of silver(I,II) fluorides with tungsten oxide tetrafluoride in anhydrous hydrogen fluoride*

3.1 Introduction

Silver fluoride (AgF) acts as a strong fluorobase in anhydrous hydrogen fluoride (HF) like alkaline metal fluorides dissolving well in HF (83.2 g / 100 g HF at 11.9°C[1]). Complex salts of AgF have been prepared by the reactions with several fluoroacids[2] although only a few crystal structures have been known due to low solubility in HF which prevents growth of single crystals.

On the other hand, silver difluoride (AgF_2) is a very weak fluorobase and reacts only with strong fluoroacids. It reacts with antimony and bismuth pentafluoride (SbF_5 and BiF_5) to form $Ag(SbF_6)_2$ and $Ag(BiF_6)_2$, respectively[3]. These compounds contain discrete divalent silver cations, Ag^{2+}. The reactions with arsenic pentafluoride (AsF_5) and boron trifluoride (BF_3) give 1 : 1 complex salts, $AgFAsF_6$ and $AgFBF_4$, respectively[4,5]. These 1 : 1 compounds contain one-dimensional polymeric cationic chains, $(AgF)_n^{n+}$, which is considered to be decomposed to monomeric Ag(II) cations in the solution acidified by AsF_5 and BF_3.

Tungsten oxide tetrafluoride (WOF_4) has been known to act as a fluoroacid to form several complex salts, such as $NaWOF_5$, $CsWOF_5$[6], $NOWOF_5$[7], $CsW_2O_2F_9$[8] and $XeF_2.WOF_4$[9]. The fluoride ion affinity of WOF_4 is known to be fairly strong although quantitative assessment is lacking.

In this chapter, WOF_4 as a fluoroacid in HF is examined through the series of reactions with AgF and AgF_2. Some chemical and physical properties of the complex salts

---

* Published in *J. Fluorine Chem.*, Vol. **74**, No. 1, 89 (1995).

will be discussed.

3.2 Reagents

Xe (Teisan K. K., purity 99.995% or more) was used as supplied. AgF was prepared by interacting Ag_2O (Wako Chemicals, purity 99% or more) with HF. Decomposition of the bifluoride, $Ag(HF)_nF$, was made at 80°C under vacuum. AgF_2 was prepared by fluorinating $AgNO_3$ (Nakarai Tesque, purity 99.95%) in a Monel reactor at 250°C. WOF_4 was prepared by the reaction of WF_6 (Ozark-Mahoning) with water formed by a slow reaction of quartz wool (Toshiba) and HF[10]. Purification was made by sublimation at −70°C under a reduced pressure.

3.3 Results

$AgF + 2WOF_4$

AgF (50 mg, 0.394 mmol) and WOF_4 (225 mg, 0.816 mmol) were interacted for several hours in HF (~1 cm^3) at room temperature. After removing HF, an ivory solid was obtained. No weight change was observed after the reaction. X-ray diffraction showed the absence of the starting materials. The solid was ascribed to the 1 : 2 complex salt, $AgW_2O_2F_9$, by the comparison of the vibrational spectra of the solid with those of $CsW_2O_2F_9$[8].

$AgF + WOF_4$

The mixture of AgF (123 mg, 0.962 mmol) and WOF_4 (266 mg, 0.964 mmol) was loaded into one arm (Tube A) of a T-shaped reactor and HF (~1 cm^3) was condensed on the mixture at −196°C. An ivory precipitate was formed after warming Tube A to room temperature. The supernatant solution was decanted to the other arm (Tube B) and the

precipitate was washed several times with HF condensed back to Tube A. Finally, after evaporating HF, an ivory solid (~270 mg) in Tube A and a colorless solid in Tube B were obtained. Additional evacuation with warming of Tube B changed the color of the solid to bright yellow (the weight : ~80 mg). A large weight loss (~40 mg, probably caused by sticking of the sample in the T-union) prevented the determination of the composition by gravimetry. X-ray diffraction showed that the yellow solid was AgF and the ivory solid was the same as obtained by the interaction of AgF + $2WOF_4$.

$AgF + WOF_4$ (slow evacuation of HF)

AgF (107 mg, 0.843 mmol) and WOF_4 (227 mg, 0.823 mmol) were loaded in one arm (Tube A) of a T-shaped reactor and HF (~1 cm^3) was condensed on the mixture at -196°C. An ivory solid was formed as described above. On removing HF very slowly by condensing in the end of the other arm cooled at 0°C, a colorless crystalline solid was formed in Tube A. No weight uptake was observed after the reaction. X-ray diffraction detected neither AgF nor WOF_4. The solid is ascribed to the 1 : 1 complex salt, $AgWOF_5$, by comparing the vibrational spectra with those of $NOWOF_5$[7].

$AgF_2 + 2WOF_4$

AgF_2 (168 mg, 1.15 mmol) and WOF_4 (640 mg, 2.32 mmol) were interacted in HF (~2 cm^3) in the presence of F_2 at room temperature. After stirring for ~24 hours, a dark-purple solid was obtained. No weight change was observed after the reaction. No phases of the starting materials were observed in the X-ray powder pattern. The solid is considered to be the 1 : 2 complex salt, $AgFW_2O_2F_9$, from the comparison of the vibrational spectra with those of $AgW_2O_2F_9$ which contains $W_2O_2F_9^-$ anion.

$AgF_2 + WOF_4$

AgF_2 (103 mg, 0.706 mmol) and WOF_4 (187 mg, 0.678 mmol) were interacted in

HF (~2 cm^3) in the presence of F_2 at room temperature. On evacuating HF very slowly, a dark-purple solid was obtained. No weight change was observed after the reaction. This solid was ascribed to the mixture of $AgFW_2O_2F_9$ and unreacted AgF_2 by X-ray diffraction.

$AgW_2O_2F_9 + F_2$

$AgW_2O_2F_9$, which was prepared above, was interacted with F_2 in HF (~1 cm^3) at room temperature. The color of the precipitate (ivory) turned to brown after stirring for a while. Additional interaction for 24 hours changed the color of the precipitate to dark-purple. X-ray diffraction of the precipitate detected $AgFW_2O_2F_9$ and AgF_2.

$AgFW_2O_2F_9 + Xe$

$AgFW_2O_2F_9$ prepared above was interacted with Xe in HF (~1 cm^3) at room temperature. In ~24 hours, the color of the precipitate changed gradually from dark-purple to brown. After evacuating HF at room temperature, a sublimable and highly reactive colorless solid was crystallized at the upper part of the reaction tube by warming the bottom of it. The solid was identified as $XeF_2.WOF_4$[9] by Raman spectroscopy. X-ray diffraction showed that the residual solid in the bottom of the tube was the mixture of AgF_2 and $AgW_2O_2F_9$.

3.4 Discussion

It is known that WOF_4 dissolves to form a monomeric anion, WOF_5^-, and a dimeric anion, $W_2O_2F_9^-$ in HF, by the following equilibria[7]:

$$2HF + WOF_4 \rightleftharpoons H_2F^+ + WOF_5^- \quad (1)$$

$$nHF + 2WOF_5^- \rightleftharpoons W_2O_2F_9^- + (HF)_nF^- \quad (2)$$

According to these equilibria, the 1 : 2 complex salt of AgF and WOF_4, $AgW_2O_2F_9$, is

formed in the presence of excess HF. The 1 : 1 complex salt, $AgWOF_5$, is formed by slow removal of HF, in other words, by shifting the following equilibrium to the left:

$$2AgWOF_5 + nHF \rightleftharpoons Ag(HF)_nF + AgW_2O_2F_9 \quad (3)$$

$AgW_2O_2F_9$ is also prepared by interacting stoichiometric amounts of AgF and WOF_4 in HF:

$$AgF + 2WOF_4 \rightarrow AgW_2O_2F_9 \quad (4)$$

The X-ray powder patterns of $AgWOF_5$ and $AgW_2O_2F_9$ are listed in Table 3-1. Table 3-2 shows the vibrational spectra. The spectra of $NOWOF_5$[7] and $CsW_2O_2F_9$[8] are also included for comparison. The peaks for WOF_5^- are assigned for C_{4v} symmetry[11]. The spectra of $AgWOF_5$ and $AgW_2O_2F_9$ are quite similar to those of $NOWOF_5$ and $CsW_2O_2F_9$, respectively.

Table 3-1 X-ray powder diffraction patterns of $AgWOF_5$, $AgW_2O_2F_9$ and $AgFW_2O_2F_9$.

$AgWOF_5$		$AgW_2O_2F_9$			$AgFW_2O_2F_9$	
d / Å	Intensity	*d* / Å	Intensity	*hkl**	*d* / Å	Intensity
4.92	mw	4.32	w	013	6.62	w
4.47	s	4.13	s	103	5.19	vw
4.31	w	3.92	s	212	4.77	m
4.18	w	3.79	w	$\bar{2}21$, 221	4.60	m
3.97	w	3.65	m	023	4.39	vw
3.75	s	3.50	vw	032	4.17	s
3.57	s	3.42	s	222	3.80	s
3.42	s	3.23	m	014	3.68	mw
3.17	mw	2.59	w	$\bar{2}41$, 241	3.33	vs
3.09	m	2.47	vw	$\bar{1}43$	3.14	mw
2.81	w	2.42	vw	$\bar{1}25$	2.83	m
2.69	w	2.22	vw	225	2.62	m
2.58	w	2.17	w	$\bar{4}31$	2.52	w
2.48	w	2.00	m	$\bar{2}53$	2.38	m
2.10	m	1.96	s	226		
1.88	m					

Abbreviations used: s, strong; m, medium; v, very; w, weak.
* a_o = 10.402, b_o = 12.307, c_o = 13.639 Å, β = 90.2°; space group, $P2_1/c$[12].

Table 3-2 Vibrational spectra[a] of solid $AgWOF_5$, $AgW_2O_2F_9$, $AgFW_2O_2F_9$ and some related compounds.

$AgWOF_5$		$AgW_2O_2F_9$		$AgFW_2O_2F_9$		$NOWOF_5$[b]		$CsW_2O_2F_9$[c]		Assignments	
Raman	IR	Raman	IR	Raman	IR	Raman	IR	Raman	IR	$WOF_5^-(C_{4v})$[d]	$W_2O_2F_9^-$[c]
989vs	992s,br	1026s	1009s,br	988s	1010s,br	1001s	1003s	1036s	1048vs	$\nu_1(A_1)$, ν(W=O)	ν(W=O out of phase)
		1021s							1035vs		ν(W=O in phase)
									822vw		
									790vw		
690	692ms,sh	707ms	711ms	690m	711ms,sh	684mw	680sh	700m	704s	$\nu_2(A_1)$, ν(W-F_t)	$\nu_s(WF_4$ in phase)
	632s,br		645s,br		645s,br		610vs,br		628vs,br	$\nu_8(E)$, $\nu(WF_4)$	$\nu_{as}(WF_4)$
		610w	597s,br	615ms	602s,br	591vw		610vw		$\nu_5(B_1)$,$\nu(WF_4)$	$\nu_s(WF_4$ out of phase)
440w	445vs	440w	447s		447		455ms		440vs	$\nu_3(A_1)$,$\nu(WF_4)$	ν_{as}(WFW)
									400vw		
330m		320s		335ms		327m				$\nu_9(E)$,ρ_w(W-F_t)	
291		282w				292sh				$\nu_4(A_1)$,$\pi(WF_4)$	

[a]Frequencies are given in cm^{-1}. Abbreviations used: sh, sharp; br, broad; s, strong; m, medium; v, very; w, weak. [b]The spectra reported in ref. 7. The peaks corresponding to N-O are not listed. [c]Ref. 8. [d]Ref. 11.

It has been reported that AgF_2 reacts with strong fluoroacids to give cationic Ag(II), $(AgF)_n^{n+}$ and/or Ag^{2+}[4,5,13,14]. Two isomers, $AgF^+W_2O_2F_9^-$ and $Ag^{2+}(WOF_5^-)_2$, are possible for the 1 : 2 compound of AgF_2 and WOF_4. The vibrational spectra of this compound are listed in Table 3-2. It is evident that this compound contains $W_2O_2F_9^-$ by comparing the spectra with those of $AgWOF_5$ and $AgW_2O_2F_9$. The powerful oxidizing ability discussed below indicates that this compound contains $(AgF)_n^{n+}$. Therefore this compound is concluded to be $AgFW_2O_2F_9$. The X-ray powder pattern is listed in Table 3-1.

$AgFW_2O_2F_9$ is stable under an inert gas but irradiation of this compound sealed in a quartz glass capillary by Ar laser (488 and 514.5 nm, 50-250 mW) causes decomposition probably to $AgW_2O_2F_9$ and fluorine, the latter seems to have etched the quartz wall. The Raman spectrum was obtained by using a Kr laser (647.1 nm, 50 mW) beam which does not cause decomposition (Table 3-2).

Interaction of equimolar amounts of AgF_2 and WOF_4 does not form the 1 : 1 complex salts such as $AgFWOF_5$, but gives a mixture of $AgFW_2O_2F_9$ and unreacted AgF_2. WOF_4 is considered to act as a stronger fluoroacid by forming $W_2O_2F_9^-$ rather than forming WOF_5^-, the latter being unable to form an $(AgF)_n^{n+}$ salt.

Ag^+ is oxidized by F_2 to form cationic Ag(II) such as Ag^{2+} and $(AgF)_n^{n+}$ in the presence of SbF_5, AsF_5 and BF_3[5,13]. The formation of $AgF^+W_2O_2F_9^-$ by the reaction of $AgW_2O_2F_9$ with F_2 demonstrates that the fluoroacidity of WOF_4 by forming $W_2O_2F_9^-$ is at least as strong as that of BF_3.

$$AgW_2O_2F_9 + 1/2F_2 \rightarrow AgFW_2O_2F_9 \qquad (5)$$

The formation of AgF_2 (brown) is observed at the beginning of the reaction. Ag^+ is oxidized to Ag(II) by F_2 in the presence of a trace amount of WOF_4, formed according to the equilibria expressed by eqs. (1) and (2). However, AgF_2 would precipitate instead of $AgFW_2O_2F_9$ when the solution is not acidic enough due to the low solubility of $AgW_2O_2F_9$ in HF. Since the reaction rate of AgF_2 and WOF_4 is slow, because the former

is insoluble again, $AgFW_2O_2F_9$ is formed very slowly as the fluoroacidity is increased by the precipitation of AgF_2.

According to the crystal structure of $H_3O^+W_2O_2F_9^-$[15], $W_2O_2F_9^-$ consists of two WOF_4 units linked by a fluorine bridge trans to the tungsten-oxygen bonds. At the same time as this work was carried out, Shen *et al.* also performed a series of reactions of AgF and AgF_2 with WOF_4[12]. They succeeded in growing a single crystal of $AgW_2O_2F_9$ and determined the crystal structure, in which they found two types of fluorine-bridged dimeric anions, slightly different in bond angles and conformation with each other. The assignment of the powder pattern of $AgW_2O_2F_9$ in Table 3-1 was made based on their result.

Xe is oxidized to Xe(II) by cationic Ag(II) in HF at room temperature[13]. $AgFW_2O_2F_9$ also oxidizes Xe to Xe(II) by the following reaction in HF:

$$5AgFW_2O_2F_9 + 2Xe \rightarrow 2XeF_2.WOF_4 + 4AgW_2O_2F_9 + AgF_2 \qquad (6)$$

Since the fluorobasicity of XeF_2 is stronger than that of AgF_2, XeF_2 substitutes AgF_2 in $AgFW_2O_2F_9$ to form $XeF_2.WOF_4$. All Ag(II) is not consumed for the oxidation of Xe to Xe(II) due to the precipitation of AgF_2 which does not oxidize Xe unless further WOF_4 is added to the solution.

References

1 A. W. Jache and G. H. Cady, *J. Phys. Chem.*, **56**, 1106 (1952).

2 R. D. W. Kemmitt, D. R. Russel and D. W. A. Sharp, *Inorg. Chem.*, 4408 (1963).

3 C. Shen, G. Lucier, B. Žemva, W. J. Casteel, Jr., J. Münzenberg and N. Bartlett, *Proc. of the 14th International Symposium on Fluorine Chemistry*, 34 (1994).

4 D. Gantar and B. Frlec, *Acta Cryst.*, C**43**, 618 (1987).

5 W. J. Casteel, Jr., G. Lucier, R. Hagiwara, H. Borrmann and N. Bartlett, *J. Solid State Chem.*, **96**, 84 (1992).

6 J. H. Canterford and R. Colton, "*Halides of the Second and Third Row Transition Metals*," John Wiley & Sons Ltd., (1968).

7 R. Bougon, T. Bui Huy and P. Charpin, *Inorg. Chem.*, **14**, 1822 (1975).

8 W. W. Wilson and K. O. Christe, *Inorg. Chem.*, **20**, 4139 (1981).

9 J. H. Holloway, G. J. Schrobilgen and P. Taylor, *J. Chem. Soc., Chem. Commun.*, 40 (1975).

10 J. M. Shreeve, "*Inorganic Synthesis*," John Wiley & Sons Inc., **24**, 37 (1986).

11 K. Nakamoto, "*Infrared and Raman Spectra of Inorganic and Coordination Compounds*," 4th ed., John Wiley & Sons (1986).

12 C. Shen, *Ph. D. thesis of University of California, Berkeley* (1992).

13 B. Žemva, R. Hagiwara, W. J. Casteel, Jr., K. Lutar, A. Jesih and N. Bartlett, *J. Am. Chem. Soc.*, **112**, 4846 (1990).

14 D. Gantar, I. Leban, B. Frlec and J. H. Holloway, *J. Chem. Soc. Dalton Trans.*, 2379 (1987).

15 B. F. Hoskins, A. Linden and T. A. O' Donnell, *Inorg. Chem.*, **26**, 2223 (1987).

CHAPTER 4

Reaction of silver fluoride and uranium hexafluoride in anhydrous hydrogen fluoride*

4.1 Introduction

Uranium hexafluoride is expected to be a powerful fluorinating agent if one notes the first U-F bond dissociation energy (143 kJ mol^{-1}[1]) is lower than F-F bond energy. In fact, UF_6 fluorinates SO_3 in gas phase to give $S_2O_6F_2$ like F_2 and XeF_2[2], which is a good example of the fluorination power of it.

For the fluorination reaction in solution, water is not a suitable solvent because UF_6 reacts with it to give UO_2F_2. The highest oxidation state of uranium, 6+, is stable in the form of uranyl ion, UO_2^{2+}, in aqueous solution. Liquid anhydrous hydrogen fluoride (HF) is one of the best candidates as solvents since it is stable against strong oxidizers, and one can avoid formation of stable uranyl ions. This chapter demonstrates the oxidizing power of UF_6 in HF which is able to fluorinate the cationic Ag(I) to Ag(II) at ambient temperature and clarify the reaction mechanism.

4.2 Reagents

AgF was prepared as described in Chapter 3. UF_6 was prepared by fluorinating UO_2 (Furukawa Denki Kogyo, depleted uranium) in a nickel metal reaction vessel at around 500°C, and distilled into a Monel metal container after evacuating volatile gases at 0°C for a while. UF_5 (β-form) was prepared by irradiating UV light of a mercury lamp (Hitachi UM-102) on a gaseous mixture of UF_6 and carbon monoxide (Takachiho

---

* Published in *Eur. J. Solid State Inorg. Chem.*, **32**, 283 (1995).

Kagaku Kogyo, spectroscopic grade) in a Pyrex glass bulb. $AgFBF_4$ was prepared by fluorinating $AgBF_4$ prepared by the interaction of AgF and BF_3 in liquid hydrogen fluoride[3]. Hydrogen fluoride (Daikin Kogyo, purity 99 % or more) was dried over K_2NiF_6 (Ozark-Mahoning) to remove trace amount of water. Fluorine (Daikin Kogyo, purity, 99.7 %) and xenon (Teisan K. K., purity 99.995 % or more) were used as supplied. No impurities were detected by IR spectroscopy in the gaseous samples (~200 mm Hg) transferred to a gas cell with silver chloride windows. The purity of the solid materials was checked by X-ray powder diffraction.

4.3 Results

$AgF + UF_6$ in HF (interacted overnight)

UF_6 (>10 mmol) was condensed over AgF (4.54 mmol) with HF (~4 cm^3) in an FEP tube at –196°C. At room temperature, a saturated colorless solution was formed with a colorless precipitate of UF_6 at the bottom of the reaction tube. After starting agitation of the solution with a stirring bar for a few minutes, a red solid gradually precipitated from the solution. The color of the precipitate slowly turned dark brown. The bubbling almost ceased after overnight reaction. Volatile materials in the tube were all condensable at -196°C. The weight uptake of the product indicates that 2 moles of AgF reacts with 1 mole of UF_6. Elemental analyses of Ag and U of the product agreed with this result (obsd., Ag: 36.4, U: 39.4, F(the rest): 24.2 wt%, calcd., Ag: 35.6, U: 39.3, F: 25.1 wt%). The X-ray powder diffraction detected a cubic phase (a_0 = 8.513 Å, see Table 4-1) in addition to AgF_2[4] and $AgUF_6$[5] in the product.

$AgF + UF_6$ in HF (interacted for 20 minutes)

In the one end of a T-shaped FEP tube (Tube A), AgF (1.48 mmol) dissolved in HF (~2 cm^3) was interacted with UF_6 (2.7 mmol) to give a colorless solution. After

starting the agitation of the solution with a stirring bar for a few minutes, a red solid gradually precipitated from the solution. After 20 minutes of stirring, the solution was decanted to the side tube (Tube B). From the solution in Tube B, a white solid precipitated which gradually turned yellow by evacuation. All the lines in the X-ray diffraction powder pattern of the precipitate in Tube A were ascribed to those of AgF[6], AgF_2[4], $AgUF_6$[5] and the cubic phase identified above. Only AgF was detected from the powder pattern of the yellow solid remained in Tube B.

$Xe + AgF + UF_6$ in HF

AgF (4.8 mmol) and UF_6 (7.3 mmol) were condensed with HF (~4 cm^3) to prepare a saturated solution. Xenon gas was introduced in the tube (the total pressure was around 1.4 atm at room temperature). A red solid gradually precipitated from the solution as in the case of the reaction without xenon. The color of the precipitate changed to dark brown after overnight reaction. The solution was always stirred during the reaction. A week later, the volatile materials (the total pressure was unchanged from the beginning of the reaction) were evacuated at 0°C after sampling a part of it for IR measurement. X-ray powder diffraction detected only AgF_2[4] and $AgUF_6$[5] in this solid. Only HF and UF_6 were observed in IR spectra of the volatile materials. From the weight uptake, the Ag / U ratio of the residual solid was two, the same as in the case without supplying xenon.

$AgFBF_4$ + UF_5 (β-form) in HF

$AgFBF_4$ (0.913 mmol) was interacted with β-UF_5 (0.901 mmol) in liquid HF (~2 cm^3) at room temperature. A gas evolution was observed during the reaction. IR spectroscopy detected UF_6 from the volatiles. A significant weight loss (302 mg, 0.86 mmol, assuming only UF_6 was released) was observed after evacuation. X-ray powder diffraction of the residual solid detected $AgBF_4$[7] and unreacted β-UF_5[8].

Decomposition of the reaction product

The reaction product of AgF + UF_6 sealed in a quartz glass capillary in which the cubic phase was detected by X-ray diffraction was kept at room temperature over a month. In the X-ray diffraction powder pattern, the cubic phase disappeared and only the AgF_2[4] and $AgUF_6$[5] were observed. No evolution of UF_6 was confirmed on the same sample of a large quantity kept in a sealed Pyrex glass ample. UF_6 was not collected by cooling the one end of the tube at liquid nitrogen temperature. About 1 g of the sample was put in water (2 cm^3) in a FEP test tube. A gas evolution occurred from the green solution formed.

4.4 Discussion

The ionization potential of $Ag^+(g)$ (21.49 eV[3]) is the highest of all the singly charged metal cations except alkaline metals. Fluorinations of AgF by strong fluorinating agents such as F_2[9], XeF_2[10], ClF_3[10] and BrF_3[11], using HF or themselves as solvents, all failed at ambient temperature. The calculated free enthalpy changes of these reactions are large negative values[12]. The failure of the reactions should have some kinetic reasons. A possible explanation is that these fluorinating agents are all strong electrophiles and cannot effectively attack cations in solution.

In HF, 2 moles of AgF reacts with 1 mole of UF_6 as follows.

$$2AgF + UF_6 \rightarrow AgF_2 + AgUF_6 \qquad (1)$$

The free enthalpy change of this reaction has been calculated to be -67 ± 15 kJ mol^{-1}[12]. When UF_6 is interacted with HF solution saturated with AgF, a red solid precipitates in the beginning which gradually turns dark brown. Although the formation of AgF_2 was denied in the earlier work[10], we confirmed the existence in the product of every run in experiments by X-ray powder diffraction (Table 4-1).

Table 4-1 X-ray powder data for the reaction product of AgF and UF_6.

Intensity	d Å	$10^4/d^2$ $Å^{-2}$ (obs.)	hkl $AgUF_6$	$10^4/d^2$ $Å^{-2}$ (calc.)	hkl AgF_2	$10^4/d^2$ $Å^{-2}$ (calc.)	hkl Ag_2UF_8	$10^4/d^2$ $Å^{-2}$ (calc.)
vw	6.025	275					110	276
m	5.455	336	100	337				
vw	5.113	383					111	414
m	4.264	550					200	552
vw	3.999	625	002	628				
s	3.858	672	110	674			210	690
vw	3.487	822	111	831			211	828
s	3.233	956	102	965				
m	3.131	1020			111	1014		
vvw	3.017	1098					220	1104
vw	2.907	1183			200	1187		
vw	2.759	1314	112	1302	020	1314		
w	2.717	1355	200	1348			310	1380
vw	2.566	1519					311	1518
vw	2.439	1681	210	1685			222	1656
m	2.309	1876	211	1842				
w	2.209	2049	113	2087				
vw	2.130	2204					400	2208
s	2.082	2307	212	2313			322 401	2346
w	2.000	2500	004	2512	220	2495	411 330	2484
vw	1.960	2603					331	2622
m	1.921	2710	220	2696				
w	1.897	2832	221 104	2853 2849	022	2863		
w	1.810	3052	300	3033			332	3036
m	1.775	3174	114	3186				
m	1.727	3353	310 222	3370 3324	311	3380		
vvw	1.665	3607			131	3629		
vw	1.648	3682	302	3661				
vw	1.614	3839	204 321	3860 3860				
vw	1.579	4011	312	3998				
vw	1.565	4083			133	4120		

$AgUF_6$: a_0 = 5.4491(8), c_0 = 7.9704(12) Å; space group, $P4_2/mcm$[5].
AgF_2 : a_0 = 5.813, b_0 = 5.529, c_0 = 5.073 Å; space group, Pbca[4].
Ag_2UF_8 : a_0 = 8.513 Å, cubic.

When the reaction product is interacted with water, oxygen evolution and disproportionation of the U(V) to U(VI) and U(IV) are observed.

$$4AgF_2 + 2H_2O \rightarrow 4Ag^+ + 4H^+ + 8F^- + O_2\uparrow \quad (2)$$

$$2AgUF_6 + 2H_2O \rightarrow 2Ag^+ + UO_2^{2+} + UF_4 + 4H^+ + 8F^- \quad (3)$$

In addition to AgF_2 and $AgUF_6$, a cubic phase (a_0 = 8.513 Å) exists in the reaction product as shown in Table 4-1. This phase disappears slowly from the reaction product kept in a sealed quartz glass tube.

The solubility of UF_6 in HF is about 0.5 M and Raman bands of UF_6 in the solution are almost unchanged from those of pure material[13], suggesting that the following equilibria[14] shift to the left side.

$$3HF \rightleftharpoons H_2F^+ + HF_2^- \quad (4)$$

$$UF_6 + HF_2^- \rightleftharpoons UF_7^- + HF \quad (5)$$

When a fluorobase is dissolved in HF, the concentration of bifluoride ion is increased according to the following equilibrium.

$$MF + HF \rightleftharpoons M^+ + HF_2^- \quad (6)$$

Therefore the concentration of UF_7^- is also increased according to eq. 5. In the present study, the solubility of UF_6 is remarkably increased by dissolving AgF which acts as a fluorobase in HF. It has been reported that UF_8^{2-} ion is also formed in the basic condition[14].

$$UF_7^- + HF_2^- \rightleftharpoons UF_8^{2-} + HF \quad (7)$$

It is considered that the red solid formed at the beginning of the reaction is a metastable complex salt of AgF and UF_6 which decomposes to AgF_2 and $AgUF_6$. While the hepta- and octafluorouranates (VI), MUF_7 and M_2UF_8 (M = Na, K, Rb, Cs, NO, NH_4), have been identified by X-ray diffraction[14,15], no structural informations are available for $AgUF_7$ or Ag_2UF_8. If $AgUF_7$ is this intermediate phase, the decomposition would proceed as follows.

$$2AgUF_7 \rightarrow AgF_2 + AgUF_6 + UF_6 \quad (8)$$

In case that Ag_2UF_8 is the intermediate phase, the decomposition reaction would occur without the evolution of UF_6.

$$Ag_2UF_8 \rightarrow AgF_2 + AgUF_6 \qquad (9)$$

Actually no evolution of UF_6 was observed from the reaction product sealed in a Pyrex glass ample. It is concluded that the red precipitate is Ag_2UF_8 which is insoluble in HF and decomposes to AgF_2 and $AgUF_6$. The oxidation of cationic Ag(I) to Ag(II) is considered to be accomplished through the nucleophilic attack of the fluorouranate (VI) anion. Isolation of $AgUF_7$ attempted by evacuating the HF quickly just before Ag_2UF_8 precipitates failed.

In Fig. 4-1 the formula volumes of several fluorouranates of monovalent metals are plotted against the cationic radii[14,15,16]. In the region where cationic radius exceeds

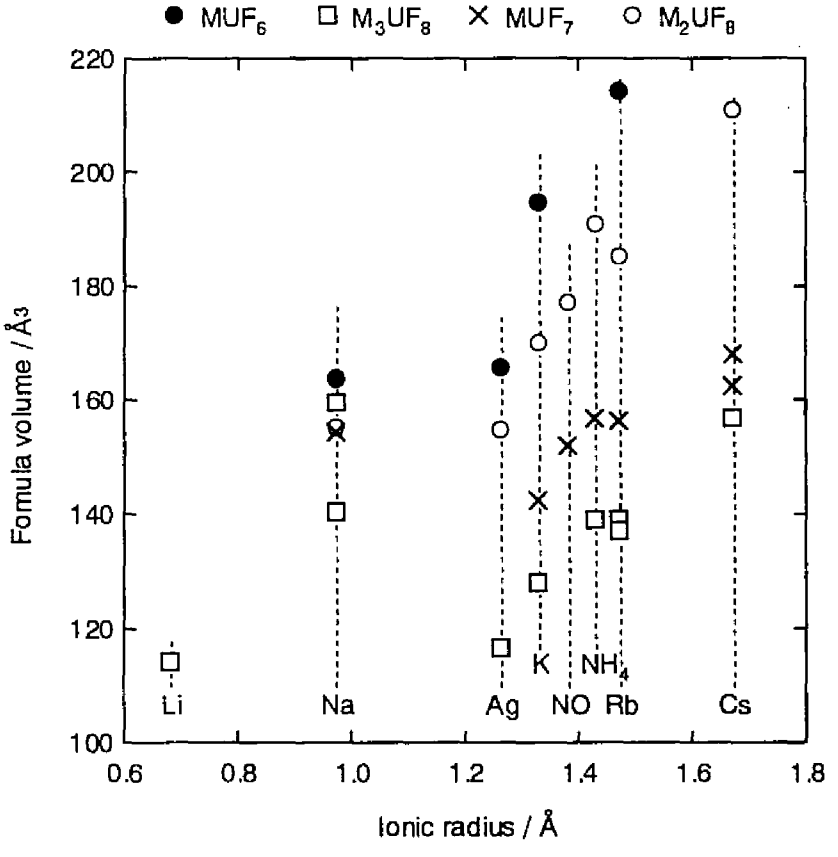

Fig. 4-1 Relations between the formula volume of some M_xUF_y complex salts and ionic radius of M^+.

1.2 Å, linear relationships exist between these parameters for these penta- and hexavalent fluorouranates including Ag_2UF_8. Formula volumes of all the sodium fluorouranates deviate from this tendency taking similar sizes regardless of the types of complex salts. This is probably due to the large differences in sizes between the sodium ion and fluorouranate anions which prevent the effective close packing of the cations and anions.

The instability of Ag_2UF_8 prevented from obtaining a good X-ray powder pattern enough to refine the structure. So, here, the discussion will be limited to preliminary model structures constructed as follows. First of all, the lattice volume approximately corresponds to four times that of the formula unit. Miller indices of X-ray diffraction lines identified as those of Ag_2UF_8 are all even or odd reflections except 110 line. Therefore, the heavy atoms, silver and uranium, are presumably located on, or, at least closely to the special positions which satisfy a face-centered symmetry. Assuming UF_8^{2-} anion is spherical, it must be closely packed in the cubic lattice. From these requirements, it is automatically derived that the uranium positions must be (0, 0, 0) and (1/2, 1/2, 0) in a cubic lattice. Another heavy atom, silver should be placed at the interstitial sites of UF_8^{2-} anions such as (1/4, 1/4, 1/4) to fulfill the stoichiometry and face-centered symmetry. There is a possibility that it is slightly shifted from the special position without

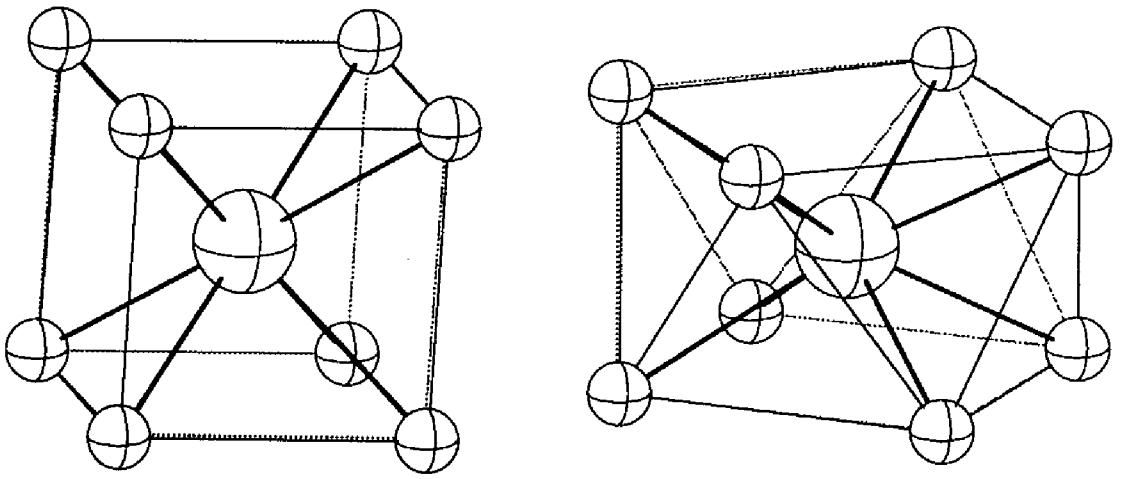

(a) Cubic (b) Square antiprism

Fig. 4-2 Geometries of octa-coordinated UF_8^{2-} anion.

significantly changing the peak intensities in the powder pattern. From these facts, the crystal structure of Ag_2UF_8 is reasonably concluded to be closely related to an inverse fluorite type. From the requirement of cubic symmetry of the lattice, at least UF_8^{2-} at (0, 0, 0) should possess a cubic geometry although it is slightly less stable than the square antiprism (D_{4d})[17] (Fig. 4-2). The cubic geometry has been found in $M_3U^{V}F_8$ complex salts[18] while it has been only proposed in $Na_2U^{VI}F_8$ from the results of vibrational spectroscopy[14]. Consequently, it was revealed that the possible space groups are limited to $Pm\bar{3}m$, P432 and $Pm\bar{3}$.

The optimized positional parameters of the Ag_2UF_8 structure for each space group are listed in Table 4-2. Here the geometry of UF_8^{2-} is assumed to be cubic or square

Table 4-2 Space groups and positional parameters of the models of Ag_2UF_8.

$Pm\bar{3}m$				P432				$Pm\bar{3}$			
Atom	*x*	*y*	*z*	Atom	*x*	*y*	*z*	Atom	*x*	*y*	*z*
Ag(8g)	0.3004	0.3004	0.3004	Ag(8g)	0.3712	0.3712	0.3712	Ag(8i)	0.2830	0.2830	0.2830
F1(8g)	0.1424	0.1424	0.1424	F1(8g)	0.1424	0.1424	0.1424	F1(8i)	0.1424	0.1424	0.1424
F2(24l)	0.5000	0.2985	0.1424	F2(24k)	0.4165	0.2984	0.1150	F2(12j)	0.3576	0.2986	0.0000
U1(1a)	0.0000	0.0000	0.0000	U1(1a)	0.0000	0.0000	0.0000	F3(12k)	0.5000	0.2014	0.3576
U2(3c)	0.5000	0.5000	0.0000	U2(3c)	0.5000	0.5000	0.0000	U1(1a)	0.0000	0.0000	0.0000
								U2(3c)	0.5000	0.5000	0.0000
Interatomic distances / Å				Interatomic distances / Å				Interatomic distances / Å			
Ag - F1		2.330		Ag - Ag		2.193		Ag - F1		2.073	
Ag - F2		2.167		Ag - F2		2.300		Ag - F2		2.495	
F1 - F1		2.425		Ag - F2		2.900		Ag - F3		2.073	
F1 - U1		2.100		F1 - F1		2.425		F1 - F1		2.425	
F2 - F2		1.879		F1 - F2		2.695		F1 - F2		2.568	
F2 - F2		2.425		F1 - U1		2.100		F1 - U1		2.100	
F2 - U2		2.101		F2 - F2		2.420		F2 - F2		2.425	
				F2 - F2		2.626		F2 - F3		2.425	
				F2 - F2		2.627		F2 - U2		2.100	
				F2 - U2		2.100		F3 - F3		2.425	
								F3 - U2		2.100	

Lattice parameter : a_0 = 8.513 Å.

antiprismatic and U-F bond length to be 2.1 Å which is slightly longer than that in UF_6 (1.994 Å[16]). The schematic illustrations of these models are shown in Fig. 4-3 (a)-(c). All the geometries of UF_8^{2-} anions must be cubic in both $Pm\bar{3}m$ and $Pm\bar{3}$ from requirement of the symmetry. In P432 lattice, UF_8^{2-} at the face center is allowed to take square antiprism geometry. In this geometry, two squares of the fluorine atoms in UF_8^{2-} are staggered to each other taking closer approach due to the decrease of repulsion. The position of silver atom was determined to maximize the distance between silver and fluorine atoms.

From the calculation of the interatomic distances in each model, the possibility of the $Pm\bar{3}m$ model is ruled out by the too small distance between the fluorine atoms (24l) from adjacent two UF_8^{2-} anions at the face-centered positions (F2-F2, 1.879 Å). These fluorine atoms are apart enough in P432 and $Pm\bar{3}$ models. In the $Pm\bar{3}$ model, Ag-F distances are optimized to be 2.073 and 2.495 Å, the former being smaller than the sum of the ionic radii of silver and fluoride ions. On the other hand, silver and fluorine atoms are well separated in the P432 model. However, the structure is not acceptable because eight silver atoms (8g) are too closely gathered in the center of the cell. Therefore the $Pm\bar{3}$ model is concluded to be the best candidate for a structure of Ag_2UF_8.

If the $Pm\bar{3}$ model structure is correct, there should be appreciable covalent character between silver and fluorine atoms which explains the shorter bond length. The bond length, 2.073 Å, estimated in this model is close to that typical for covalent compounds (e.g. 2.07 Å for AgF_2[4]). The oxidation of Ag(I) to Ag(II) might occur through ligand-bridged (inner sphere) mechanism in which "active complex," $(Ag\text{-}F\text{-})_2UF_6$, rearranges to AgF_2 and $AgUF_6$.

Figure 4-4 shows a preliminary simulation of X-ray powder profile for the $Pm\bar{3}$ model. The observed lines are marked with open circles on them. The simulation was made by RIETAN program[19] assuming the isotropic thermal parameters of 1.0 for uranium and silver atoms and 2.0 for fluorine atoms. The intensity of (100) line was not

(a) $Pm\bar{3}m$

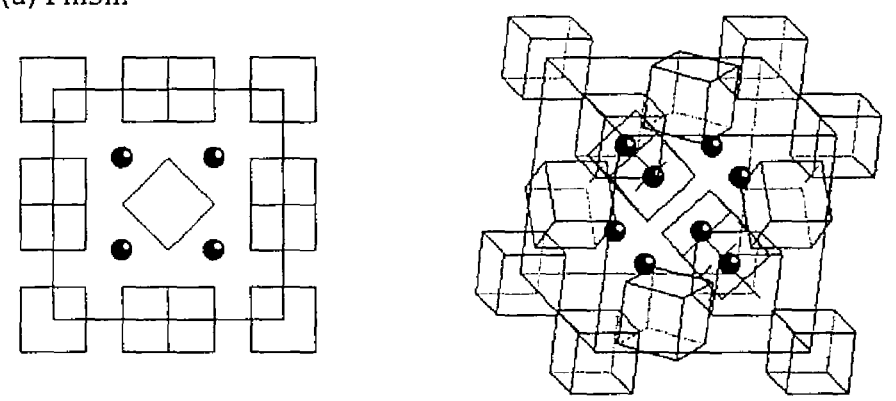

(b) P432

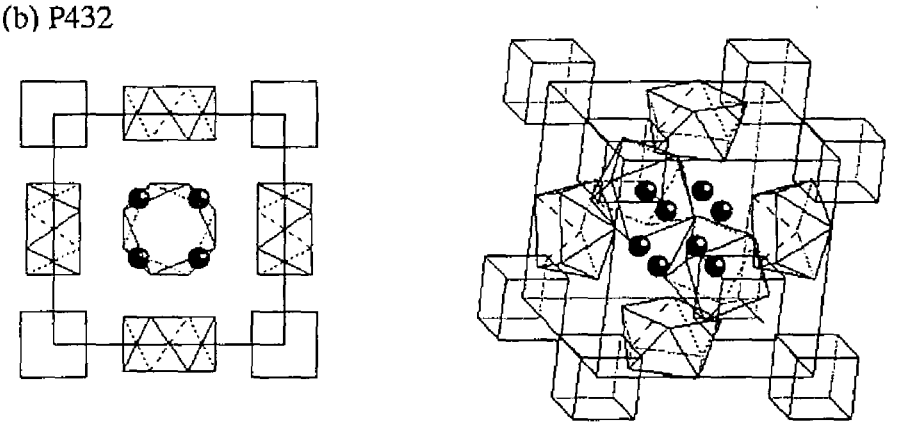

(c) $Pm\bar{3}$

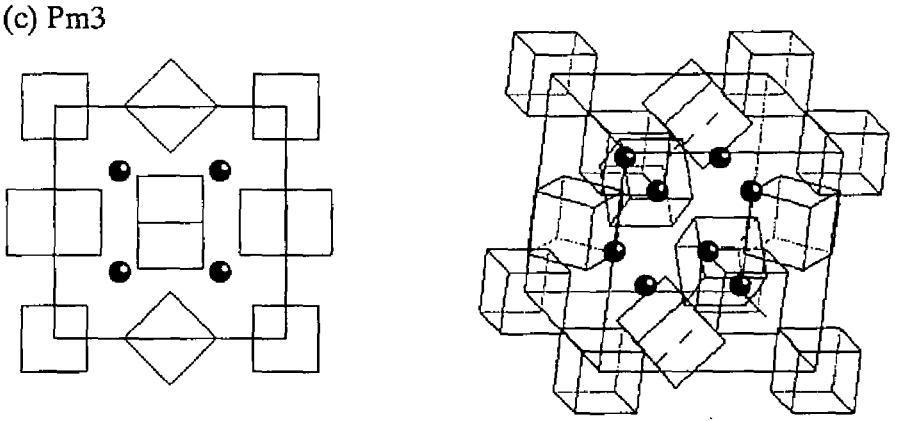

Fig. 4-3 Examined crystal structure models of Ag_2UF_8.

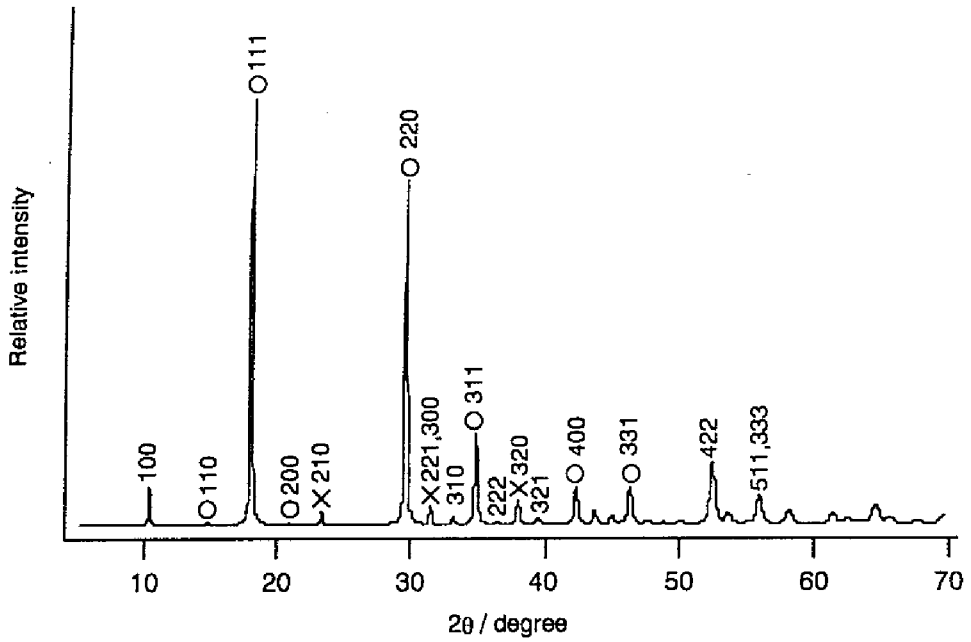

Fig. 4-4 Simulated X-ray powder profile of Ag_2UF_8 assuming the $Pm\bar{3}$ model. The peaks with open circles are observed by X-ray diffraction. Peaks with X should overlay with those of $AgUF_6$ and AgF_2.

collected in the pattern due to the geometrical limitation of the powder camera. The matching of the relative peak intensities in the observed and simulated patterns are not good enough. A further examination to obtain a better powder pattern profile is necessary for determination of the detailed structure of Ag_2UF_8.

The direct fluorination of xenon by UF_6 is thermodynamically unfavorable. The fluorination reaction of xenon by UF_6 in AgF solution of HF was examined since the free enthalpy change of the following reaction is calculated to be -16 ± 20 kJ mol^{-1}.

$$2AgF + 2UF_6 + Xe \rightarrow XeF_2 + 2AgUF_6 \qquad (10)$$

The formation of XeF_2 was however, not actually observed at ambient temperature. It is not clear that the failure of this reaction is due to whether a thermodynamic or kinetic reason. From this result, the possibility of the formation of Ag(II)-U(VI) complex salt

like $AgFUF_7$ or $AgUF_8$ from AgF_2 and UF_6 is also denied since the cationic Ag(II) oxidizes xenon to Xe(II) in HF[3,7,8]:

$$AgF_2 + UF_6 \not\rightarrow AgFUF_7 \text{ or } AgUF_8 \qquad (11)$$

The fluoride ion affinity of UF_6 would be too low to stabilize the AgF^+ or Ag^{2+} ion. Although the fluoride ion affinity of the UF_5 is much higher than UF_6, U(V) is easily oxidized to U(VI) by cationic Ag(II) in HF.

$$AgFBF_4 + UF_5 \rightarrow AgBF_4 + UF_6 \qquad (12)$$

So it is obvious that the formation of the Ag(II)-U(V) complex salt such as $AgFUF_6$ or $AgUF_7$ does not occur.

References

1 F. Weigel, "*The Chemistry of Actinide Elements,*" Vol. 1, Chapt. 5, *Uranium*; J. J. Katz, G. T. Seaborg and L. R. Morss, Ed., Chappman and Hall Ltd, 314 (1986).

2 N. Bartlett and F. O. Sladky, "*Comprehensive Inorganic Chemistry,*" Vol. 1, Chapt. 6, *The Chemistry of Krypton, Xenon and Radon*, Pergamon Press, Oxford and New York, 213, (1973).

3 B. Žemva, R. Hagiwara, W. J. Casteel, Jr., K. Lutar, A. Jesih and N. Bartlett, *J. Am. Chem. Soc.*, **112**, 4846 (1990).

4 P. Charpin, P. Plurien and P. Mériel, *Bull. Soc. Franc. Mineral Crist.*, **93**, 7 (1970).

5 R. Bougon and P. Plurien, *C. R. Acad. Sci. Paris*, **260**, 4217 (1965); P. Charpin, *C. R. Acad. Sci. Paris*, **260**, 1914 (1965)

6 N. P. Galkina ed., "*Osnovnye Svojstva Neorganicheskih Ftoridov,*" Moskva Atomizdat, (1976).

7 D. W. A. Sharp and A. G. Sharpe, *J. Chem. Soc.*, 1855 (1956).

8 R. R. Ryan, R. A. Penneman, L. B. Asprey and R. T. Paine, *Acta Cryst.*, **B32**, 3311 (1976).

9 N. Bartlett, W. J. Casteel Jr. and R. Hagiwara, unpublished results.

10 J. G. Malm, *J. Fluorine Chem.*, **23**, 267 (1983).

11 I. Sheft, H. H. Hyman and J. J. Katz, *J. Am. Chem. Soc.*, **75**, 5221 (1953).

12 P. A. O'hare and J. G. Malm, *J. Chem. Thermodynamics*, **16**, 753 (1984).

13 B. Frlec, H. H. Hyman, *Inorg. Chem.*, **6**, 1596 (1967).

14 R. Bougon, P. Charpin, J. P. Desmoulin and Malm, *Inorg. Chem.*, **15**, 2532 (1976).

15 J. G. Malm, H. Selig and S. Siegel, *Inorg. Chem.*, **5**, p. 130 (1966).

16 D. Brown, "*Halides of the Lanthanides and Actinides,*" Chapt. 2, *Fluorides and*

Oxyfluorides, John Wiley & Sons Ltd., (1968) and references contained therein.

17 D. L. Kepert, *Inorganic Stereochemistry*, Springer, Berlin (1982).

18 W. Rüdorff and H. Leutner, *Ann. Chemie.*, 632, 1 (1960).

19 F. Izumi, "*The Rietveld Method*," edited by R. A. Young, Oxford University Press, Oxford (1993), Chap. 13; Y.-I. Kim and F. Izumi, *J. Ceram. Soc. Jpn.*, **102**, 401 (1994).

CHAPTER 5

Reactions of uranyl fluoride with some fluorobases in anhydrous hydrogen fluoride*

5.1 Introduction

Uranyl fluoride (UO_2F_2) is an ionic compound containing a uranyl cation (UO_2^{2+}), surrounded by 6 fluoride ions with a distance of 2.50 Å. Some complex ions, $UO_2F_{2+n}^{n-}$ (n = 1, 2, 3), have been found by spectroscopic measurements in aqueous solutions of UO_2F_2 containing a fluorobase such as KF[1]. In fact, the concentration of fluoride ion in the aqueous solution of UO_2F_2 is unable to be measured precisely by a fluoride ion selective electrode because of the complex formation.

Anhydrous MUO_2F_3 and $M_3UO_2F_5$ (M : singly charged metals) are obtained from their hydrates prepared in aqueous solution[2]. The structure of $UO_2F_5^{3-}$ ion in $M_3UO_2F_5$ (M = K, NH_4 and Cs) has been reported. On the other hand, $UO_2F_3^-$ ion in MUO_2F_3 (M = Cs) has not been characterized. Double salts, $K_3(UO_2)_2F_7$ and $K_5(UO_2)_2F_9$, also have been prepared in aqueous solution[2]. The reaction of UO_2F_2 and silver(I) fluoride (AgF) in acetone has been found to form $Ag(UO_2)_2F_5$[3].

In this chapter, fluoroacidity of UO_2F_2 is discussed based on the results on the reactions with alkaline metal fluorides and AgF in anhydrous hydrogen fluoride (HF). The compounds obtained were characterized by X-ray powder diffraction and vibrational spectroscopy.

---

* Published in *J. Fluorine Chem.*, Vol. **74**, No. 1, 89 (1995).

5.2 Reagents

AgF was prepared in the same manner as described in Chapter 3. CsF (Nakarai Tesque, extra pure reagent) and KF (Wako Chemicals, purity 98% or more) were dried under vacuum at ~300°C. U_3O_8 was obtained by heating UO_2 (Furukawa Denki Kogyo, depleted uranium) in an alumina crucible in air at ~800°C. UO_2F_2 was prepared by fluorinating U_3O_8 in a Monel container at 200°C.

5.3 Results

$CsF + UO_2F_2$

CsF (176 mg, 1.16 mmol) and UO_2F_2 (355 mg, 1.15 mmol) were interacted in HF (~1 cm^3) at room temperature. On stirring for several hours, a pale yellow solid was obtained after evacuating volatile materials at room temperature. A small weight uptake (26 mg, 1.3 mmol as HF) was observed. The X-ray powder pattern of the solid obtained after successive evacuation at ~70°C was identical with that of $CsUO_2F_3$ prepared in aqueous solution[4]. The Raman spectrum of $CsUO_2F_3$ could not be obtained due to the strong fluorescence of the sample.

$KF + UO_2F_2$

KF (32 mg, 0.55 mmol) and UO_2F_2 (172 mg, 0.56 mmol) were interacted in HF (~1 cm^3) at room temperature. After stirring for several hours, a light green solid was obtained after evaporating HF very slowly. X-ray diffraction showed that the solid was a mixture of $K_3UO_2F_5$[5] and UO_2F_2. The Raman spectrum of $K_3UO_2F_5$ could not be obtained due to the strong fluorescence of the sample.

$AgF + UO_2F_2$

AgF (35 mg, 0.28 mmol) and UO_2F_2 (85 mg, 0.28 mmol) were interacted in HF at room temperature. A light yellow solid was obtained after stirring for 20 hours. No weight uptake was observed after removing volatile materials. X-ray diffraction showed no peaks corresponding to the starting materials. The solid is considered to be the 1 : 1 compound of AgF and UO_2F_2 by the vibrational spectra of the solid.

$3AgF + UO_2F_2$

AgF (233 mg, 1.84 mmol) and UO_2F_2 (189 mg, 0.614 mmol) were loaded in one arm (Tube A) of a T-shaped reactor and interacted in HF (~ 2 cm^3) at room temperature. After stirring for several hours, the supernatant solution over the precipitate was decanted to Tube B and the precipitate was washed several times with HF which was condensed back to Tube A. A light yellow solid in Tube A was obtained by removing volatile materials and a colorless solid in Tube B was crystallized from the solution used for washing the precipitate. The color of the solid turned to bright yellow by the additional evacuation while warming Tube B. X-ray diffraction showed that the solid in Tube A was the mixture of UO_2F_2 and the 1 : 1 compound obtained by the interaction of AgF + UO_2F_2. The solid in Tube B was only AgF.

Excess $AgF + UO_2F_2$

UO_2F_2 (145 mg, 0.471 mmol) was placed in one arm (Tube A) of a T-shaped reactor and AgF (654 mg, 5.15 mmol) in the other arm (Tube B). HF (~1 cm^3) was condensed in Tube B to prepare a saturated solution of AgF with a trace amount of white precipitate. The solution was decanted to Tube A and the mixture was stirred for several hours. The supernatant solution was decanted to Tube B. In Tube A, a bright yellow solid was obtained after evacuating HF with heating so as to decompose $Ag(HF)_nF$. X-ray diffraction showed that the solid in Tube A was a mixture of AgF and the 1 : 1 compound

of AgF and UO_2F_2 and that the solid remained in Tube B was only AgF.

5.4 Discussion

UO_2F_2 acts as a fluoroacid to give some compounds with MF (M : univalent metal) in aqueous solutions[2]. The anhydrous 1 : 1 compound prepared so far is only $CsUO_2F_3$[4] the structure of which has not yet been determined. The existence of the complex anion, $UO_2F_3^-$, has not been claimed in the solid state although it was identified in the gaseous phase by Knudsen' s effusion method in combination with mass-spectrometry[6] and in the solution by Raman spectroscopy[1]. The formation of some oxofluorocomplex anions is expected in $M_3UO_2F_5$ and MUO_2F_3 since the uranium atom in UO_2^{2+} is coordinated by ligands forming strong bonds with some covalency[7]. In fact, the anhydrous 3 : 1 compounds, $M_3UO_2F_5$ (M = K, Cs and NH_4), are well characterized and a pentagonal bipyramidal anion, $UO_2F_5^{3-}$, was found in $K_3UO_2F_5$[5]. In this anion, five fluorine atoms coordinate to uranium atom within the plane perpendicular to the linear O-U-O axis to form a regular pentagon (Fig 5-1).

In the reaction of equimolar amounts of CsF and UO_2F_2 in HF, the solvated salt, $CsUO_2F_3 \cdot nHF$, seems to be formed like the hydrate prepared from the aqueous solution.

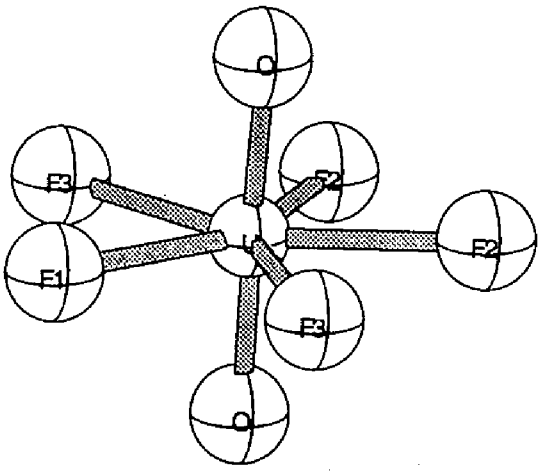

Fig. 5-1 Dioxopentafluorouranate anion in $K_3UO_2F_5$.

This compound loses HF at ~ 70°C to give $CsUO_2F_3$. On the other hand, the reaction of equimolar amounts of KF and UO_2F_2 in HF does not give the 1 : 1 compound, KUO_2F_3, but the mixture of $K_3UO_2F_5$ and unreacted UO_2F_2.

A novel 1 : 1 compound, $AgUO_2F_3$, is formed by the reaction of equimolar amounts of AgF and UO_2F_2 in HF. The X-ray powder pattern of $AgUO_2F_3$ is shown in Table 5-1. It is suggested that $AgUO_2F_3$ contains some oxofluoroanions from the vibrational spectra as shown in Fig. 5-2 and Table 5-2. If the uranium were present only in the form of bare cationic UO_2^{2+}, a single peak around 900 cm^{-1} should be observed in the Raman spectrum. The possibility of formation of a double salt containing UO_2^{2+} is excluded from the spectrum of the sample.

$AgUO_2F_3$ is solvolized by washing with HF:

$$AgUO_2F_3 + nHF = Ag^+ + (HF)_nF^- + UO_2F_2 \qquad (1)$$

In order to obtain a pure sample of $AgUO_2F_3$, it is necessary to remove HF very slowly from the system to shift the equilibrium to the left. The growth of a single crystal is

Table 5-1 X-ray powder diffraction pattern of $AgUO_2F_3$.

d / Å	Intensity	*d* / Å	Intensity
9.32	w	2.52	w
7.73	w	2.42	mw
5.47	w	2.15	mw
4.96	vw	2.09	w
4.14	vw	2.01	ms
3.99	w	1.97	m
3.77	m	1.95	w
3.70	m	1.88	m
3.29	m	1.84	m
3.07	s	1.82	w
2.93	w	1.78	w
2.66	mw	1.72	mw
2.62	mw	1.70	w

Abbreviations used: s, strong; m, medium; v, very; w, weak.

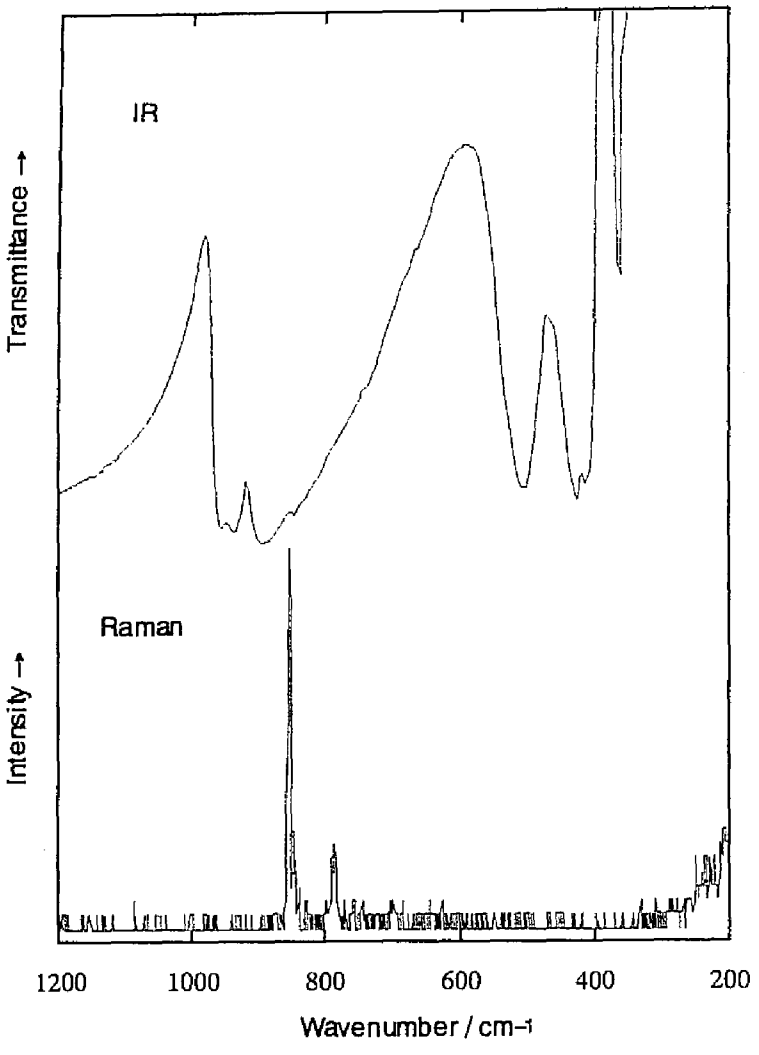

Fig. 5-2 Vibrational spectra of $AgUO_2F_3$.

practically impossible in HF due to the low solubility of $AgUO_2F_3$.

The reaction of CsF with UO_2F_2 gives both the 3 : 1 and 1 : 1 compounds in aqueous solution, however, only the latter being formed in HF. Only the 3 : 1 compound is formed by the reaction of KF and UO_2F_2 in both the solutions. The reaction of AgF and UO_2F_2 in HF provides only the 1 : 1 compound even in HF saturated with AgF. These observations cannot be explained by the simple comparative chemistry of the stability of ionic salts.

The fluoroacidity of UO_2F_2 in HF does not seem to be exceedingly higher than that

of HF due to the low solubility as expected from its fluoride ion affinity slightly higher than that of HF[6,8]. The stabilities of the compounds of UO_2F_2 with strong fluorobases such as MF (M = K, Cs and Ag) are higher than those of $M(HF)_nF$. However, the solvolysis of the compounds seems to occur in excess HF resulting in precipitating UO_2F_2 as observed in the reaction of AgF and UO_2F_2.

Table 5-2 Vibrational spectra of $AgUO_2F_3$. Frequencies are given in cm^{-1}. Abbreviations used: sh, sharp; br, broad; s, strong; m, medium; v, very; w, weak.

Raman	IR
	953ms
	935ms
	894s,br
851s,sh	
784m,sh	
	505m,sh
	425m,sh
	412m,sh
	360w,sh

References

1 C. Nguyen-Trung, G. M. Begun and D. A. Palmer, *Inorg. Chem.*, **31** 5280 (1992).

2 D. Brown, "*Halides of the Lanthanides and Actinides*," John Wiley & Sons Ltd., 33 (1968).

3 I. P. Sokolov, V. P. Seleznev, Yu. Ya. Kharitonov and G. A. Yagodin, Deposited Doc., VINITI 401-79, 7 (1979).

4 L. L. Zaitseva, L. V. Lipis, V. V. Fomin and N. T. Chebotarev, *Russ. J. Inorg. Chem.*, **7**, 795 (1962).

5 Z. B. Mukhametshina, M. L. Kotsar', V. P. Seleznev, A. A. Tsvetkov, B. N. Sudarikov and B. V. Gromov, *Russ. J. Inorg. Chem.*, **18** 696 (1973).

6 I. V. Sidorova, A. T. Pyatenko, L. N. Gorokhov and V. K. Smirnov, *Teplofizaka Vyskikh Temperatur*, **22**, 1120 (1984).

7 J. J. Katz, G. T. Seaborg and L. R. Morss, "*The Chemistry of the Actinide Elements*," Second Ed., Chapman and Hall Ltd. (1986).

8 S. A. Harrell and D. H. McDaniel, *J. Am. Chem. Soc.*, **86** 4497 (1964).

CHAPTER 6

Reactions of uranyl fluoride with some fluoroacids in anhydrous hydrogen fluoride*

6.1 Introduction

Property of uranyl fluoride (UO_2F_2) as a fluoroacid in anhydrous hydrogen fluoride (HF) has been discussed in Chapter 5. UO_2F_2 is an ionic compound containing uranyl cation, UO_2^{2+}. The lattice energy of UO_2F_2, 2315 kJ mol^{-1}[1], is a little smaller than that of barium fluoride (BaF_2, 2352 kJ mol^{-1}[2]). Thus, UO_2F_2 is expected to act as a fluorobase like BaF_2 in HF. However, it has been examined only for the reactions with HF-SbF_5 system[3,4] which is one of the strongest superacids.

Preparation of a mixed valence compound, $U_2O_2F_7$, is expected to be made by the acid-base reaction of UO_2F_2 and UF_5 in HF. $U_2O_2F_7$ has been prepared by the reaction of $U^{VI}O_2F_2$ with $U^{V}F_5$ under ~3 atm of UF_6 atmosphere at 370°C[5]. However, it has not been characterized enough. UF_5 acts as a fluoroacid in HF by forming UF_6^- anion, the fluoride ion affinity (–423 kJ mol^{-1}[6,7]) of which being comparable to that of PF_5. It also acts as a dibasic and tribasic fluoroacid by forming UF_7^{2-} and UF_8^{3-} anions, respectively. The complex salts of UF_5 and some fluorobases have been prepared in HF[8]. On the other hand, UF_5 acts as a fluorobase when it is interacted with strong fluoroacids, such as SbF_5 and AsF_5, forming some adducts, $UF_5.nSbF_5$ and $UF_5.nAsF_5$[9]. It is important to examine the property of UO_2F_2 as a fluorobase in order to clarify the reaction of UO_2F_2 and UF_5.

In this chapter, the properties of UO_2F_2 as a fluorobase in HF are studied by the reactions with some fluoroacids, BF_3, PF_5, TaF_5, GeF_4, AsF_5, BiF_5 and UF_5. The

---

* A part of this chapter was published in *J. Fluorine Chem.*, Vol. **74**, No. 1, 89 (1995).

discussion will be made on the compounds obtained by these reactions.

6.2 Reagents

F_2 (Daikin Kogyo, purity 99.7%), PF_5 (Nippon Sanso), TaF_5 (Ozark-Mahoning), AsF_5 (Matheson) and BF_3 (Nippon Sanso) were used as supplied. GeF_4 was prepared by fluorinating powdered Ge metal in a Monel container at 300°C, and distilled into another container after evacuating volatile gases at -196°C for a while. Antimony pentafluoride (SbF_5, PCR, purity 97 %) was used for reactions by distillation to avoid the contamination of SbF_3. BiF_5 was prepared by fluorination of Bi_2O_3 (Nakarai Tesque, purity 99.9%) and purified by vacuum sublimation at ~70°C. Commercially supplied BiF_5 (Ozark-Mahoning, purity 97%) was also used without further purification. UO_2F_2 was prepared in the same manner as described in Chapter 5. Preparation of β-UF_5 is described in Chapter 4.

6.3 Results

UO_2F_2 + excess AsF_5

UO_2F_2 (190 mg, 0.617 mmol) was interacted with excess AsF_5 in HF (~2 cm^3) at room temperature. UO_2F_2 dissolves immediately to give a yellow solution. On evacuating HF slowly, a yellow-green solid was precipitated. Although a significant weight uptake (81 mg, 0.48 mmol as AsF_5) was observed just after the reaction, X-ray diffraction on the final product showed only the pattern of UO_2F_2.

UO_2F_2 + liquid AsF_5 without HF solvent

UO_2F_2 (244 mg, 0.792 mmol) was placed in a reaction tube and AsF_5 (~1 cm^3) was condensed on it at –77°C. UO_2F_2 was not dissolved in this case. After stirring the mixture

for 2 hours, a green solid was formed. The color of the remaining solid after evacuating excess AsF_5 at –77°C faded and the pressure in the tube increased with elevation of the temperature. The amount of the released gas was estimated to be about 1.3 mmol by tensimetry. IR spectroscopy showed that the gas was pure AsF_5. X-ray diffraction revealed that the residual solid was UO_2F_2.

UO_2F_2 + excess BF_3

UO_2F_2 (447 mg, 1.45 mmol) was interacted with excess BF_3 in HF (~2 cm^3) at room temperature. The color change of the precipitate, gas consumption and weight uptake were not observed. X-ray diffraction identified only UO_2F_2 in the solid.

UO_2F_2 + excess GeF_4

UO_2F_2 (423 mg, 1.37 mmol) was interacted with excess GeF_4 in HF (~2 cm^3) at room temperature. A green precipitate was formed after stirring the liquid for a while. The color of the solid faded on evacuating HF. No weight change was observed after the reaction. X-ray diffraction showed that the residual solid was UO_2F_2.

UO_2F_2 + TaF_5

UO_2F_2 (389 mg, 1.26 mmol) was interacted with TaF_5 (704 mg, 2.55 mmol) at room temperature for ~ 20 hours in HF. Dissolution of UO_2F_2 was not observed during the reaction. X-ray diffraction identified UO_2F_2 and TaF_5 in the solid remained after evacuation of HF.

UO_2F_2 + 2BiF_5

UO_2F_2 (110 mg, 0.357 mmol) was interacted with BiF_5 (209 mg, 0.688 mmol) at room temperature for ~ 20 hours in HF. A yellow green precipitate was formed and the supernatant solution slightly colored yellow. An yellow green solid was obtained after

evacuating HF. No weight change was observed after the reaction. X-ray powder diffraction detected no starting materials.

$UO_2F_2 + BiF_5$

UO_2F_2 (160 mg, 0.519 mmol) and BiF_5 (158 mg, 0.520 mmol) were reacted in HF for ~ 20 hours at room temperature. An yellow green solid was obtained after evacuating HF. No weight change was observed after the reaction. X-ray powder diffraction pattern showed that the solid was the mixture of UO_2F_2 and the compound prepared by the reaction of $UO_2F_2 + 2BiF_5$.

$UO_2F_2 + 3BiF_5$

UO_2F_2 (40 mg, 0.13 mmol) and BiF_5 (111 mg, 0.365 mmol) were reacted in HF for ~ 20 hours at room temperature. An yellow green solid was obtained after evacuating HF. No weight change was observed after the reaction. X-ray powder diffraction showed that the solid was the mixture of BiF_5 and the compound prepared in the reaction of $UO_2F_2 + 2BiF_5$.

$UO_2F_2 + UF_5$

UO_2F_2 (54 mg, 0.18 mmol) and β-UF_5 (54 mg, 0.17 mmol) were reacted in HF for ~ 48 hours at room temperature. No weight change was observed after the reaction. X-ray powder diffraction detected only UO_2F_2 and UF_5.

UO_2F_2 + excess SbF_5

$UO_2F_2.2SbF_5$ was prepared by the following procedures as described in ref. 3: UO_2F_2 (652 mg, 2.12 mmol) was interacted with excess SbF_5 in HF for ~20 hours at room temperature. UO_2F_2 was readily dissolved completely to give a yellow solution. After evacuating HF and SbF_5, a yellow green solid was obtained. The solid was

determined to be $UO_2F_2.3SbF_5$ by the weight uptake of the sample (1411 mg, 6.511 mmol as SbF_5). Then, $UO_2F_2.3SbF_5$ (393 mg, 0.410 mmol) was decomposed under dynamic vacuum at ~140°C, giving a yellow green solid. From the weight, the composition was estimated to be $UO_2F_2.1.6SbF_5$. A small amount of UO_2F_2 was contaminated in the sample by further decomposition of $UO_2F_2.2SbF_5$.

6.4 Discussion

Although UO_2F_2 is insoluble in liquid HF, it dissolves when HF is acidified by AsF_5, the solution giving the typical yellow color of UO_2^{2+}. However, the compound of UO_2F_2 and AsF_5 formed at −77°C in HF is not stable at room temperature and decomposes to UO_2F_2 and AsF_5. Based on the amount of the released AsF_5, the UO_2F_2 / AsF_5 ratio of the compound is approximately 1 : 2. It is known that the reaction of UO_2F_2 and SbF_5 in HF gives several compounds stable at room temperature, $UO_2F_2.nSbF_5$ (n = 2, 3, 4)[3,4].

$UO_2F_2.3SbF_5$ is characterized as an ionic solid containing monomeric SbF_6^- and dimeric $Sb_2F_{11}^-$, $UO_2^{2+}(SbF_6^-)(Sb_2F_{11}^-)$[3]. $UO_2F_2.2SbF_5$ is presumably expressed as $UO_2^{2+}(SbF_6^-)_2$ from the comparison of its IR spectrum with that of $UO_2F_2.3SbF_5$. The enthalpy change of the decomposition of $UO_2F_2.2AsF_5$ is estimated from that of $UO_2F_2.2SbF_5$ at 245°C[3] taking account of the difference in the fluoride ion affinities of SbF_5 and AsF_5[10,11]. The estimation here is made assuming; a) the lattice energies of $UO_2F_2.2SbF_5$ and $UO_2F_2.2AsF_5$ are approximately the same because of the similarity of the molecular volumes of SbF_6^- and AsF_6^-, b) the difference in enthalpy changes of the decomposition of $UO_2F_2.2SbF_5$ at room temperature and 245°C is negligible.

The entropies of $UO_2F_2(s)$, $SbF_5(g)$ and $AsF_5(g)$ are literally available[12] and those of $UO_2F_2.2SbF_5(s)$ and $UO_2F_2.2AsF_5(s)$ were evaluated by Latimer' s method[13]. The free enthalpy changes of the reactions of UO_2F_2 with SbF_5 and AsF_5 at room

temperature are evaluated by combining the enthalpy changes and entropies estimated above:

$$UO_2F_2(s) + 2SbF_5(g) \rightarrow UO_2F_2.2SbF_5(s) \qquad \Delta G^\circ = -169 \text{ kJ mol}^{-1} \qquad (1)$$

$$UO_2F_2(s) + 2AsF_5(g) \rightarrow UO_2F_2.2AsF_5(s) \qquad \Delta G^\circ = 9 \text{ kJ mol}^{-1} \qquad (2)$$

The ΔG° values agree with the observations that $UO_2F_2.2SbF_5$ is stable while $UO_2F_2.2AsF_5$ is not which decomposes to UO_2F_2 and AsF_5 at room temperature. The difference in the stabilities is mainly due to the difference in the fluoride ion affinities. The reaction of UO_2F_2 and TaF_5 does not give a compound, the fluoride ion affinity of the latter being smaller than that of AsF_5.

UO_2F_2 does not react with BF_3 to give a stable compound. The lattice energy of the complex salt of UO_2F_2 and BF_3 is expected to be larger than those of SbF_6^- and AsF_6^- salts because of the smaller volume of BF_4^-. However, the fluoride ion affinity of BF_3 is weak compared to AsF_5 and SbF_5, which offsets this advantage for the formation of the complex salt.

The reaction of UO_2F_2 with GeF_4 appears to proceed in HF, however, the salt is not stable. The fluoroacidity of GeF_4 by accepting two fluoride ions to form GeF_6^{2-} is probably not strong enough to form a complex salt, $UO_2^{2+}GeF_6^{2-}$, in spite of the advantage of the larger lattice energy which arises from the doubly charged ions. Even if GeF_4 acts as a monobasic fluoroacid, its fluoroacidity is weaker than that of AsF_5, the complex salt such as $UO_2^{2+}(GeF_5^-)_2$ not being stabilized.

The reaction of UO_2F_2 with BiF_5 gives only a 1 : 2 compound, $UO_2F_2.2BiF_5$, while several compounds, $UO_2F_2.nSbF_5$ (n = 2, 3, 4), are known as mentioned above. The stable complex salts containing a dimeric anions of BiF_5, $Bi_2F_{11}^-$, have not been reported. The X-ray powder patterns of $UO_2F_2.2BiF_5$ and $UO_2F_2.2SbF_5$ are shown in Table 6-1. As can be seen from the table, $UO_2F_2.2BiF_5$ is isomorphous with $UO_2F_2.2SbF_5$. IR spectrum of $UO_2F_2.2BiF_5$ is shown in Fig. 6-1. The similarity in the spectra of $UO_2F_2.2BiF_5$ and $UO_2F_2.2SbF_5$ (Fig 6-1) also supports that geometrically closely related molecular entities

Table 6-1 X-ray powder patterns of $UO_2F_2.2BiF_5$ and $UO_2F_2.2SbF_5$.

$UO_2F_2.2BiF_5$		$UO_2F_2.2SbF_5$	
Intensity	$10^4 / d^2$ Å^{-2}	Intensity	$10^4 / d^2$ Å^{-2}
w	184	w	203
w	278	w	279
		mw	418*
vw	467		
s	513	s	513
		mw	573*
m	626		
s	679	s	701
ms	745	ms	762
w	845	w	873
w	999	mw	1041
vw	1142		
vw	1204		
w	1338	w	1376
w	1516	w	1548
vw	1632	w	1656
w	1693	w	1724
vw	1762	w	1785
w	1851		
s	2046	m	2036
		mw	2126*
w	2200	w	2290
mw	2277	w	2353
w	2361		
ms	2479	mw	2558
w	2571	w	2638
w	2697		
mw	2991	m	3085
w	3119		
w	3205		
vw	3272		
w	3359		
ms	3484		

*Impurity ascribed to UO_2F_2 formed by subsequent decomposition of $UO_2F_2.2SbF_5$.

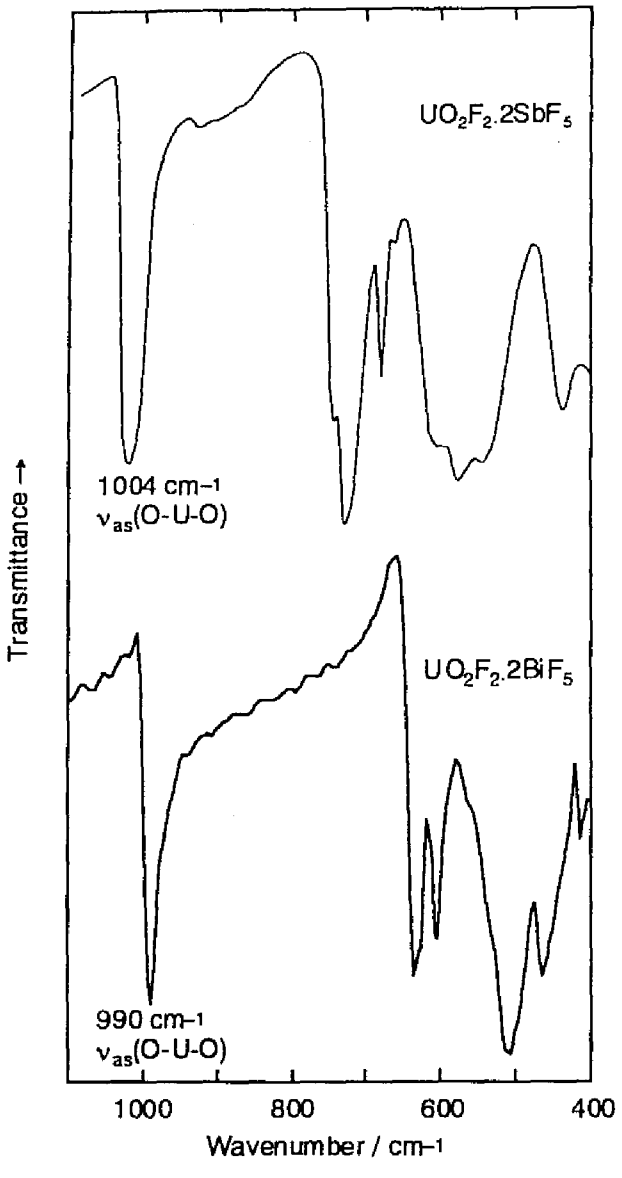

Fig. 6-1 IR spectra of $UO_2F_2.2BiF_5$ and $UO_2F_2.2SbF_5$.

exist in both the compounds. The peak corresponding to the asymmetric stretching of O-U-O (1004 cm^{-1}) in $UO_2F_2.2SbF_5$ is shifted to a lower wavenumber (990 cm^{-1}) in $UO_2F_2.2BiF_5$. This suggests that uranium is less positively charged in $UO_2F_2.2BiF_5$, therefore the fluoride ion affinity of BiF_5 is lower than that of SbF_5. On the other hand, the instability of $UO_2F_2.2AsF_5$ compared to $UO_2F_2.2BiF_5$ suggests that the fluoride ion affinity of BiF_5 is larger than that of AsF_5.

UO_2F_2 is concluded to be a weak fluorobase in HF reacting only with strong fluoroacids such as AsF_5, BiF_5 and SbF_5. The reaction of UO_2F_2 with UF_5 does not give a compounds like $UO_2F_2.2UF_5$ since the fluoride ion affinity of UF_5 is smaller than that of AsF_5[6,7] and not enough to withdraw the second fluoride ion from UO_2F_2. However, several compounds, such as $MF_2.2UF_5$ (M = Ba, Sr, Zn, Sn and Co, probably $M(UF_6)_2$), have been reported to be formed by the reactions of MF_2 and UF_5 in HF[14] although the lattice enthalpies of MF_2 are not less than that of UO_2F_2. Formation of $MF_2.2UF_5$ would be assisted by the fluorobasicity of MF_2 in HF and the stability of the compound. The fluorobasicity of UO_2F_2 insoluble in HF is not so strong as is expected from the lattice enthalpy. This would be the reason why formation of $U_2O_2F_7$ like $(UO_2F)^+UF_6^-$ or $UO_2^{2+}UF_7^{2-}$ does not occur by the reaction of UO_2F_2 and UF_5 in HF at room temperature.

References

1 L. V. Kobets and D. S. Umreiko, *Russ. J. Inorg. Chem.*, **30**, No. 12, 1795 (1985).

2 D. R. Lide ed., "*HANDBOOK of CHEMISTRY and PHYSICS*," 74th ed., CRC press (1993-1994).

3 J. Fawcett, J. H. Holloway, D. Laycock and D. R. Russell, *J. Chem. Soc. Dalton Trans.*, 1355 (1982).

4 J. H. Holloway, D. Laycock and R. Bougon, *J. Chem. Soc. Dalton Trans.*, 1635 (1982).

5 K. Asada, K. Ema and T. Iwai, *Bull. Chem. Soc. Jpn.*, **60** 3189 (1987).

6 J. L. Beauchamp, *J. Chem. Phys.*, **64**, 929 (1976).

7 J. J. Katz, G. T. Seaborg and L. R. Morss ed., "*The Chemistry of the Actinide Elements,*" Chapman and Hall Ltd., 169 (1986).

8 R. A. Penneman, G. D. Sturgeon and L. B. Asprey, *Inorg. Chem.*, **3**, 1, 126 (1964).

9 J. H. Holloway, G. M. Staunton, K. Rediess, R. Bougon and D. Brown, *J. Chem. Soc. Dalton Trans.*, 2163 (1984).

10 D. D. Gibler, *Ph. D. thesis of the University of California, Berkeley*, (1973).

11 T. E. Mallouk, G. L. Rosenthal, G. Müler, R. Brusasco and N. Bartlett, *Inorg. Chem.*, **23**, 3167 (1984).

12 N. P. Galkina ed., "*Osnovnye Svojstva Neorganicheskih Ftoridov*," Moskva Atomizdat, (1976).

13 D. A. Johnson, "*Some Thermodynamic Aspects Of Inorganic Chemistry*," Cambridge University Press (1968).

14 B. Frlec, D. Gantar and B. Volavšek, *Vestn. Slov. Kem. Drus.*, **30**, 277 (1983).

CHAPTER 7

Acid-base reactions of rare earth trifluorides in anhydrous hydrogen fluoride*

7.1 Introduction

Rare earth (RE) elements exhibit similar chemical behaviors because of their similarities in sizes and stable trivalent oxidation states. This makes the mutual separation of RE elements difficult. Rare earth trifluorides (REF_3) are stable ionic compounds and not soluble in water or anhydrous hydrogen fluoride (HF). However, they dissolve in highly acidic solutions, such as HF-BF_3 and HF-AsF_5. Moreover, it has been reported that the divalent oxidation states, unstable in aqueous solutions, is stabilized in anhydrous HF[1].

Several compounds of REF_3 and alkaline metal fluorides (MF) are also prepared from their fused melts[2]. The crystal structure of $MREF_4$ (hexagonal, space group $P\bar{6}$) shows that these compounds are not complex salts in which the fluoroanions of rare earth elements are involved but double salts of MF and REF_3 since the bond lengths of RE and fluorine atoms correspond to the sum of the individual cationic and anionic radii of them[3]. On the other hand, two types of the crystal structures of M_3REF_6 have been reported by Reshetnikova *et al.* [4]. One of them is a cubic, α-K_3AlF_6 type ($Fm\bar{3}m$[5]) and the other is a tetragonal, Cs_3YF_6 type (I4/mmm[6]). In both cases, the existence of REF_6 octahedra was identified by the ν_3 mode in IR spectra. Whether the compounds M_3REF_6 are complex or double salts is still controversial since the detailed crystal structures have not been obtained.

REF_3 acts as a fluorobase in highly acidic condition as described above. Clifford *et*

---

* To be submitted to *J. Fluorine Chem.*

al. have reported the formation of rare earth fluoroantimonates in HF-SbF_5[7]. Recently, formation of rare earth fluoroborates and fluoroarsenates were reported by Lutar *et al.* although the detailed characterization is still under way because of its difficulty[8].

This chapter deals with the reactions of rare earth trifluorides with some fluorobases and fluoroacids. The reactions and compounds are discussed based on the results of gravimetry, X-ray diffraction and vibrational spectroscopy.

7.2 Reagents

REF_3's were obtained from Wako Chemicals (purity 99.5%) and dried under vacuum at 300°C until the pressure above the samples became less than 10^{-3} torr. Some REF_3's were prepared by the reaction of HF with their trichloride hexahydrates (Wako Chemicals, purity 99.5%). The hexahydrates were dehydrated in the same manner as will be described in Chapter 8. Sodium, potassium and cesium fluorides (NaF, KF and CsF, Nakarai Tesque, more than 98 %) were dried under vacuum at 300°C. Silver fluoride (AgF) was prepared in the same manner as described in Chapter 2. Boron trifluoride (BF_3, Nippon Sanso, purity 99.8%) and bismuth pentafluoride (BiF_5, Ozark-Mahoning, purity 97 %) were used as supplied. Antimony pentafluoride (SbF_5, PCR, purity 97 %) was distilled to eliminate SbF_3. The purity of solid materials was checked by X-ray powder diffraction. The purity of gaseous reagents was checked by IR spectroscopy. The compounds obtained were characterized by gravimetry, X-ray diffraction, ICP (Inductively Coupled Plasma) and vibrational spectroscopy.

7.3 Results

PrF_3 + MF (M = Na, K, Cs and Ag)

The mixtures of PrF_3 and MF (M = Na, K, Cs and Ag) in an FEP reactor was

interacted in HF (~2 cm^3) with stirring for several hours at room temperature. The supernatant solution was not colored in each case. After removal of liquid HF by pumping, the reactor was subsequently evacuated with elevating temperature to ~80°C. In the case of AgF, the silver bifluoride was decomposed by elevating temperature which caused the change of color of the solid. The phases in the solids were identified by X-ray powder diffraction. The initial conditions and results are summarized in Table 7-1.

$REF_3 + BF_3$

REF_3 was interacted with BF_3 in HF (~2 cm^3) for several hours at room temperature. The dissolution of PrF_3 and NdF_3 was observed by coloring of the solutions. A solid was obtained after evacuating excess BF_3 and HF. The initial conditions and results of gravimetry and X-ray powder diffraction are summarized in Table 7-2.

Table 7-1 Initial conditions and results of the reactions of MF and PrF_3.

	Initial condition			Result
MF	Weight of PrF_3 / mg	Weight of MF / mg	Molar ratio of MF : PrF_3	Phases detected by X-ray powder diffraction
NaF	328	69	1 : 1	PrF_3, $NaHF_2$
KF	300	264	1 : 1	PrF_3, $K(HF)_nF$
CsF	130	300	3 : 1	PrF_3, $Cs(HF)_nF$
AgF	502	322	1 : 1	PrF_3, AgF
AgF	60	1018	26 : 1	PrF_3, AgF

Table 7-2 Initial conditions and results of the reactions of REF_3 and BF_3.

REF_3	Initial amount of REF_3 mg (mmol)	Reaction time	Weight uptake mg	Ratio of BF_3 / REF_3	Phases detected by X-ray diffraction	
					$REF_3 nBF_3$	REF_3
YF_3[a]	115 (0.788)	1 day	81	1.5	Obs.	Obs.
	180 (1.23)	1 day	104	1.25		Obs.
LaF_3[a]	132 (0.673)	3 days	83.2	1.82	Obs.	
LaF_3	220 (1.12)	1 day	194	2.55	Obs.	
CeF_3	240 (1.22)	1 day	42	0.51	Obs.[b]	Obs.
	206 (1.05)	3 days	45	0.64	Obs.[b]	Obs.
PrF_3	212 (1.07)	1 day	139	1.91	Obs.[b]	
	116 (0.586)	2 hours	39	0.98	Obs.[b]	Obs.
	210 (1.06)	2 hours	62	0.86	Obs.[b]	Obs.
	203 (1.03)	3 days	161	2.32	Obs.[b]	
	268 (1.35)	5 days	190	2.07	Obs.[b]	
	155 (0.783)	1 day	60	1.1	Obs.[b]	Obs.
	521 (2.63)	5 days	432	2.42	Obs.[b]	
NdF_3[a]	254 (1.26)	2 days	206	2.41	Obs.[b]	
SmF_3[a]	216 (1.04)	1 day	90	1.27	Obs.[b]	
	197 (0.950)	1 day	142	2.20	Obs.[b]	
EuF_3	214 (1.02)	5 days	47	0.69		Obs.
EuF_3[a]	118 (0.565)	2 days	74	1.9	Obs.[b]	
GdF_3[a]	259 (1.21)	1 days	185	2.26	Obs.[b]	
	248 (1.16)	1 days	154	1.96	Obs.	
TbF_3	237 (1.10)	14 hours	28	0.376		Obs.
TbF_3[a]	121 (0.560)	1 day	69	1.8	Obs.	
DyF_3	156 (0.711)	1 day	48	1.0	Obs.	
	238 (1.08)	4 days	129	1.76	Obs.	
HoF_3	239 (1.08)	2 days	9	0.1		Obs.
ErF_3[a]	176 (0.786)	1 day	75	1.41	Obs.	Obs.
ErF_3	243 (1.08)	1 day	0	0		Obs.
TmF_3	403 (1.78)	4 days	6	0.05		Obs.
YbF_3	245 (1.07)	1 day	3	0.04		Obs.
YbF_3[a]	191 (0.830)	5 days	87	1.5	Obs.	Obs.
LuF_3	255 (1.10)	1 day	25	0.34		Obs.

[a] prepared from the corresponding trichloride.

[b] isomorphic pattern was obtained (Orthorhombic).

$PrF_3 + BiF_5$

PrF_3 (126 mg, 0.637 mmol) and BiF_5 (586 mg, 1.93 mmol) were interacted in HF (~2 cm^3) for ~20 hours at room temperature. The dissolution of PrF_3 was observed by the green color of the supernatant solution. A pale green solid was obtained after evacuating HF. No peak was observed in the X-ray powder photograph. No weight change was observed after the attempt to separate excess BiF_5 from the product by vacuum sublimation at ~100°C. The X-ray powder photograph of the sample after the sublimation gave no peaks.

In a separate experiment, PrF_3 (67 mg, 0.34 mmol) and BiF_5 (521 mg, 1.71 mmol) were interacted in HF (~2 cm^3) for ~20 hours at room temperature. X-ray powder diffraction of a solid obtained after evacuating HF detected only the unreacted BiF_5. The decrease of the weight by 71 mg (0.23 mmol as BiF_5) was observed after vacuum sublimation. The X-ray powder photograph of the sample after the sublimation gave no peaks, either.

$PrF_3 + SbF_5$

PrF_3 (100 mg, 0.505 mmol) was interacted with excess SbF_5 in HF (~2 cm^3) for ~20 hours at room temperature. PrF_3 completely dissolved in HF to give a green solution. A pale green solid was obtained after evacuating excess SbF_5 and HF. The weight uptake of the solid was 481 mg (2.22 mmol as SbF_5). X-ray diffraction of the solid showed a complex pattern different from that of PrF_3.

7.4 Discussion

Reactions of PrF_3 with fluorobases

PrF_3 does not react with monobasic metal fluorides (NaF, KF, CsF and AgF) in HF whereas double salts like $MREF_4$ and M_3REF_6 are formed in their melts[2]. The

solubility of REF_3 in HF is so low that the dissolution of REF_3 by forming RE(III) species like REF_{3+n}^{n-} does not occur at room temperature. The dissolution of REF_3 was not observed even in a highly basic solution such as HF saturated with AgF. NaF, KF ,CsF and AgF react only with the solvent HF to form their bifluorides, $M(HF)_nF$. Thus, REF_3 does not act as a fluoroacid in HF.

In contrast to the HF system, formation of compounds of REF_3 and NOF, $NORE_2F_7$, $NOREF_4$ and $(NO)_3RE_2F_9$ has been reported in the NO_2-HF solution (NO_2 : HF = 20 : 80 in mol%)[9]. In NO_2-HF system, NOF and HNO_3 are formed by the following equilibrium[10]:

$$N_2O_4 + HF \rightleftharpoons NOF + HNO_3 \qquad (1)$$

The solubility of RE in this system has been reported to be 0.4 ~ 0.8 kg m^{-3} for Y, La, Ce, Pr, Nd and Sm at 25°C[11]. It is not clear in this case whether REF_3 acts as a fluoroacid or not since the compounds have not been characterized. However, the formation of the compounds of NOF and REF_3 is considered to be promoted by the dissolution of REF_3 in the solution.

Reactions of REF_3 with fluoroacids

REF_3 dissolves more or less in HF in the presence of fluoroacids. PrF_3 (pale green solid) dissolves in HF with BF_3, BiF_5 and SbF_5 to give pale green solutions. The solubility is larger in HF-BiF_5 and SbF_5 solutions than in HF-BF_3. REF_3 is considered to act as a fluorobase under a highly acidic condition, for example;

$$REF_3 + 3nHF \rightarrow RE^{3+}(sol) + 3(HF)_nF^-. \qquad (2)$$

NdF_3 (red purple solid) also dissolves in acidified HF. The dissolution of the colorless heavy earth fluorides was not observed in the present study.

The formation of REF_3-BF_3 compounds where RE = Y, La, Cs, Pr, Nd, Sm, Eu, Gd, Tb, Dy, Er and Yb was confirmed by gravimetry and X-ray powder diffraction (see Table 7-2). The formation of REF_3-BF_3 compounds seems to be very slow probably due

to the low solubility of REF_3 in HF. The presence of REF_3 remained in some products is explained by incomplete reaction and/or the decomposition of the compounds during the pumping. Recently, Mazej *et al.* reported that a partial liberation of BF_3 and AsF_5 from the compounds of REF_3-BF_3 and REF_3-AsF_5 occurs under a dynamic vacuum at room temperature[12]. There is a tendency that free REF_3 is found in the product of heavy earth. For light earth series, free CeF_3 was exceptionally detected with the compound of BF_3. In the case of PrF_3-BF_3 system, the overnight interaction was not enough to complete the reaction, the unreacted PrF_3 being remained. The stability of the compound seems to decrease as the ionic radius of RE^{3+} decreases. Fig. 7-1 shows the lattice enthalpy of REF_3 at 25°C represented by the following equation:

$$REF_3(s) \rightarrow RE^{3+}(g) + 3F^-(g) \qquad \Delta H_L \qquad (3)$$

The lattice enthalpy is calculated by a thermodynamic cycle combined with the enthalpy of formation of REF_3[13], RE^{3+}[14] and F^- (= –247 kJ mol^{-1}[14]). There is almost linear

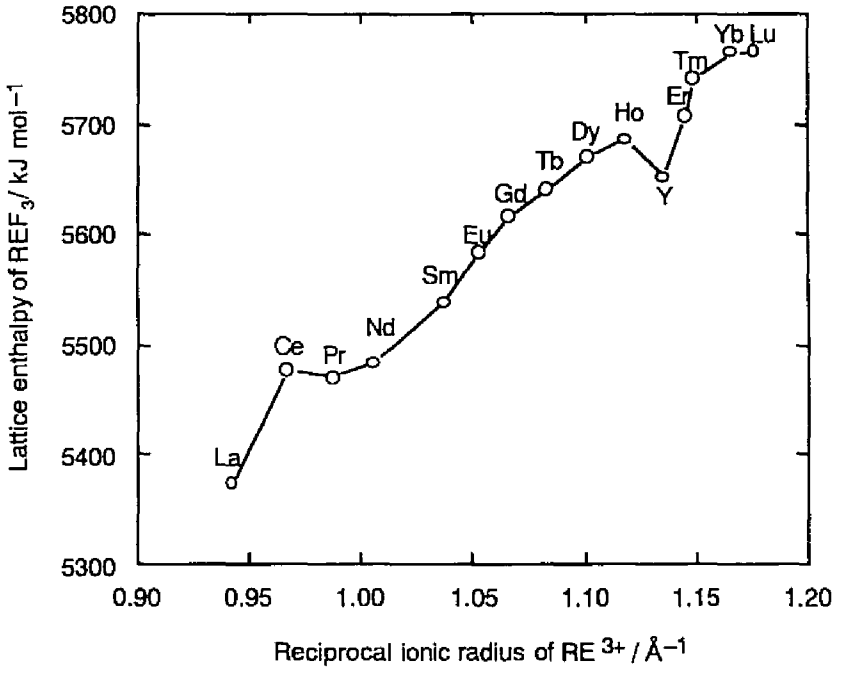

Fig. 7-1 Dependence of the lattice enthalpy of REF_3 on the reciprocal ionic radius of RE^{3+}.

relationship between ΔH_L and reciprocal ionic radius of RE^{3+}. Fluorobasicity of REF_3 generally decreases with the increase of ΔH_L, the coulombic interaction between RE^{3+} and F^- being increased to stabilize REF_3.

HoF_3 and TmF_3 do not react with BF_3 in spite of the formation of that of YbF_3 which has a smaller ionic radius than they have. The reactivity of REF_3 with BF_3 in HF seems to be governed not only by thermodynamic but also kinetic factors. The starting REF_3's prepared from their trichlorides are more 'reactive' than commercially supplied ones as seen in the results of EuF_3 TbF_3, ErF_3 and YbF_3. The difference might be explained by the kinetic reason caused by the difference in the crystallite sizes of REF_3 prepared from their trichlorides and that commercially supplied. The line widths in the X-ray powder patterns of REF_3's (Fig. 7-2) prepared from their trichlorides are broader than

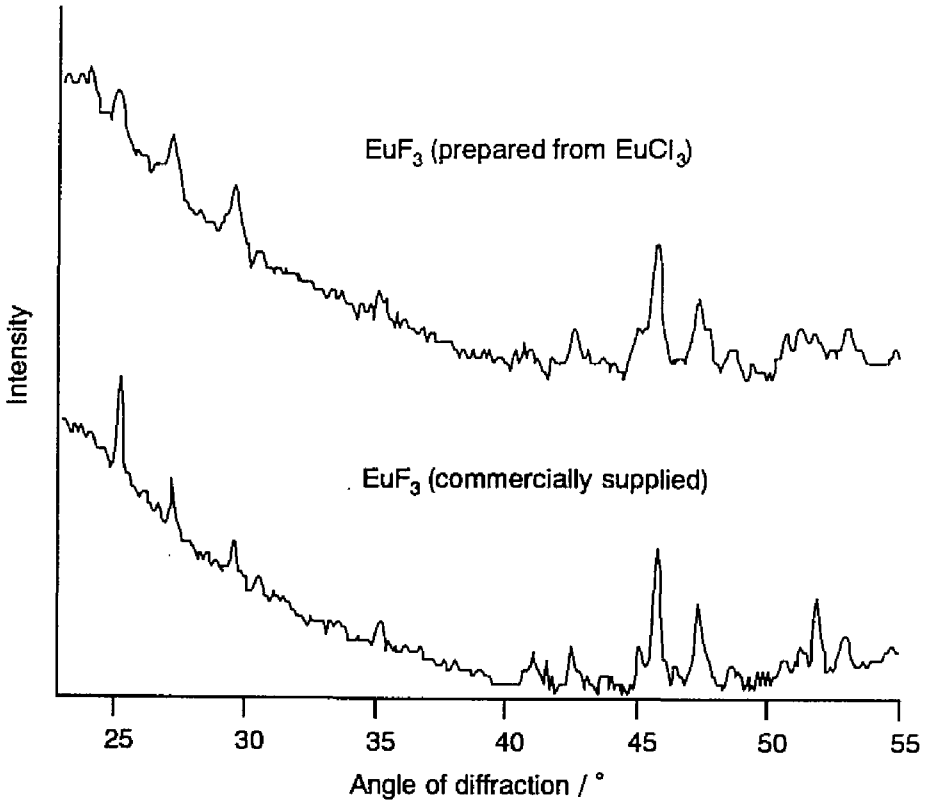

Fig. 7-2 X-ray powder diffraction profiles of EuF_3's prepared from $EuCl_3$ and commercially supplied.

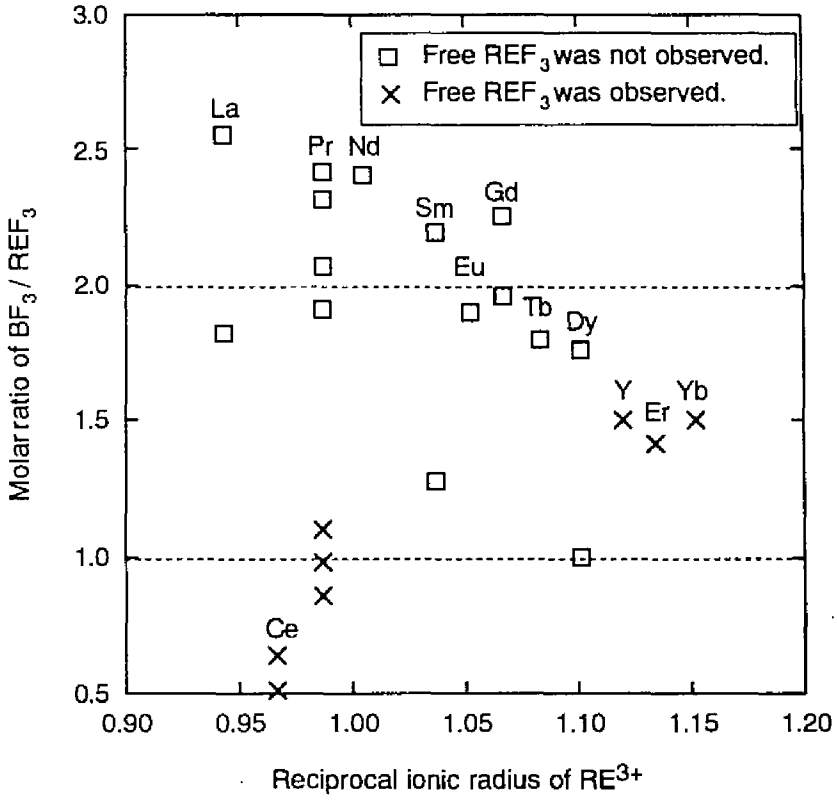

Fig. 7-3 Variation of the molar ratio of REF_3-BF_3.

those of trifluorides commercially supplied. There is a possibility that all the REF_3's including even the trifluorides of Ho, Tm and Lu react with BF_3 if they are prepared from their trichlorides and have lower crystallinity, which has not been proved yet.

For vacuum stable compounds, the molar ratios, BF_3 / REF_3, are listed in Table 7-2 assuming that the weight uptake of the sample after the reaction was caused only by BF_3. In the case of PrF_3, the ratio is ~2.3. When it is smaller than this value, the pattern of PrF_3 is observed in the X-ray powder photograph. The BF_3 / PrF_3 ratio of the product not containing free PrF_3 was also confirmed to be ~2.3 by ICP spectroscopy of prascodymium and boron. Fig. 7-3 summarizes the ratios of BF_3 / REF_3 of the products in which the REF_3-BF_3 compounds were detected by X-ray diffraction. The square marks in the plot represent the products not containing free REF_3 and the X marks denote the products with some free REF_3. There is a tendency that the ratio generally decreases with

decreasing the ionic radius of RE^{3+}. Anyway, roughly speaking, BF_3 / REF_3 ratios are around two. The ratios lower than two found in Y, Ce, Er and Yb might be explained by the decomposition during the pumping since the presence of free REF_3 is always found in the samples. The compositions of the compounds obtained by Mazej *et al.* [12] were classified into two groups; BF_3 / REF_3 = 2 for light earths and 1 for heavy earths. Their results differ from ours in the compositions of the compounds of heavy earths. However, neither the presence of free REF_3 nor the formation of the compound have been detected since their products are X-ray amorphous. Thus, the existence of the 1 : 1 compounds of REF_3-BF_3 is still controversial.

The X-ray powder pattern of the compound of PrF_3 and BF_3 was indexed as an orthorhombic unit cell with the lattice parameters of a_0 = 11.389, b_0 = 6.325 and c_0 = 6.869 Å, as listed in Table 7-3. The possible space group, Pnc2 or Pncm, is expected from the systematic extinction of the observed lines. The X-ray powder patterns of the compounds of REF_3-BF_3 (RE = Ce, Nd, Sm, Eu, and Gd) are isomorphous with that of PrF_3-BF_3 compound. In Table 7-4, the lattice parameters of the isomorphous series are listed and Fig. 7-4 shows the relation between the cubic root of the lattice volume of the isomorphous series and the reciprocal ionic radius of RE^{3+}. The cubic root of the lattice volume almost linearly increases with the ionic radius of RE^{3+}. The X-ray powder patterns of the compounds of REF_3-BF_3 (RE = Tb, Dy, Y, Er, and Yb) are not isomorphous with that of PrF_3-BF_3. The crystal structures of the products are classified into, at least, three types: the structure of LaF_3-BF_3, that of REF_3-BF_3 (RE = Ce, Nd, Sm, Eu, and Gd), and that of REF_3-BF_3 (RE = Tb, Dy, Y, Er, and Yb). The X-ray powder patterns of the last group are not confirmed to be isomorphous because only broad and weak lines were observed. The dependence of the cubic root of the lattice volume on the ionic radius of RE^{3+} and the dissolution of the compound in acetonitrile (CH_3CN) at room temperature suggest that the compounds are ionic.

Table 7-3 X-ray powder diffraction pattern of PrF_3-BF_3 (orthorhombic, a_0=11.389 Å, b_0=6.325 Å, c_0=6.869 Å). Possible space group is Pnc2 or Pncm(Pmna).

hkl	Int.	Obs. $10^4/d^2$ Å^{-2}	Calc. $10^4/d^2$ Å^{-2}	*hkl*	Int.	Obs. $10^4/d^2$ Å^{-2}	Calc. $10^4/d^2$ Å^{-2}
011	m	451	462	231	m	2770	2770
111	s	526	539	313	m	2861	2851
210	s	553	558	330	ms	2938	2944
211	mw	779	770	422	m	3084	3081
002	s	842	848	132	m	3176	3175
102	m	912	925	611	m	3240	3237
310	m	939	944	413	m	3321	3391
020	ms	1001	1000	004	m	3392	3391
120	m	1070	1077	430	m	3531	3483
112	m	1170	1175	204	m	3697	3699
400	ms	1229	1234	612	m	3857	3873
212	m	1406	1406	040	w	4006	3999
410	mw	1462	1483	423	vw	4126	4141
302	w	1595	1542	711	vw	4262	4240
411	mw	1704	1695	024	mw	4417	4391
312	m	1789	1792	124	m	4478	4468
122	mw	1944	1925	224	ms	4701	4699
402	ms	2097	2081	800	mw	4957	4934
510	mw	2175	2177	242	ms	5156	5156
130	m	2315	2327	441	mw	5453	5445
511	s	2371	2389	514	m	5573	5568
031	ms	2461	2462	802	ms	5810	5782
230	vs	2553	2558	730	m	6028	6027

Abbreviations used: s, strong; m, medium; w, weak; v, very.

Table 7-4 Lattice parameters of the isomorphous series of REF_3-BF_3 compounds.

Compound	a_0 / Å	b_0 / Å	c_0 / Å	V / Å^3
CeF_3-BF_3	11.43	6.343	6.905	500.6
PrF_3-BF_3	11.39	6.325	6.869	494.8
NdF_3-BF_3	11.36	6.319	6.881	494.0
SmF_3-BF_3	11.28	6.258	6.807	480.0
EuF_3-BF_3	11.18	6.225	6.772	471.3
GdF_3-BF_3	11.28	6.209	6.761	473.5

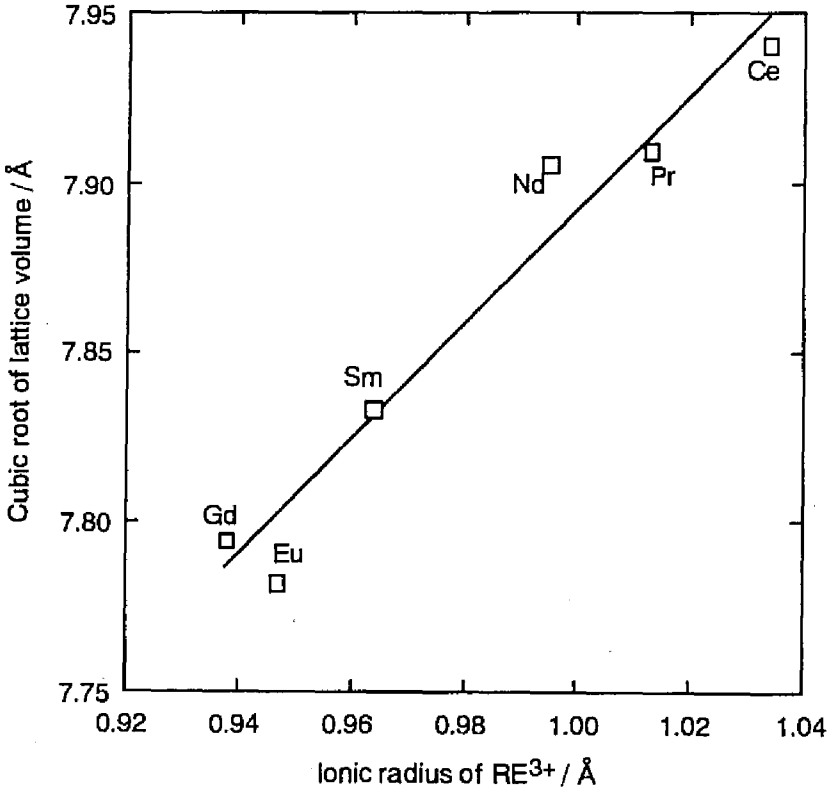

Fig. 7-4 Dependence of the cubic root of the lattice volume of REF_3-BF_3 compounds on the ionic radius of RE^{3+}.

The IR spectra of REF_3-BF_3 compounds are shown in Fig. 7-5. The broad and split peaks around 1100 cm^{-1} are assigned to the ν_3 mode of BF_4^- by comparing with the spectrum of $NaBF_4$ (also shown in Fig. 7-5) which contains discrete BF_4^- (T_d). The splitting of the ν_3 mode in the spectra of REF_3-BF_3 would be explained by the strong interaction of the fluorine atoms in BF_4 units with rare earth atom. This might be explained by the formation of a large complex cation like $RE(FBF_3)_n^{(3-n)+}$. A complex cation of RE(III) coordinated by SO_2 have been reported in $[RE(SO_2)_x(AsF_6)_2]^+AsF_6^-$ prepared in SO_2 solvent[15]. The similarity in the spectra of the compounds of PrF_3 and SmF_3 also supports that their structures are closely related with each other. The spectra of the compounds of LaF_3, DyF_3 and YF_3 are obviously different from those of the isomorphous series reflecting the differences in their structures.

The reactions of PrF_3 with SbF_5 and BiF_5 also gave stable compounds. The ratios of BiF_5 / PrF_3 and SbF_5 / PrF_3 were 3.03 ~ 4.26 and 4.40, respectively. The complex pattern was obtained for the product of PrF_3 and SbF_5, while only a few weak peaks were observed for the product of PrF_3 and BiF_5. The formation of the X-ray amorphous phases has been also reported in the compounds of REF_3 with BF_3 and AsF_5[8]. The stoichiometry of these compounds are again not straightforward as is expected from the formal ionic charge balances of RE^{3+}, MF_6^- and $M_2F_{11}^-$ (M = Bi and Sb).

Figure 7-6 shows the IR spectra of BiF_5 and the compound of PrF_3 and BiF_5. The peak around 620 cm^{-1} is assigned to ν_3 mode of BiF_6 unit with O_h symmetry. BiF_5 has a tetragonal α-UF_5 structure in which a trans-linked chain of BiF_6 octahedra via fluorine bridging bonds exists along *c*-axis[16]. The close frequency of ν_3 mode for PrF_3-BiF_5 compound to that of BiF_5 suggests that the former does not contain discrete BiF_6^- anions but fluorine-bridged structures such as $(-FBiF_5-)_n$ or (-Pr-F-BiF_5) since the ν_3 mode of discrete BiF_6^- anion appears at lower frequency, for example, around 570 cm^{-1} as seen in $CsBiF_6$[17].

Compared with the compounds of PrF_3 and BiF_5, the IR spectrum of the compound

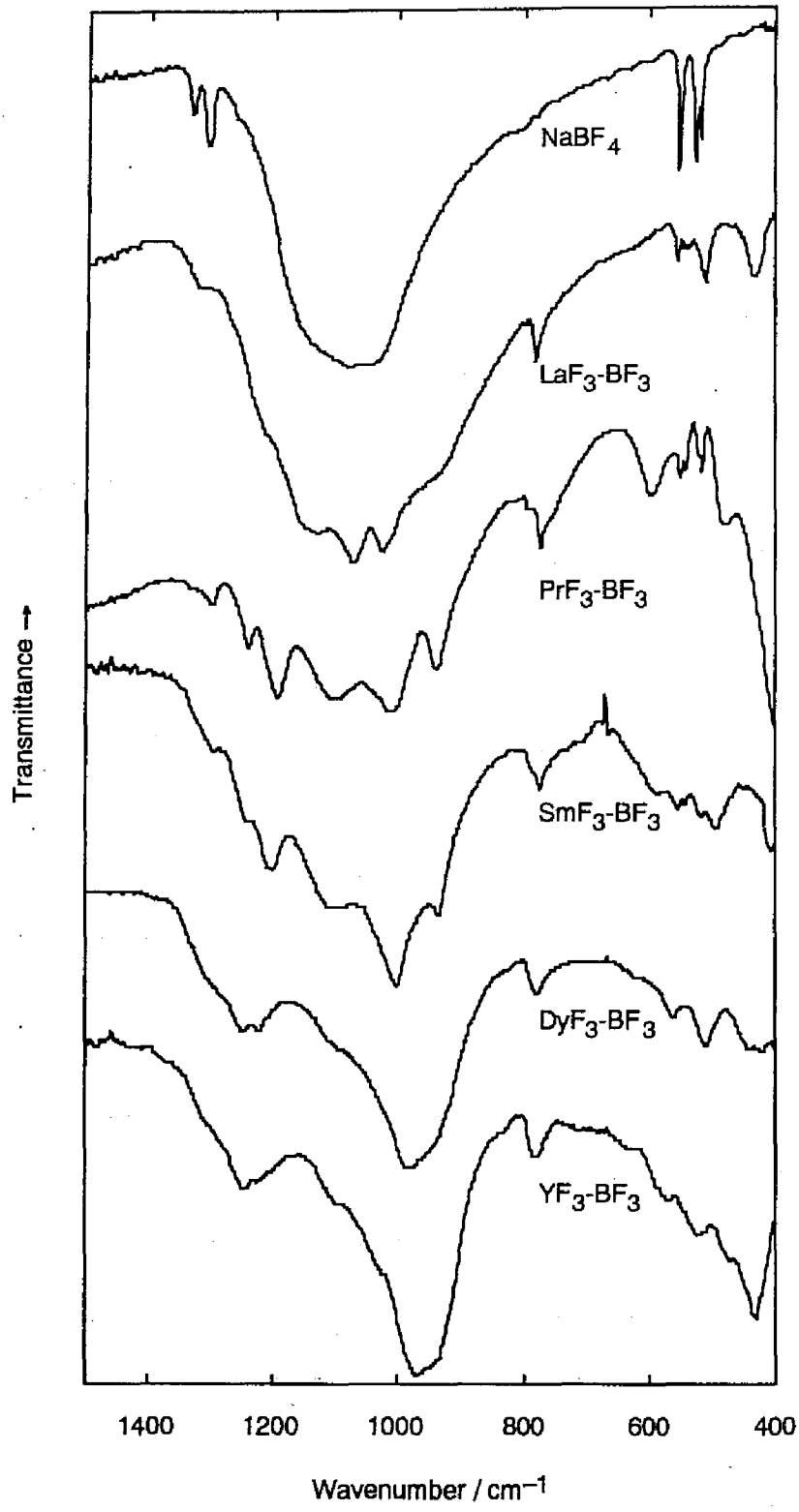

Fig. 7-5 IR spectra of the compounds of REF_3 and BF_3. The spectrum of $NaBF_4$ is also shown for comparison.

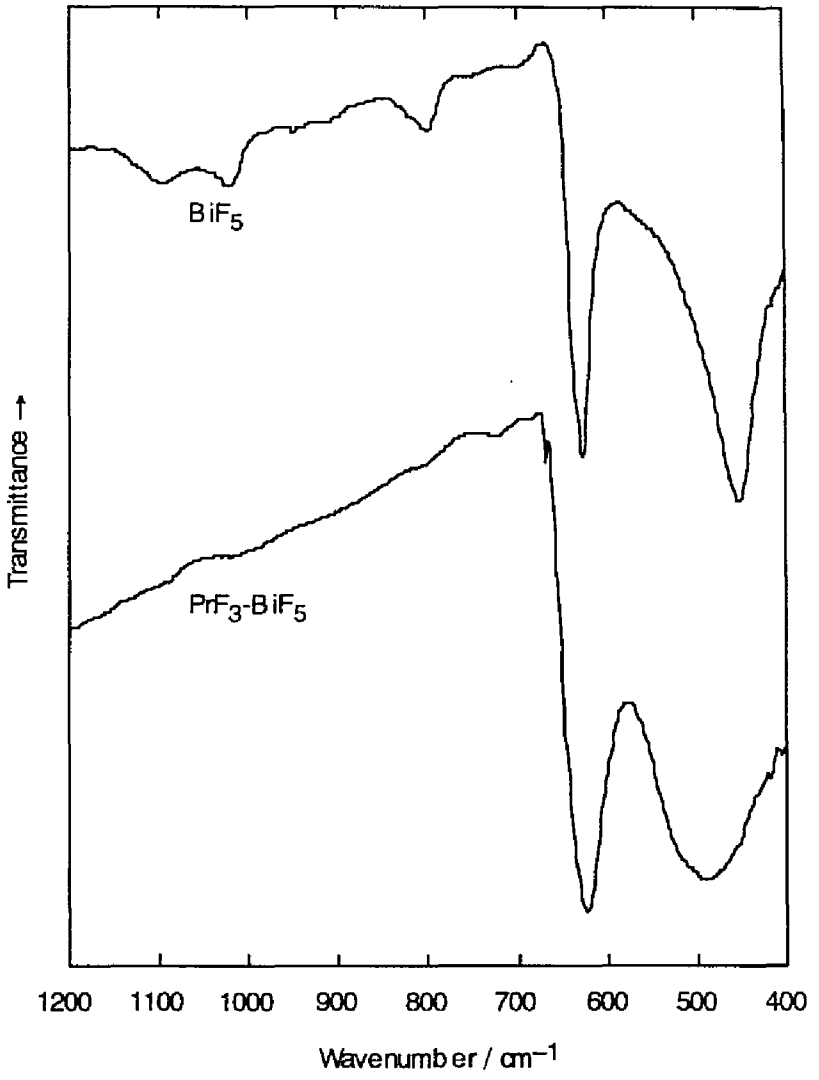

Fig. 7-6 IR spectra of BiF_5 and the compound of PrF_3 with BiF_5.

of SbF_5 is more complex as shown in Fig. 7-7. The groups of peaks around 650 ~ 750 and 500 ~ 550 cm^{-1} are ascribed to the Sb-F(terminal) and Sb-F(bridging) stretching bands, respectively, by comparison with the spectra of $[Re_2F_9O_2][Sb_2F_{11}]$[18], $UO_2F_2.3SbF_5$[19], $UO_2F_2.4SbF_5$[20] and so on. Thus, this compound probably contains fluorine-bridged structures such as $Sb_2F_{11}^-$, $(-FSbF_5-)_n$ and Pr-F-SbF_5 units.

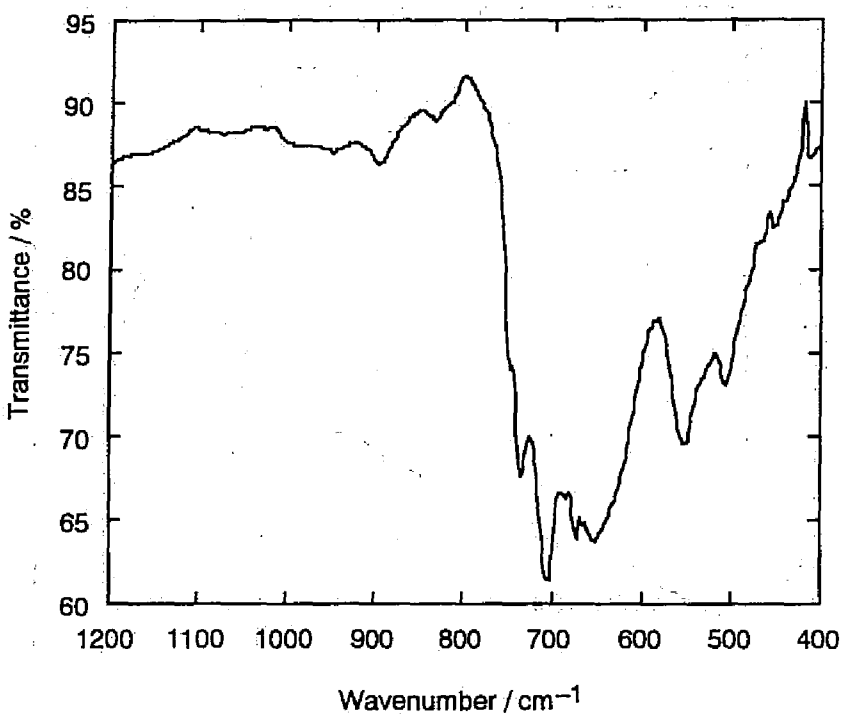

Fig. 7-7 IR spectrum of the compound of PrF_3 and SbF_5.

References

1 C. G. Barraclough, R. W. Cockman and T. A. O'Donnell, *Inorg. Chem.*, **30**, 340 (1991).

2 D. Brown, "*Halides of the Lanthanide and Actinide,*" John Wiley & Sons Ltd., (1968).

3 J. H. Burns, *Inorg. Chem.*, **4**, 6, 881 (1965).

4 L. P. Reshetnikova, I. B. Shaimuradov, V. A. Efremov and A. V. Novoselova, *Dokl. Akad. Nauk. SSSR*, **215**, 4, 877 (1974).

5 E. G. Steward and H. P. Rooksby, *Acta. Cryst.*, **6**, 49 (1953).

6 H. Bode and E. Voss, Z. *Anorg. Allgen. Chem.*, **290**, 1 (1957).

7 A. F. Clifford, H. C. Beachell and W. M. Jack, *J. Inorg. Nucl. Chem.*, **5**, 57 (1957).

8 K. Lutar, M. Fele-Beuermann, S. Milićev and B. Žemva, *Proc. of the 14th International Symposium on Fluorine Chemistry*, 2 (1994).

9 N. Sato and A. Kigoshi, *Thermochimica Acta*, **57** 141 (1982).

10 N. Sato and A. Kigoshi, *AIChE Journal*, Vol. 28, **3**, 522 (1982).

11 A. Kigoshi, *J. Japan Inst. Metals*, Vol. 21, **10**, 769 (1982).

12 Z. Mazej, K. Lutar and B. Žemva, *Proc. of the 11th European Symposium on Fluorine Chemistry*, 129 (1995).

13 N. P. Galkina ed., "*Osnovnye Svojstva Neorganicheskih Ftoridov,*" Moskva Atomizdat, (1976).

14 D. R. Lide ed., "*HANDBOOK of CHEMISTRY and PHYSICS,*" 74th ed., CRC press (1993-1994).

15 C. Ruf, U. Behrens, E. Lork and R. Mews, *Proc. of the 11th European Symposium on Fluorine Chemistry*, 27 (1995).

16 W. H. Zachariasen, *Acta Cryst.*, **2**, 296 (1949).

17 K. O. Christe, W. W. Wilson and C. J. Schack, *J. Fluorine Chem.*, **11**, 71 (1978).

18 G. J. Schrobilgen, J. H. Holloway and D. R. Russell, *J. Chem. Soc. Dalton Trans*, 1411 (1984).

19 J. Fawcett, J. H. Holloway, D. Laycock and D. R. Russell, *J. Chem. Soc. Dalton Trans.*, 1355 (1982).

20 J. H. Holloway, D. Laycock and R. Bougon, *J. Chem. Soc. Dalton Trans.*, 1635 (1982).

CHAPTER 8

Acid-base reactions of rare earth trichlorides in molten LiCl-KCl eutectic*

8.1 Introduction

Rare earth (RE) elements are important for syntheses of various functional materials having unique catalytic and magnetic properties. The electrochemical process in molten alkaline halides is one of the strong candidates to synthesize such materials because of their wide electrochemical windows. The electrochemical syntheses of some alloys containing rare earth elements have been investigated in LiCl-KCl eutectic melt to control the bulk or surface composition[1,2]. These chlorides are hygroscopic and the perfect elimination of oxide species from a considerable amount of melt is technically difficult, which sometimes causes the precipitation of the oxides (RE_2O_3) or oxide chlorides (REOCl). The precipitation of the compounds occasionally affects electrochemical measurements in molten chlorides.

REOCl is easily formed by heating hydrated $RECl_3$ in air at around 300°C[3]. Under this condition, the formation of RE_2O_3 does not occur. Therefore, it has been considered that REOCl is dominantly formed in rare earth molten chlorides contaminated by O^{2-}. Picard *et al.* studied the stabilities of REOCl and RE_2O_3 for some rare earth elements (La, Ce, Pr, Nd, Gd and Y) in LiCl-KCl eutectic[4]. They showed that formation of RE_2O_3 for Pr, Nd and Gd occurs at higher oxide ion concentration and only Y_2O_3 precipitates regardless of the oxide ion concentration. However, the available thermodynamic data of REOCl's are not comprehensive, especially those of heavy rare earths, compared to those of RE_2O_3's and $RECl_3$'s and the thermodynamic explanation

---

* Published in *J. Electrochem. Soc.*, Vol. **142**, No. 7, 2196 (1995).

for formation of the precipitates has not been made systematically in this system.

In this chapter, identification of the precipitates was carried out in LiCl-KCl eutectic containing $RECl_3$ at several O^{2-} concentrations including 'zero' at 450°C. The thermodynamic data of REOCl at high temperatures are estimated and applied to LiCl-KCl eutectic containing RE(III) and O^{2-} to predict the precipitates to be formed in the melts.

8.2 Experimental

Materials

All the reagents were handled in a glove box of Ar atmosphere. LiCl and KCl (Wako Chemicals, purity 99.0 and 99.9%, respectively) were dried in Pyrex glass ampoules under vacuum elevating the temperature to 200°C and holding it for several hours until the pressure becomes below 10^{-3} Torr. They were transferred into the glove box and mixed (eutectic composition, LiCl : KCl = 59 : 41 in molar fraction). Li_2O (Mitsuwa's Chemicals, purity 95%) was dried under vacuum and heated up to 550°C to decompose the trace amount of LiOH to Li_2O. Anhydrous $RECl_3$'s were prepared from $RECl_3 \cdot 6H_2O$'s (Wako Chemicals, purity 99.5% or more). They were carefully dehydrated under vacuum at lower temperatures less than 200°C and heated up to ~300°C with the intermittent treatment with dry HCl to convert contaminated REOCl to $RECl_3$. X-ray powder diffraction detected no impurities in the prepared samples.

Preparation and identification of the precipitates

The composition of $RECl_3$ in LiCl-KCl eutectic, 1 or 3 mol%, was chosen because the identification of the precipitates in LiCl-KCl becomes difficult by X-ray diffraction below this composition. The temperature was fixed to 450°C for all the experiments. The melting point of LiCl-KCl eutectic is 353°C and 450°C is often chosen as a reaction temperature for electrochemical measurements because Pyrex glass is stable and the

vaporization of LiCl is negligible.

LiCl-KCl eutectic, $RECl_3$ (1 or 3 mol%) and Li_2O (1 or 3 mol%, $pO^{2-} \sim 2$) were mixed and loaded in a Pyrex glass reaction tube connected to a Whitey stainless steel valve. The tube was connected to a vacuum line to keep the ambient pressure of Ar in the tube. The temperature was elevated to 450°C by a transparent electric furnace to observe the melting of the mixture and the formation of precipitate. After holding the temperature for several hours, the tube was cooled and transferred to the glove box. The precipitate was collected from the cooled melts and charged in a quartz glass capillary to prepare the sample for X-ray powder diffraction. Experiments without Li_2O were carried out to examine the precipitates from the melt not containing O^{2-}.

8.3 Results and discussion

8.3.1 The precipitates in the absence of oxide ion

The addition of 3 mol% of $LaCl_3$ and $NdCl_3$ to LiCl-KCl eutectic at 450°C gives clear colorless and purple melts, respectively. The addition of 1 mol% of $GdCl_3$ gives a clear colorless melt, the precipitate being formed when it is increased to 3 mol%. The addition of 1 mol% of YCl_3 and $YbCl_3$ gives the formation of precipitates in the melts. The precipitates are found to be the 3 : 1 compounds of KCl and $RECl_3$, K_3RECl_6 (RE = Gd, Y and Yb)[5]. Neither the formation of RE_2O_3 nor REOCl was observed in all the experiments.

The formation of K_3RECl_6's has been reported in KCl-$RECl_3$ systems[5], their X-ray powder patterns having not been indexed yet. In this investigation, the X-ray powder pattern of α-K_3YCl_6 (low temperature form, a phase transition occurring in the cooling process.) is indexed as a simple cubic cell with the lattice parameter, a_0 = 10.55 Å and Z = 4 as shown in Table 8-1. The X-ray powder patterns of K_3RECl_6 for Gd and Yb are isomorphous, their lattice parameters, a_0, being 10.65 and 10.53 Å, respectively. In the

Table 8-1 X-ray powder pattern of α-K_3YCl_6. The index was made as a simple cubic unit cell with the lattice parameter, a_0= 10.55 Å.

Intensity	d_{obs} / Å	d_{calc} / Å	*hkl*
m	5.998	6.091	111
m	5.199	5.275	200
s	3.686	3.730	220
w	3.308	3.336	310
w	2.931	2.926	320
vw	2.819	2.820	321
s	2.644	2.638	400
w	2.499	2.487	411, 330
w	2.430	2.420	331
s	2.152	2.154	422
w	2.028	2.030	333, 511

Abbreviations used: s, strong; m, medium; w, weak; v, very.

crystal structure of the related compound, $Cs_2NaBkCl_6$ (cubic, a_0 = 10.8050 Å) [6], the bond length between Bk(III) and Cl^- corresponds to the sum of the ionic radii of Bk(III) and Cl^-. It is strongly suggested that K_3RECl_6 is also a double salt rather than a complex salts containing a discrete anion, such as $RECl_6^{3-}$.

It seems that the precipitation of K_3RECl_6 is more likely to occur as the ionic radius of RE^{3+} decreases by lanthanide contraction which causes the increase of the coulomb interaction between RE^{3+} and Cl^-.

8.3.2 The precipitates in the presence of oxide ion

When 3 mol% of Li_2O is added to LiCl-KCl eutectic containing 3 mol% of $RECl_3$ (RE = La and Nd), REOCl is precipitated. In the melt containing 1 mol% of Li_2O and $RECl_3$ (RE = Y, Yb), the precipitation of RE_2O_3 is observed. When a small amount of Li_2O (~0.5 mol%) is added to the melt containing 1 mol% of $GdCl_3$, the precipitation of GdOCl is observed. Further addition of Li_2O (~1 mol%) gives the precipitation of both Gd_2O_3 and GdOCl.

The formation of RE_2O_3 or REOCl in these melts is reasonably explained from the potential-pO^{2-} diagrams. In order to construct the potential-pO^{2-} diagrams, the RE(III)/RE(0) standard electrode potentials and the standard chemical potential of O^{2-} in LiCl-KCl eutectic at 450°C are required in addition to the free enthalpies of formation of $RECl_3$, RE_2O_3 and REOCl (see Appendix). The RE(III)/RE(0) standard electrode potentials are literally available only for La, Ce, Pr, Nd, Gd and Y[4,7,8]. The standard chemical potential of the O^{2-} was estimated by the measurements of the solubility of some metal oxides (ZnO, CoO, MgO, FeO, NiO, UO_2, UO_3, PdO, Bi_2O) in LiCl-KCl eutectic at 450°C[9,10], which was employed for the calculation here:

$$\frac{\mu^0(O^{2-})}{2.303RT} = 9.3 \quad \text{(in molar fraction)} \tag{1}$$

Only the following redox equilibria are taken into account in LiCl-KCl eutectic containing the trivalent rare earth species, RE(III), and O^{2-} because at this temperature the formation of divalent species can be ignored for La, Gd and Y:

$$RE(III) + 3e = RE(0) \tag{i}$$

$$RE_2O_3 + 6e = 2RE(0) + 3O^{2-} \tag{ii}$$

$$REOCl + 3e = RE(0) + O^{2-} + Cl^- \tag{iii}$$

For these equilibria, the potential against Cl_2/Cl^- electrode are expressed as follows;

$$E = E^0_{RE(III)/RE} + \frac{2.303RT}{3F}\log X_{RE(III)} \tag{2}$$

$$E = \frac{\Delta G_f(REOCl)}{3F} - \frac{\mu^0(O^{2-})}{3F} + \frac{2.303RT}{3F}pO^{2-} \tag{3}$$

$$E = \frac{\Delta G_f(RE_2O_3)}{6F} - \frac{\mu^0(O^{2-})}{2F} + \frac{2.303RT}{2F}pO^{2-} \tag{4}$$

where $X_{RE(III)}$ is the concentration of trivalent rare earth elements in molar fraction and pO^{2-} represents the logarithmic concentration of O^{2-} in molar fraction defined as:

$$pO^{2-} = -\log X_{O^{2-}} \tag{5}$$

The potentials in eqs.(3) and (4) depend linearly on pO^{2-}. Although the absolute value of $\mu^0(O^{2-})$ is still controversial, it does not affect the comparison of the relative stability of REOCl to RE_2O_3.

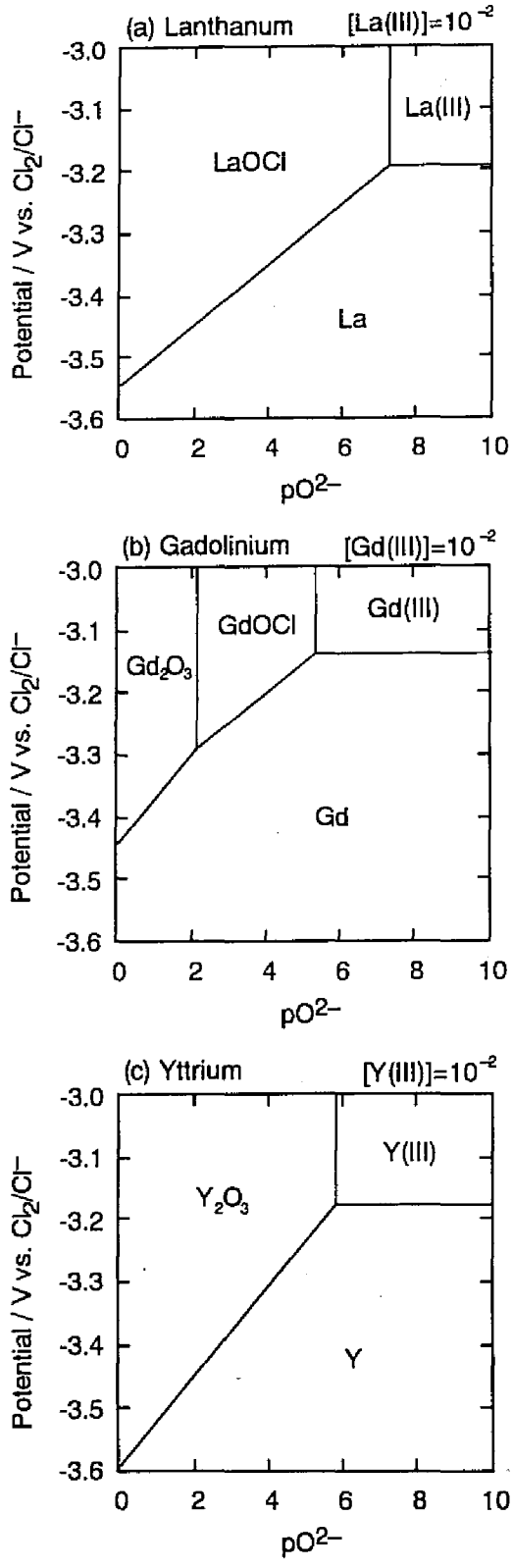

Fig. 8-1 Potential-pO^{2-} diagrams for (a) lanthanum, (b) gadolinium and (c) yttrium in LiCl-KCl eutectic at 450°C. The concentrations of RE(III) and O^{2-} are given in molar fraction.

Figure 8-1 shows typical examples of the potential-pO^{2-} diagrams for La, Gd and Y systems. The concentration of $RECl_3$ in LiCl-KCl eutectic is chosen to be 1 mol%. Since LaOCl is thermodynamically more stable than La_2O_3 at 450°C, LaOCl selectively precipitates in the melt containing O^{2-} (a), which agrees with the result of the previous workers[4]. On the other hand, only Y_2O_3 is formed because the relative stability of Y_2O_3 to YOCl is reversed in this case (b). In LiCl-KCl-$GdCl_3$ system, the formation of Gd_2O_3 is preferred in the lower pO^{2-} region. But the precipitation of GdOCl becomes favorable as pO^{2-} increases because the relative stability of Gd_2O_3 against GdOCl is reversed at pO^{2-} ~ 2 (c).

To judge whether the formation of RE_2O_3 or REOCl occurs for each element, the relative stability of RE_2O_3 against REOCl was estimated in terms of the free enthalpy change of the following reaction;

$$REOCl + \frac{1}{2}O^{2-} = \frac{1}{2}RE_2O_3 + Cl^- \qquad \text{(iv)}$$

$$\Delta G = \frac{1}{2}\Delta G_f(RE_2O_3) - \Delta G_f(REOCl) - \frac{1}{2}\mu^0(O^{2-}) + \frac{2.303RT}{2}pO^{2-} \qquad (6)$$

Figure 8-2 shows the plot of ΔG against the reciprocal ionic radii of rare earth elements when $pO^{2-} = 2$ at 450°C. The tendency is that the formation of RE_2O_3 becomes more favorable than that of REOCl as the ionic radius of RE^{3+}[11] is decreased except in the case of Yb. The stability of RE_2O_3 to REOCl is comparable around the ionic radius of Gd^{3+}. The formation of RE_2O_3 and REOCl is considered to be sensitive to the concentration of O^{2-} for the elements lying near the zero line in the plot.

The values of ΔG for reaction (iv) are considered to be governed by the difference in the formation enthalpies of REOCl and RE_2O_3 if the entropy changes of reaction (iv) are similar for all the elements. Because both REOCl and RE_2O_3 are ionic compounds, the difference in their formation enthalpies is attributed to the difference in the lattice energies of RE_2O_3 and REOCl. This coincides with the observation that, except for a few heavier rare earths, ΔG shows a roughly linear correlation with the reciprocal ionic radius of RE^{3+}.

It should be noted that the heating of all the hydrated $RECl_3$ in air at 450°C always gives REOCl[3], which would be explained by slow kinetics of the oxidation in the solid state compared to that in melts of heavy earth chlorides.

8.3.3 Dehydration of rare earth trichloride hydrates

Except $LaCl_3$, anhydrous $RECl_3$ cannot be prepared by the thermal dehydration of hydrated $RECl_3$, the formation of REOCl being unavoidable even in the inert gas. Figure 8-3 shows the logarithms of equilibrium constants of the hydrolysis of $RECl_3$[12,13,14, 15,16], log K_{Hyd}, for some rare earth elements at 100, 200 and 300°C. At 100°C, the formation of REOCl is negligible for all the rare earth elements. Even at 200°C, for light

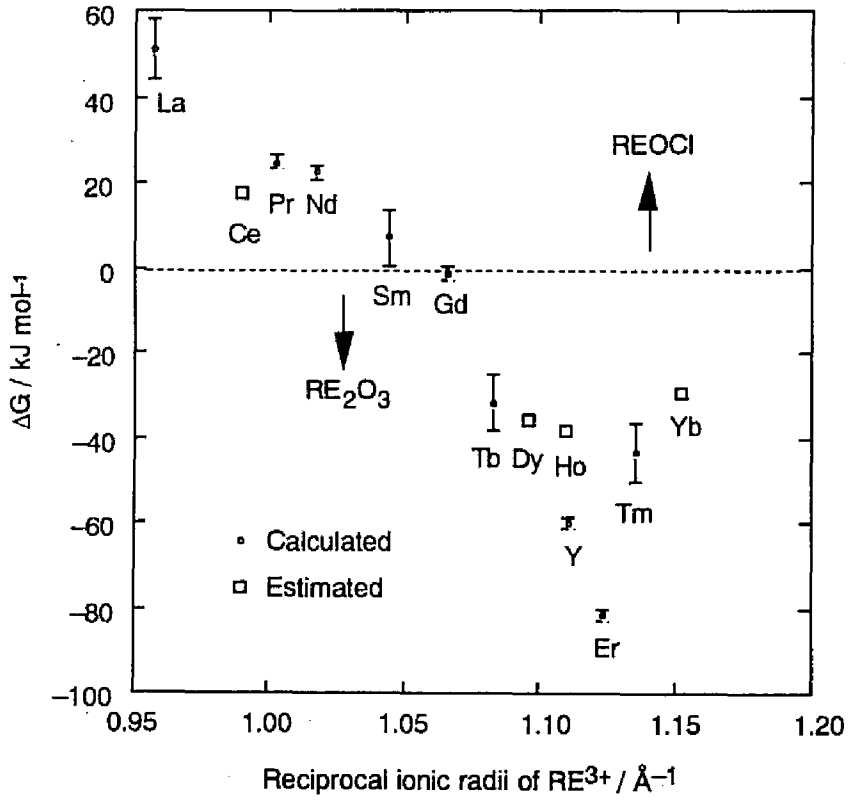

Fig. 8-2 Dependence of the free enthalpy changes, ΔG, of the reaction;

$$REOCl + \frac{1}{2}O^{2-} = \frac{1}{2}RE_2O_3 + Cl^-$$

on the reciprocal ionic radii of RE^{3+} in LiCl-KCl eutectic when $pO^{2-} = 2$ at 450°C.

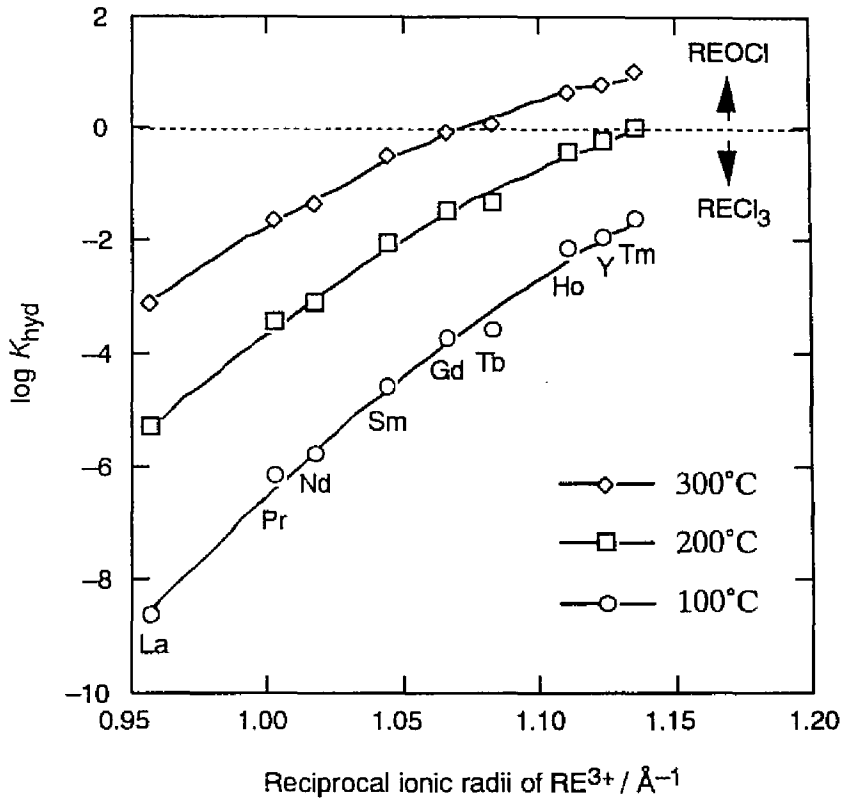

Fig. 8-3 Calculated equilibrium constants of the hydrolysis of $RECl_3$, K_{hyd};

$$RECl_3(s) + H_2O(g) \rightleftharpoons REOCl(s) + 2HCl(g) \qquad K_{hyd} = \frac{p_{HCl}^2}{p_{H_2O}}$$

at 100, 200 and 300°C.

earths, the hydrolytic formation of REOCl is still unfavorable. However, on the other hand, the dehydration is considered not to be complete because $RECl_3 \cdot H_2O$ is rather stable kinetically and not dehydrated unless the temperature exceeds ~300°C[3]. At 300°C, pure anhydrous $LaCl_3$ would be formed by thermal dehydration while the formation of REOCl occurs to a greater or lesser degree for other heavier rare earths in the same condition. In the case of Ho, Y and Tm, REOCl would be the major product. Therefore, the dehydration of hydrated heavy earth trichlorides, including Y, to obtain anhydrides should be carried out at temperatures below 200°C to minimize the formation of REOCl, followed by heating gradually to ~300°C with intermittent treatment of dry HCl and

elimination of H_2O from the system. Since the rate of conversion of REOCl to $RECl_3$ seems to be very slow in solid-gas reaction, it is difficult to obtain pure anhydrous $RECl_3$ from the reagents containing a large amount of REOCl formed by hydrolysis.

8.4 Estimation of ΔG_f(REOCl) at 450°C (723K)

Since the formation enthalpies of REOCl are not literally available, the estimation was made in the following manner.

The reaction thermodynamics of the hydrolysis of some $RECl_3$'s (RE = La, Ce, Pr, Nd, Sm, Gd, Tb, Y, Er and Tm) have been studied by several workers[12,13,14,15,16]:

$$RECl_3(s) + H_2O(g) = REOCl(s) + 2HCl(g) \qquad (v)$$

ΔC_p, for reaction (v) was estimated for La[12].

$$\Delta C_p = -12 - 1.5\times10^{-3}T + \frac{1.8\times10^{-5}}{T} \qquad (\text{in J K}^{-1}) \qquad (8)$$

Assuming ΔC_p' s for other rare earth elements are the same, the free enthalpy changes, ΔG_{hyd}, is given by;

$$\Delta G_{hyd} = H_0 + 2.7\times10^{-2}T\log T + 7.5\times10^{-6}T^2 - \frac{92}{T} + I\times10^{-3}T$$

(in kJ). (9)

The constants, H_0 and I, were re-calculated in this study from the equilibrium constants reported in refs 12-16 by means of the weighed least-square refinement. The errors in H_0 and I are estimated at 1.6% or less for all the elements. Then the enthalpy changes, ΔH_{hyd}, and the entropy changes, ΔS_{hyd}, of reaction (v) are calculated from the following equations:

$$\Delta H_{hyd} = H_0 + \int_0^T \Delta C_p dt$$

$$= H_0 - 1.2\times10^{-2}T - 7.5\times10^{-7}T^2 - \frac{1.8\times10^2}{T} \qquad (\text{in kJ}) \qquad (10)$$

$$\Delta S_{hyd} = \frac{\Delta H_{hyd} - \Delta G_{hyd}}{T}$$

$$= -12(1 + \ln T) - 1.5\times10^{-3}T - \frac{9.2\times10^4}{T^2} + I \qquad (\text{in J K}^{-1}) \qquad (11)$$

The difference in ΔH_{hyd} is attributed to the difference in the formation enthalpies of $RECl_3$ and REOCl, $\Delta H_f(REOCl)$ and $\Delta H_f(RECl_3)$, respectively. Since REOCl is an ionic compound, $\Delta H_f(REOCl)$ is written as eq.(12):

$$\Delta H_f(REOCl) = \Delta H_L(REOCl) - \Delta H_f(RE^{3+}) - \Delta H_f(O^{2-}) - \Delta H_f(Cl^-) \quad (12)$$

where $\Delta H_f(RE^{3+})$, $\Delta H_f(O^{2-})$ and $\Delta H_f(Cl^-)$ are the formation enthalpies of gaseous RE^{3+}, O^{2-} and Cl^-, respectively and $\Delta H_L(REOCl)$ is the lattice energy of REOCl. As $RECl_3$ is also an ionic solid, $\Delta H_f(REOCl)$ is given by;

$$\Delta H_f(RECl_3) = \Delta H_L(RECl_3) - \Delta H_f(RE^{3+}) - 3\,\Delta H_f(Cl^-). \quad (13)$$

From eqs.(12) and (13), the difference of ΔH_f of REOCl and $RECl_3$, $\Delta\Delta H_f$ is given by;

$$\Delta\Delta H_f = \Delta H_f(REOCl) - \Delta H_f(RECl_3)$$

$$= [\Delta H_L(REOCl) - \Delta H_L(RECl_3)] - \Delta H_f(O^{2-}) + 2\,\Delta H_f(Cl^-). \quad (14)$$

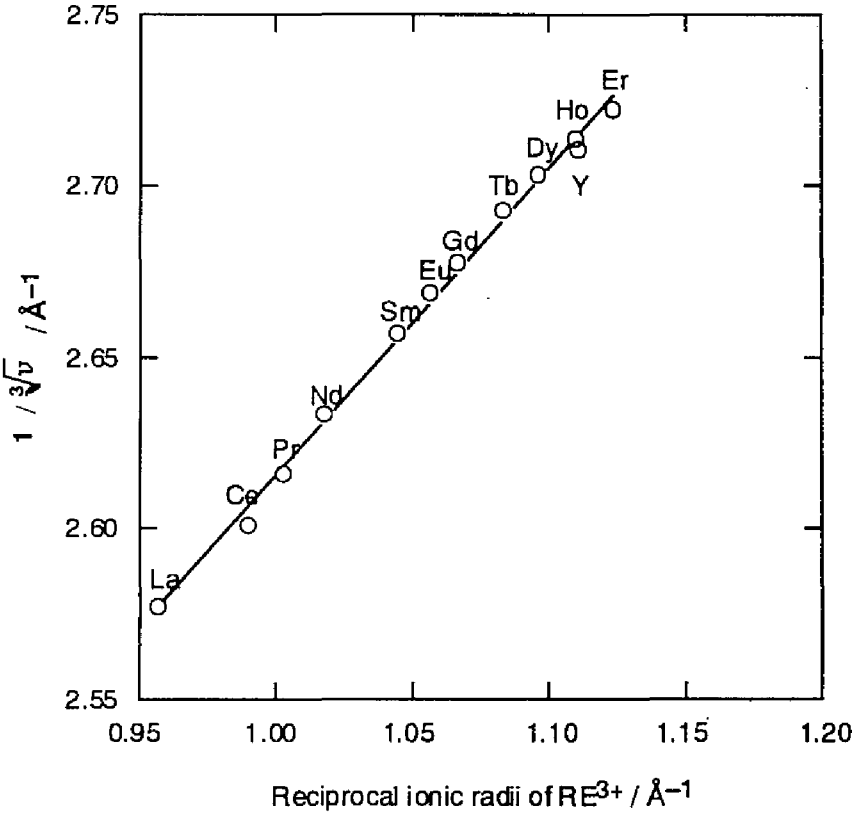

Fig. 8-4 Dependence of the reciprocal cube roots of the formula volumes, $1/\sqrt[3]{v}$, of REOCl on the reciprocal ionic radii of RE^{3+}.

Since the last two terms are independent of the metals, ΔH_{hyd} depends only on the difference between $\Delta H_L(RECl_3)$ and $\Delta H_L(REOCl)$.

The crystal structures of REOCl are the same regardless of the metals, i.e., a tetragonal PbClF-type[17]. On the other hand, the crystal structures of $RECl_3$ are classified into three types; hexagonal UCl_3-type for La to Gd, orthorhombic $PuBr_3$-type for Tb and monoclinic $AlCl_3$-type for Dy to Lu and Y[17]. The influences of the difference in the crystal structures of $RECl_3$ to ΔH_{hyd} and ΔS_{hyd} should be checked.

Figure 8-4 shows the plots of the reciprocal cube roots of the formula volumes, $1/\sqrt[3]{v}$, of REOCl, versus the reciprocal ionic radii or RE^{3+}. The $\Delta H_L(REOCl)$ is considered to depend linearly on $1/\sqrt[3]{v}$ of REOCl. Since the crystal structures of REOCl are all the same, the plot shows the linear correlation between $1/\sqrt[3]{v}$ of REOCl, i.e. ΔH_L (REOCl), and the reciprocal ionic radii of RE^{3+}. Figure 8-5 shows the lattice energies of

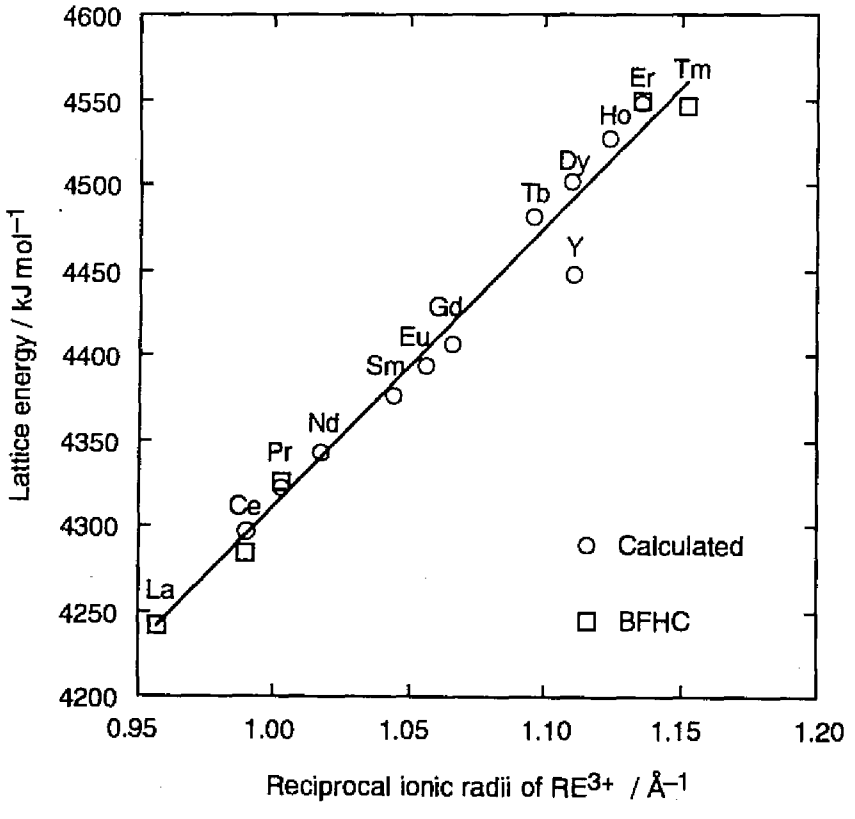

Fig. 8-5 Dependence of the calculated lattice energies of $RECl_3$ on the reciprocal ionic radii of RE^{3+} at 25°C (BFHC = Born-Fajans-Haber Cycle).

$RECl_3$ at 25°C[11] against the reciprocal ionic radii of RE^{3+}. Although the three types of crystal structures of $RECl_3$ exist, there is also a good linear relationship between ΔH_L ($RECl_3$) and the reciprocal ionic radii of RE^{3+} at 25°C. Thus the difference in the crystal structures of $RECl_3$ does not affect the dependence of ΔH_{hyd} on the reciprocal ionic radii of RE^{3+} as shown in Fig. 8-6. By inter- and extrapolating the line, the ΔH_{hyd} at 450°C (723K) for Ce, Pm, Eu, Dy, Ho, Yb and Lu are estimated as listed in Table 8-2.

In Table 8-2, the values of ΔS_{hyd} are similar for La to Gd, ~130 J K^{-1}, and for Er to Tm, ~110 J K^{-1}. This difference would be caused by the difference in the crystal structures of $RECl_3$. Therefore, the average values of ΔS_{hyd} for La to Gd are applied to Ce, Pm and Eu, and the average values of ΔS_{hyd} for Y, Er and Tm are employed to Dy, Ho, Yb and Lu. Although yttrium is one of the light earths in terms of atomic weight, it should be classified as a heavy rare earth in the sense of its chemical properties. The values of

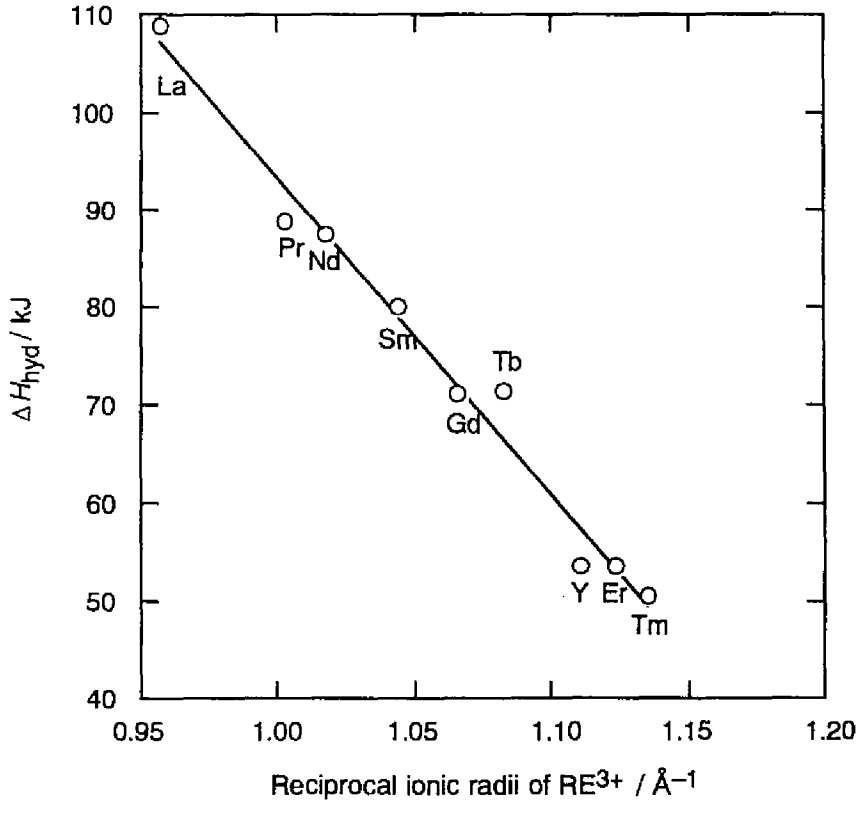

Fig. 8-6 Dependence of the enthalpy changes of the hydrolysis of $RECl_3$ on the reciprocal ionic radii of RE^{3+} at 450°C.

ΔG_{hyd} are also shown in Table 8-2.

Based on these calculations, the free enthalpy changes of formation, ΔG_f^{723}, the formation enthalpies, ΔH_f^{723} and the entropies, S^{723}, of REOCl at 450°C (723K) are obtained by combining with those of $RECl_3$, H_2O and HCl at this temperature[18]. Some ΔG_f^{723} are not listed in Table 8-2 since the values of $\Delta G_f(RECl_3)$ are not literally available.

Table 8-2 Thermodynamic data of the hydrolysis reaction of $RECl_3$ and those of REOCl at 450°C (723K). The values with asterisks(*) are extra- or interpolated from the other data.

RE	$r_{RE^{3+}}$	$RECl_3 + H_2O = REOCl + 2HCl$			REOCl		
		ΔG_{hyd}^{723}	ΔH_{hyd}^{723}	ΔS_{hyd}^{723}	ΔG_f^{723}	ΔH_f^{723}	S^{723}
	Å	kJ	kJ	J K^{-1}	kJ mol^{-1}	kJ mol^{-1}	J mol^{-1} K^{-1}
La	1.045	14.1	109	132	–894	–986	165
Ce	1.010	14.6*	107*	128*	–874*	–975*	162*
Pr	0.9970	–1.00	88.9	124	–883	–989	160
Nd	0.9830	–4.80	87.4	128	–872	–975	161
Pm	0.9700	–4.82*	87.7*	128*			
Sm	0.9580	–14.9	79.9	131	–868	–968	165
Eu	0.9470	–13.3*	79.2*	128*		–866*	
Gd	0.9380	–18.2	71.2	124	–852	–957	156
Tb	0.9230	–20.6	71.3	127	–845	–948	162
Dy	0.9120	–12.3*	66.5*	109*	–837*	–957*	141*
Ho	0.9010	–16.5*	62.3*	109*	–847*	–967*	140*
Y	0.9000	–23.8	53.6	107	–837	–945	128
Er	0.8900	–25.9	53.6	110	–811	–928	143
Tm	0.8800	–28.1	50.7	109	–840	–961	139
Yb	0.8680	–29.3*	49.5*	109*	–825*	–936*	138*
Lu	0.8610	–34.4*	44.4*	109*			

References

1 G. Xie, K. Ema, Y. Ito and Zhao Min Shou, *J. Appl. Electrochem.*, **23**, 753 (1993).

2 G. S. Picard, Y. E. Mottot and B. L. Trémillon, *Proc. of 4th International Symposium on Molten Salts*, vol 84-2, 585 (1984).

3 G. Haeseler and F. Matthes, *J. Less-common Metals*, **9**, 133 (1965).

4 G. S. Picard, Y. E. Mottot and B. L. Trémillon, *Proc. of 5th International Symposium on Molten Salts*, vol. 86-1, 189 (1986).

5 D. V. Drobot, B. G. Korshunov and G. P. Borodulenko, *Russ. J. Inorg. Chem.*, **13**, 855 (1968).

6 L. R. Morss and J. Fuger, *Inorg. Chem.*, **8**, 1433 (1969).

7 A. J. Bard, "*Encyclopedia of Electrochemistry of the Elements Vol. X Fused Salt Systems*," Marcel Dekker, Inc., New York (1976).

8 Z. Y. Qiao, S. Duan and D. Inman, *J. Appl. Electrochem.*, **19**, 937 (1989).

9 N. Masuko, M. Okada and T. Hisamatsu, *Yoyuen*, **6**, 570 (1963).

10 N. Masuko, M. Okada and T. Hisamatsu, *Yoyuen*, **6**, 570 (1963).

11 D. R. Lide ed., "*HANDBOOK of CHEMISTRY and PHYSICS*," 74th ed., CRC press (1993-1994).

12 C. W. Koch, A. Broido, and B. B. Cunningham, *J. Am. Chem. Soc.*, **74**, 2349 (1952).

13 C. W. Koch and B. B. Cunningham, *J. Am. Chem. Soc.*, **75**, 796 (1953).

14 C. W. Koch and B. B. Cunningham, *J. Am. Chem. Soc.*, **76**, 1471 (1954).

15 F. Weigel and V. Wishnevsky, *Chem. Ber.*, **103**, 193 (1970).

16 F. Weigel and V. Wishnevsky, *Chem. Ber.*, **103**, 1976 (1973).

17 D. Brown, "*Halides of the Lanthanides and Actinides*", John Wiley & Sons Ltd., 152 (1968).

18 I. Barin, O. Knacke and O. Kubaschewski, "*Thermochemical properties of inorganic substances*," Springer-Verlag Berlin Heidelberg New York, (1977).

CHAPTER 9

General conclusion

A study was made to clarify acid-base reactions of halides and oxide halides in anhydrous hydrogen fluoride (HF) and LiCl-KCl eutectic melt. For this purpose, the reactions were carried out in extremely "dry" system described in Chapter 2. Reactions were discussed mainly based on the results obtained by characterization of the salts with the aid of structural and spectroscopic analyses

In Chapter 3, the complex salts of silver(I) fluoride (AgF) and tungsten oxide tetrafluoride (WOF_4), $AgWOF_5$ and $AgW_2O_2F_9$, were obtained. The former was able to be prepared by shifting the following solvolysis equilibrium:

$$2AgWOF_5 + nHF \rightleftharpoons Ag(HF)_nF + AgW_2O_2F_9 \quad (1)$$

The complex anions, WOF_5^- and $W_2O_2F_9^-$ were identified in the compounds by vibrational spectroscopy. The reaction of silver(II) fluoride (AgF_2) and WOF_4 gave only a 1 : 2 compound, $AgFW_2O_2F_9$, containing a $W_2O_2F_9^-$ anion as follows:

$$AgF_2 + 2WOF_4 \rightarrow AgFW_2O_2F_9 \quad (2)$$

This compound was also prepared by the reaction of $AgW_2O_2F_9$ with F_2:

$$AgW_2O_2F_9 + 1/2\ F_2 \rightarrow AgFW_2O_2F_9 \quad (3)$$

The fluoride ion affinity of WOF_4 by forming $W_2O_2F_9^-$ anion is larger than that by forming WOF_5^-. The oxidizing ability of $AgFW_2O_2F_9$ is so strong that xenon (Xe) is oxidized to Xe(II) giving $Xe^{II}F_2.WOF_4$ according to the following equation:

$$5AgFW_2O_2F_9 + 2Xe \rightarrow 2XeF_2.WOF_4 + 4AgW_2O_2F_9 + AgF_2 \quad (4)$$

Chapter 4 revealed the oxidizing ability of uranium hexafluoride (UF_6). The reaction of AgF and UF_6 resulted in formation of AgF_2 and $AgUF_6$. Formation of an intermediate complex salt, Ag_2UF_8, was detected by X-ray powder diffraction. A cubic structure of

Ag_2UF_8 was proposed and it was suggested that the oxidation of Ag(I) to Ag(II) would occur through ligand-bridged (inner sphere) mechanism in which "active complex," $(Ag\text{-}F\text{-})_2UF_6$, rearranges to AgF_2 and $AgUF_6$. Therefore, the overall reaction of AgF and UF_6 is represented as follows:

$$2AgF + UF_6 \rightarrow (Ag_2UF_8)^* \rightarrow AgF_2 + AgUF_6 \qquad (5)$$

In Chapters 5 and 6, the properties of uranyl fluoride (UO_2F_2) as a fluoroacid and fluorobase were examined in HF. In Chapter 5, the formation of the complex salts of univalent metal fluorides (MF, M = K, Cs and Ag) was studied. Especially, the new complex salt of AgF and UO_2F_2, $AgUO_2F_3$, was prepared by the following reaction in HF:

$$AgF + UO_2F_2 \rightarrow AgUO_2F_3 \qquad (6)$$

The compound was characterized by X-ray powder diffraction and vibrational spectroscopy, the existence of a new oxofluoroanion being suggested in $AgUO_2F_3$. The fluoroacidity of UO_2F_2 in HF was concluded to be very weak, comparable to that of HF. Chapter 6 is concerned to the properties of UO_2F_2 as a fluorobase in HF based on the reactions with fluoroacids. The fluorobasicity of UO_2F_2 was concluded to be very weak not acting as a fluorobase in the reactions with fluoroacids the fluoride ion affinities of which are higher than that of AsF_5. The compound of UO_2F_2 and AsF_5 was stable only at low temperatures, at least, below −78°C. A new complex salt of UO_2F_2 and BiF_5, $UO_2F_2.2BiF_5$, was prepared and characterized:

$$UO_2F_2 + 2BiF_5 \rightarrow UO_2F_2.2BiF_5 \qquad (7)$$

The structural similarities of $UO_2F_2.2BiF_5$ to $UO_2F_2.2SbF_5$ were suggested by X-ray powder diffraction and vibrational spectroscopy. The attempts at the preparation of the mixed valence compound, $U_2O_2F_7$, from UO_2F_2 and UF_5 which occurs in their melt failed due to the stability of UO_2F_2 having very low activities of acting as both fluoroacid and fluorobase in HF at room temperature.

In Chapter 7, behaviors of rare earth trifluorides (REF_3) as fluorobase and acid were studied. The reactions of REF_3 and univalent metal fluorides (MF, M = Na, K, Cs and Ag) gave no compounds, indicating the low fluoroacidities of REF_3 in HF at room temperature. The formation of the compounds of REF_3 and BF_3, BiF_5 and SbF_5 showed that REF_3 acts as a fluorobase in acidic conditions. The compounds of REF_3 and BF_3 for most of RE's were prepared:

$$REF_3 + nBF_3 \rightarrow REF_3.nBF_3 \qquad (n \sim 2) \qquad (8)$$

The isomorphous series of the compounds were discovered from Ce to Gd having orthorhombic unit cells with a space group of Pnc2 or Pncm. The formation of the compounds of REF_3 and BiF_5 was confirmed, but the detailed properties of them have not been clarified yet.

Chapter 8 clarified the conditions of the formation of rare earth oxides (RE_2O_3) and oxide chlorides (REOCl) in LiCl-KCl eutectic melt (450°C) in the presence of oxide ion. Some thermodynamic parameters of REOCl at this temperature were estimated from the data of hydrolysis of the chlorides ($RECl_3$) taking account of the variation of the crystal structures of $RECl_3$ and REOCl with the ionic radius of RE^{3+}. A tendency that formation of RE_2O_3 becomes more favorable than that of REOCl as the decrease of the ionic radius of RE^{3+} was thermodynamically predicted and proved by experiments. The stability of RE_2O_3 and REOCl is comparable for middle earths. In this chapter, the chemical behaviors of $RECl_3$ in the melt were determined also in the absence of oxide ion. The formation of a double salt of $RECl_3$ and KCl, K_3RECl_6, was confirmed in the absence of oxide ion in the melt. The solubility of $RECl_3$ in the melt is lower for heavy earths than for light earths, resulting in the precipitation of K_3RECl_6, since the stability of K_3RECl_6 increases as the ionic radius of RE^{3+} decreases.

APPENDIX

Preparation of some reagents

This part describes detailed methods to prepare reagents used in this study. In every preparation method, care must be paid when anhydrous hydrogen fluoride (HF), hydrofluoric acid, fluorine (F_2) and other corrosive gases are used.

A.1 Preparation of silver fluoride (AgF)

Several synthetic methods were tried to prepare anhydrous AgF. The reaction of argentus oxide (Ag_2O, Wako Chemicals, purity 99% or more) with hydrofluoric acid (Nakarai Tesque, 47 vol%, guaranteed reagent grade) is the most effective way to prepare a large amount of AgF:

$$Ag_2O + 2HF \rightarrow 2AgF + H_2O \quad (1)$$

Ag_2O was put in a PTFE beaker and 47 vol% hydrofluoric acid was poured on it. Ag_2O was readily dissolved, giving a clear solution with a trace of black precipitate. The precipitate was not dissolved even in the excess hydrofluoric acid, indicating that it was not Ag_2O. The solution was filtered by a Teflon filter paper or decanted to eliminate the black precipitate. The solution was heated to 80 ~ 100°C in a fume hood to evaporate hydrofluoric acid solution and recrystallize AgF. The evaporation was repeated several times with addition of a small amount of hydrofluoric acid to avoid contamination of Ag_2O. AgF solid was obtained as a lump which was unable to be powdered. The solid was crashed into small pieces and put in a Pyrex glass reactor for vacuum drying. The solid was heated at 100 ~ 200°C for several hours until the pressure above the solid becomes less than 10^{-3} torr. No lines corresponding to other than AgF were detected by X-ray powder diffraction although a small amount of black particles was seen in the sample.

The reaction of Ag_2O with anhydrous HF was convenient way to prepare a small amount of AgF (less than ~1g) without further vacuum drying. Ag_2O was put in one arm (Tube A) of T-shaped FEP reactor (1/2' o.d.) and a large excess amount of HF was condensed on it. Ag_2O reacted readily with HF (even when gaseous HF was introduced in the reactor) evolving gases (probably H_2O and HF). The reaction was completed in several minutes to give an opaque solution. The solution should be left for several minutes to precipitate the black solid. Then the supernatant solution was decanted to the other arm (Tube B) and HF was condensed back to Tube B by cooling Tube A at –176°C. This procedure was repeated several times. In this procedure, large excess HF is preferably supplied since the vapor pressure of HF becomes very low due to the large solubility of AgF in HF at room temperature. A white solid (silver bifluoride, $Ag(HF)_nF$) was crystallized after evacuating HF. AgF was obtained by subsequent elimination of HF with heating $Ag(HF)_nF$ to 70 ~ 80°C by a water bath.

AgF is light sensitive, some black particles being formed. Therefore, it was kept in darkness by wrapping the container with aluminum foil. The purification by decantation in anhydrous HF should be carried out just before use when very pure AgF was needed for the experiment.

A.2 Preparation of tungsten oxide tetrafluoride (WOF_4)

WOF_4 was prepared by the hydrolysis of tungsten hexafluoride (WF_6, Ozark-Mahoning) as described elsewhere[1]:

$$WF_6 + H_2O \rightarrow WOF_4 + 2HF \qquad (2)$$

Since WOF_4 easily reacts with H_2O to form oxonium complex salts, H_3OWOF_5 and $H_3OW_2O_2F_9$, or tungsten bronze (blue solid), H_2O must be supplied very slowly to excess WF_6. It is a convenient way to supply H_2O formed by a sluggish reaction of silica (SiO_2) and HF:

$$SiO_2 + 4HF \rightarrow SiF_4\uparrow + 2H_2O \quad (3)$$

Quartz wool (Toshiba) was charged in an FEP tube. It must not be stuffed in the bottom of the reactor otherwise the HF whose specific gravity (0.987 g cm^{-3}[2]) is lower than that of WF_6 (3.44 g cm^{-3}[2]) does not interact with it. HF and WF_6 were condensed on it, the amount of the former being large enough to dissolve WOF_4. The reaction was continued overnight. After evacuating excess WF_6 and HF, the mixture of WOF_4 and oxonium complex salts was obtained. Then WOF_4 was separated from the mixture by sublimation at ~50°C under a reduced pressure. No impurity was detected by X-ray powder diffraction.

WOF_4 was also obtained by fluorination of WO_3 (Nakarai Tesque, purity 99.5%), which was more efficient to prepare a large amount of WOF_4:

$$WO_3 + 4F_2 \rightarrow WOF_4 + 2OF_2 \quad (4)$$

WO_3 powder was put in a Ni cup which was placed in a Monel reactor. F_2 (2 atm) was introduced in the reactor at room temperature. The reactor was heated to 300°C with the valve of the reactor closed in order to avoid the deposition of WOF_4 in the vacuum line. The reaction was continued for several hours. The reactor was then cooled down to room temperature and the gases in it were evacuated. F_2 (2 atm) was refilled again and allowed to react with WO_3 for several hours at 300°C. This process was repeated several times. Finally, a white solid deposited on the cooled lid of the reactor was collected. The purity of WOF_4 was confirmed by X-ray powder diffraction. Further purification was not necessary in this method.

A.3 Preparation of uranyl fluoride (UO_2F_2)

UO_2F_2 was prepared by fluorination of U_3O_8 powder[3]:

$$U_3O_8 + 5F_2 \rightarrow 3UO_2F_2 + 2OF_2 \quad (5)$$

U_3O_8 was prepared by oxidation of UO_2 (Furukawa Denki Kogyo, depleted uranium) in a

porcelain crucible in air at ~800°C. U_3O_8 was put in a Ni cup which was placed in a Monel reactor. F_2 (2 atm) was introduced in the reactor at room temperature. The temperature of the reactor was elevated to 200°C and held for several hours monitoring the pressure. After cooling the reactor down to room temperature and evacuating the gases in it, F_2 (2 atm) was introduced again and allowed to react with residual U_3O_8 at 200°C for several hours. This process was repeated several times. A pale yellow solid was remained in the Ni cup. Small amount of black material which was probably U_3O_8 was remained in the solid although the X-ray powder pattern of the solid detected only UO_2F_2. The reaction seems to be very slow. However, the temperature must not be elevated over 200°C because subsequent fluorination of UO_2F_2 to UF_6 occurs.

UO_2F_2 was also prepared by hydrolysis of UF_6[4,5]:

$$UF_6 + (2+n)H_2O \rightarrow UO_2F_2 \cdot nH_2O + 2HF \qquad (6)$$

Where n = ~2. UF_6 was prepared by fluorinating UO_2 (Furukawa Denki Kogyo, depleted uranium) in a nickel metal reaction vessel at around 500°C, and distilled into a Monel metal container after evacuating volatile gases at 0°C for a while. H_2O was put in an FEP reactor and frozen at –176°C. After evacuating air above the ice, excess UF_6 was condensed on it. After the interaction for several hours, a viscous yellow solution was obtained. After evacuating excess UF_6 and volatile materials with warming the reactor, a yellow solid was formed. The solid was charged in a Pyrex glass reactor and dried under vacuum at 200°C for several hours. The temperature should not exceed 200°C since the decomposition of UO_2F_2 occurs[3]. The product was confirmed to be anhydrous UO_2F_2 by X-ray powder diffraction[6] and Raman spectroscopy[7].

A.4 Preparation of uranium pentafluoride (UF_5)

UF_5 (β-form) was prepared by the reaction of UF_6 and carbon monoxide (CO, Takachiho Kagaku Kogyo, spectroscopic grade) under irradiation of UV light:

$$2UF_6 + CO \xrightarrow{h\nu} 2UF_5 + COF_2 \quad (7)$$

UF_6 was condensed in a Pyrex glass bulb (1000 cm^3) and CO (1 atm) was introduced in it. The bulb was irradiated by UV light of a mercury lump (Hitachi UM-102) for a day. A greenish solid was deposited on the wall of the bulb. After cooling the cold finger of the bulb at 0°C to trap unreacted UF_6, the gases in the bulb was evacuated and CO (1 atm) was introduced again. This step was repeated several times. The reaction is very slow and the deposition of UF_5 on the wall prevented UV light from irradiating the inside of the bulb. Therefore, it takes several days to prepare even a few grams of UF_5.

UF_5 is also prepared by proportionation of UF_6 and UF_4 in HF at room temperature[8]:

$$UF_6 + UF_4 \rightarrow 2UF_5 \quad (8)$$

and reduction of UF_6 by PF_3 in HF[9]:

$$2UF_6 + PF_3 \rightarrow 2UF_5 + PF_5 \quad (9)$$

These methods were not tried in this study.

A.5 Preparation of bismuth pentafluoride (BiF_5)

BiF_5 was prepared by fluorination of bismuth metal:

$$Bi + 5/2\ F_2 \rightarrow BiF_5 \quad (8)$$

Granular Bi (Nakarai Tesque, 99.5%) metal was put in a Ni cup which was placed in a Monel reactor. F_2 (1.5 atm) was introduced in the reactor at room temperature and interacted with Bi at 500°C for several hours with the valve of the reactor closed in order to raise the pressure of F_2 and avoid the deposition of BiF_5 in the vacuum line. The reaction was slow in this condition where Bi melted (m.p. 271.3°C[2]). A white solid was deposited on the lid of the reactor. The X-ray powder pattern of the solid detected some impurities. BiF_5 was purified by sublimation at 120°C under a reduced pressure. This preparation was not successful since unreacted Bi was always remained and difficult

to be removed from the Ni cup.

BiF_5 was also prepared by fluorination of Bi_2O_3 (Nakarai Tesque, purity 99.9%):

$$Bi_2O_3 + 8F_2 \rightarrow 2BiF_5 + 3OF_2 \quad (9)$$

Bi_2O_3 was put in a Ni cup which was placed in a Monel reactor. F_2 (~5 atm) at room temperature was transferred to the reactor by condensation. The reactor was heated at 500°C with the valve of the reactor closed in order to raise the pressure of F_2 and avoid deposition of BiF_5 in the vacuum line. The reaction was continued for several hours. A white solid deposited on the lid of the reactor was collected. X-ray powder diffraction of the solid detected no impurity.

BiF_5 is very reactive with water to form HF and ozone (O_3). Therefore, when the tools adhered with BiF_5 are washed with water, one should take much care. A brown solid (probably oxides or oxide fluorides of Bi) sticks to the tools when washed with water. It is easily removed by washing with dilute HCl solution.

References

1 J. M. Shreeve, "*Inorganic Synthesis*," John Wiley & Sons Inc., **24**, 37 (1986).

2 D. R. Lide ed., "*HANDBOOK of CHEMISTRY and PHYSICS*," 74th ed., CRC press (1993-1994).

3 J. J. Katz, "*The Chemistry of Uranium*," Dover Publications, Inc., (1951).

4 D. Brown, "*Halides of the Lanthanides and Actinides*," John Wiley & Sons Ltd., (1968).

5 J. Fawcett, J. H. Holloway, D. Laycock and D. R. Russell, *J. Chem. Soc. Dalton Trans.*, 1355 (1982).

6 W. H. Zachariasen, *Acta Cryst.*, **1**, 277 (1948).

7 D. P. Armstrong, R. J. Jarabek and W. H. Fletcher, *Appl. Spectrosc.*, **43**, No. 3, 461 (1989).

8 J. P. Masson, J. P. Desmoulin, P. Charpin and R. Bougon, *Inorg. Chem.*, **15**, No. 10, 2529 (1976).

9 J. G. Malm, *J. Inorg. Nucl. Chem.*, **42**, 993 (1980).

Acknowledgments

The author wishes to gratefully acknowledge Professor Yasuhiko Ito for giving valuable suggestions and advice over whole parts of this study. The author is extremely indebted to Associate Professor Rika Hagiwara for giving instructions on the experimental techniques and discussions on the results. The author would like to thank to Dr. Kazuhiro Wada, Mr. Masayuki Tada, and Ms. Keiko Ema for their valuable helps. The discussions with Professor Hirotake Moriyama (Kyoto University Research Reactor Institute), Dr. Junzo Umemura (Institute of Chemistry, Kyoto University), Professor Neil Bartlett (Department of Chemistry, University of California, Berkeley, USA) and Professor Boris Žemva (Jožef Stefan Institute, University of Ljubljana, Slovenia) were quite helpful for interpretations of the results in this study, which is also acknowledged. The author also thanks to Mr. Kohei Hironaka for his collaboration for the study appeared in Chapter 7. It remains for the author to thank all the colleagues in Prof. Ito's laboratory for their support and assistance.

A part of this study was financially supported by a Grant-in-Aid for Scientific Research from Ministry of Education, Science, Sports and Culture. The author thanks to the Japan Society for the Promotion of Science for Japanese Junior Scientists for the financial supports.

Janurary 9, 1996

Yasushi Katayama

Yasushi Katayama